

August 1987

Nutrient-Dissolved Oxygen Dynamics in Chesapeake Bay: The Roles of Phytoplankton and Micro-Heterotrophs Under Summer Conditions, 1985



Ref. No. [UMCEES]CBL 86-125a
(This cancels Ref. No.
[UMCEES]CBL 86-125 in
its entirety.)

NUTRIENT-DISSOLVED OXYGEN DYNAMICS IN CHESAPEAKE BAY:

The Roles of Phytoplankton and Micro-Heterotrophs

Under Summer Conditions, 1985

Final Report to

EPA Chesapeake Bay Program

by

Jon H. Tuttle, Thomas C. Malone,

Robert B. Jonas, Hugh W. Ducklow and David G. Cargo

The University of Maryland Center for Environmental & Estuarine Studies

Chesapeake Biological Laboratory
Solomons, Maryland 20688-0038

and

Horn Point Environmental Laboratories
Cambridge, Maryland 21613-0775

DISCLAIMER

This report has been reviewed by the Chesapeake Bay Program, U.S. Environmental Protection Agency, and approved for publication. Approval does not signify that the contents necessarily reflect the views and policies of the U.S. Environmental Protection Agency, nor does mention of trade names or commercial products constitute endorsement or recommendation for use.

ACKNOWLEDGEMENTS

This study was funded by grants X-003311-01-0 and X-003310-02-0 from the U.S. Environmental Protection Agency and grant NA84AA-D-00014 from the National Oceanographic and Atmospheric Administration through the University of Maryland Sea Grant College. The latter grant funded the major portion of our 1985 field program which forms the basis for much of this report. One of us (JHT) also wishes to acknowledge the support of grant OCE-8208032 from the National Science Foundation which supported the sulfur cycling research discussed briefly in this report.

We wish to thank J. Tyler Bell, Sue Hill, and Brian Wendler for excellent technical support and the captains and mates of R/V Orion and R/V Aquarius for much needed help with shipboard work. We are grateful to Gail Canaday for her typing expertise and for aid in compiling this report and to Margaret Weir for proof reading and reference compilation.

ABSTRACT

This study focused on the relationships of phytoplankton and microheterotrophs to the development and maintenance of anoxia in the mesohaline region of Chesapeake Bay. A series of 14 cruises were made from February to October, 1985, on which water quality, nutrient concentrations, phytoplankton production, and microheterotroph production and metabolism were assessed.

Phytoplankton production from February to May generates a quantity of organic matter more than adequate to cause oxygen decline in mid-Bay deep waters. The development of the summer maximum in phytoplankton productivity appears to depend upon the regeneration of nutrients from phytoplankton carbon produced in the spring which sinks into deep water and is remineralized by bacteria. These nutrients are recycled into the euphotic zone via vertical mixing and oscillations of the pycnocline.

Bacterial biomass, production, and metabolism are tightly coupled to phytoplankton production during the spring and summer. Phytodetritus is the source of carbon fueling bacterial oxygen consumption in deep waters. A relationship for predicting oxygen consumption rates from bacterial abundance estimates has been developed. Water column oxygen consumption by microheterotrophs is a major contributor to the development of anoxia during the spring and early summer. Microbial sulfur cycling then becomes an important mechanism for maintaining anoxia. The potential for the establishment of anoxia is greatest in the northern regions of the mesohaline

Chesapeake Bay. However, phytoplankton and bacterial parameters exhibit greater variation over shorter distances in an east to west direction.

Comparisons of biological measurements made in the summer of 1984, a high flow year in which anoxia was widespread, with measurements made in 1985, a low flow year in which anoxia was limited and of short duration, suggest that fundamental changes have occurred in the ecosystem of mid-Chesapeake Bay such that a significant portion of primary production is channeled into bacterial production. Thus, the severity of anoxic conditions depends upon climatic differences regulating freshwater flow, pycnocline tilting, and wind mixing rather than upon changes in biological parameters.

CONTENTS

	<u>Page</u>
Abstract	ii
Figures	vi
Tables	xv
Abbreviations and Symbols	xvi
Acknowledgment	xvii
 1. INTRODUCTION	 1
GENERAL CONSIDERATIONS	1
THE 1984 STUDY	5
THE 1985 STUDY	8
2. CONCLUSIONS	11
3. RECOMMENDATIONS	14
FURTHER RESEARCH	14
MANAGEMENT	16
4. MATERIALS, METHODS AND EXPERIMENTAL PROCEDURES	17
CRUISE SCHEDULE AND STATION DESCRIPTIONS	17
SAMPLE COLLECTION	17
DETERMINATION OF PARAMETERS	20
<u>Physical Water Quality Parameters</u>	20
<u>Particulate Organic Carbon (POC), Nitrogen (PON),</u> <u>and Nutrient Determinations</u>	20
<u>Phytoplankton Pigments and Cell Densities</u>	21
<u>Photosynthetic Production</u>	21
<u>Microbial Metabolism and Secondary Production -</u> <u>Dual Label Technique</u>	22
<u>Microbial Production-Single Label Technique</u>	23
<u>Bacterial Biomass</u>	24
<u>Microbial Oxygen Consumption</u>	25
<u>Biochemical Oxygen Demand (BOD-5)</u>	25
5. RESULTS AND DISCUSSION	27
THE 1985 ANNUAL CYCLE-HYDROGRAPHY, NUTRIENTS, PHYTOPLANKTON	27
<u>Hydrography</u>	27
<u>Dissolved Inorganic Nutrients</u>	31
<u>Dissolved Oxygen</u>	31
<u>Phytoplankton Biomass and Productivity</u>	39
<u>Lateral Variation</u>	46
1984 AND 1985 INTERANNUAL CONTRASTS -	
HYDROGRAPHY, NUTRIENTS, PHYTOPLANKTON	52
<u>Dissolved Oxygen and Vertical Stratification</u>	57
<u>Production and Fate of Phytoplankton Biomass</u>	60
<u>Nutrients and Phytoplankton Production</u>	60
THE 1985 ANNUAL CYCLE - MICROBIOLOGY	61
<u>Bacterial Abundance</u>	61

Temporal Changes along the Main Channel	61
Temporal Changes along Transect 2	63
Differences with Depth	74
North to South Differences	74
East to West Differences	74
Bacterial Size	79
<u>Bacterial Production</u>	83
Temporal Changes along the Main Channel	83
Differences with Depth	85
North to South Differences	92
East to West Differences	96
<u>Amino Acid Metabolism</u>	96
Temporal Changes along the Main Channel	96
Differences with Depth	105
North to South Differences	105
East to West Differences	109
<u>Glucose Metabolism</u>	109
Temporal Changes along the Main Channel	111
Differences with Depth	118
North to South Differences	119
<u>Oxygen Consumption</u>	119
<u>Carbon Sources for Bacteria and Oxygen Consumption</u>	127
Chlorophyll	127
Phaeopigments	133
Particulate Organic Nitrogen	133
Particulate Organic Carbon	136
Biochemical Oxygen Demand	141
1984 AND 1985 INTERANNUAL CONTRASTS - MICROBIOLOGY	150
<u>Microheterotrophs</u>	151
<u>The Role of Sulfur Cycling</u>	154
References	156

FIGURES

<u>Number</u>		<u>Page</u>
1	Site map of Chesapeake Bay illustrating transect (T1, T2, T3) locations (---) and additional deep channel stations (O) occupied during the 1985 study.	9
2	Temporal variations in the vertical distribution of temperature.	28
3	Temporal variations in the vertical distribution of salinity.	29
4	Temporal variations in the vertical distribution of sigma-t.	30
5	Temporal variations in the vertical distribution of nitrate (uM).	32
6	Temporal variations in the vertical distribution of ammonium (uM).	33
7	Temporal variations in the vertical distribution of phosphate (uM).	34
8	Frequency distributions of the atomic ratio of dissolved inorganic nitrogen (nitrate + nitrite + ammonium) to dissolved inorganic phosphorus (ortho-phosphate); open bars-surface, solid bars-near bottom.	35
9	Temporal variations in the vertical distribution of dissolved oxygen (mg/l); hatched areas indicate locations of mid-depth oxygen minima.	36
10	Variations in the vertical distributions of salinity and dissolved oxygen along the mainstem transect on cruise 10. Station numbers are indicated by closed triangles at top.	38
11	Temporal variations in the vertical distribution of chlorophyll (ug/l).	40

<u>Number</u>		<u>Page</u>
12	Frequency distributions of the ratio of particulate organic carbon (ug/l) to chlorophyll (ug/l); open bars-surface, solid bars-near bottom.	47
13	Frequency distributions of the ratio of particulate organic carbon (ug/l) to particulate organic nitrogen (ug/l); open bars-surface, solid bars-near bottom.	48
14	Lateral distributions of salinity and oxygen along the CHOP-PAX transect (from west on the left to east on the right). Solid triangles at top indicate stations along the transect.	49
15	Lateral distributions of chlorophyll (ug/l) along the CHOP-PAX transect (from west to east). Solid triangles at top indicate stations along the transect.	50
16	Temporal variations in surface salinity, vertical stability across the pycnocline, and the thickness of the hypoxic layer having oxygen concentrations less than 1 mg/l during 1984 (solid line) and 1985 (broken line); circled point is from June 1984.	53
17	Variations in the vertical distribution of salinity along the mainstem transect in June of 1984 and 1985. Numbers above solid triangles indicate CBI stations (above) and stations from this study (below).	54
18	Variations in the vertical distribution of dissolved oxygen along the mainstem transect in June of 1984 and 1985. Stations are the same as in Figure 16.	55
19	Temporal variations in the chlorophyll content of the euphotic zone and chlorophyll specific productivity of the euphotic zone during 1984 and 1985.	56
20	Mean oxygen concentration of the bottom layer in relationship to vertical stability across the pycnocline and to bottom water temperature (circle, station 32; triangle, station 3; diamond, station 24); regressions run for 12 Feb.-16 May.	58
21	Temporal variations in the mean concentration of dissolved oxygen in bottom layer (solid line) and vertical stability across the pycnocline (dashed line).	59

<u>Number</u>		<u>Page</u>
22	Time-dependent vertical variations in bacterial abundance along a north-south (station 32 to 24) main channel transect.	62
23	Lateral distributions of bacterial abundance along transect 2 for the period 13 Feb. - 16 Apr. 1985.	64
24	Lateral distributions of bacterial abundance along transect 2 for the period 29 Apr. - 23 May 1985.	65
25	Lateral distributions of bacterial abundance along transect 2 for the period 28 May - 19 June 1985.	66
26	Lateral distributions of bacterial abundance along transect 2 for the period 11 July - 15 Aug. 1985.	67
27	Lateral distributions of bacterial abundance along transect 2 for the period 11 Sep. - 10 Oct. 1985.	68
28	Variations in salinity with depth along transect 2 for the period 13 Feb. - 16 Apr. 1985.	69
29	Variations in salinity with depth along transect 2 for the period 29 Apr. - 23 May 1985.	70
30	Variations in salinity with depth along transect 2 for the period 28 May - 19 June 1985.	71
31	Variations in salinity with depth along transect 2 for the period 11 July - 15 Aug. 1985.	72
32	Variations in salinity with depth along transect 2 for the period 11 Sep. - 10 Oct. 1985.	73
33	Mean bacterial abundances within (●) and below (○) the euphotic zone for transects 1-3 during 1985. Bacterial abundances are expressed in millions of bacterial ml ⁻¹ .	75
34	Mean bacterial abundances within the euphotic zone along transects 1 (Δ), 2 (○), and 3 (□) during 1985. Bacterial abundances are expressed in millions of bacterial ml ⁻¹ .	76
35	Mean bacterial abundances below the euphotic zone along transects 1 (Δ), 2 (○), and 3 (□) during 1985. Bacterial abundances are expressed in millions of bacterial ml ⁻¹ .	77

<u>Number</u>		<u>Page</u>
36	Mean bacterial abundances along the west flank (Δ), main channel (O), and east flank (\square) of Chesapeake Bay during 1985. Values are means of data from all three lateral transects. Bacterial abundances are expressed in millions of bacterial ml^{-1} .	78
37	The percent of total bacterial abundance within the euphotic zone attributable to bacteria smaller than $1\ \mu\text{m}$ along transects 1 (Δ), 2 (O), and 3 (\square) during 1985.	80
38	The percent of total bacterial abundance below the euphotic zone attributable to bacteria smaller than $1\ \mu\text{m}$ along transects 1 (Δ), 2 (O), and 3 (\square) during 1985.	81
39	The percent of total bacterial abundance attributable to bacteria smaller than $1\ \mu\text{m}$ along the west flank (Δ), main channel (O), and east flank (\square) of Chesapeake Bay during 1985. Percentages are calculated from means of data from all three lateral transects.	82
40	Time-dependent vertical variations in bacterial production along a north-south (station 32 to 24) main channel transect. Values on contour lines represent TdR in $\text{p mol L}^{-1} \text{h}^{-1}$.	84
41	Lateral distribution of bacterial production along transect 2 for the period 13 Feb. - 21 Mar. 1985.	86
42	Lateral distribution of bacterial production along transect 2 for the period 29 Apr. - 23 May 1985.	87
43	Lateral distribution of bacterial production along transect 2 for the period 28 May - 19 June 1985.	88
44	Lateral distribution of bacterial production along transect 2 for the period 11 July - 15 Aug. 1985.	89
45	Lateral distribution of bacterial production along transect 2 for the period 11 Sep. - 10 Oct. 1985.	90
46	Mean bacterial production, expressed as TdR, within (\bullet) and below (O) the euphotic zone for transects 1-3 during 1985.	91

<u>Number</u>		<u>Page</u>
47	Mean bacterial production, expressed as TdR, along transects 1 (Δ), 2 (O), and 3 (\square) during 1985.	93
48	Mean bacterial production, expressed as TdR, within the euphotic zone along transects 1 (Δ), 2 (O), and 3 (\square) during 1985.	94
49	Mean bacterial production, expressed as TdR, below the euphotic zone along transects 1 (Δ), 2 (O), and 3 (\square) during 1985.	95
50	Mean bacterial production, expressed as TdR, along the west flank (Δ), main channel (O), and east flank (\square) of Chesapeake Bay during 1985. Values are means of data from all three lateral transects.	97
51	Time-dependent vertical variations in amino acid metabolism along a north-south (station 32 to 24) main channel transect. Solid triangles at the top indicate cruise dates. Values on contour lines represent amino acid turnover rates expressed as % of amino acid pool h^{-1} .	98
52	Lateral distribution of amino acid metabolism, expressed as amino acid turnover rates, along transect 2 for the period 13 Feb. - 21 Mar. 1985.	100
53	Lateral distribution of amino acid metabolism, expressed as amino acid turnover rates, along transect 2 for the period 29 Apr. - 23 May 1985.	101
54	Lateral distribution of amino acid metabolism, expressed as amino acid turnover rates, along transect 2 for the period 28 May - 19 June 1985.	102
55	Lateral distribution of amino acid metabolism, expressed as amino acid turnover rates, along transect 2 for the period 11 July to 15 Aug. 1985.	103
56	Lateral distribution of amino acid metabolism, expressed as amino acid turnover rates, along transect 2 for the period 11 Sep. - 10 Oct. 1985.	104
57	Mean amino acid metabolism, expressed as amino acid turnover rates, within (\bullet) and below (O) the euphotic zone for transects 1-3 during 1985.	106
58	Mean amino acid metabolism, expressed as amino acid turnover rates, within the euphotic zone along transects 1 (Δ), 2 (O), and 3 (\square) during 1985.	107

<u>Number</u>		<u>Page</u>
59	Mean amino acid metabolism, expressed as amino acid turnover rates, below the euphotic zone along transects 1 (Δ), 2 (O), and 3 (\square) during 1985.	108
60	Mean amino acid metabolism, expressed as amino acid turnover rates, along the west flank (Δ), main channel (O), and east flank (\square) of Chesapeake Bay during 1985. Values are means of data from all three lateral transects.	110
61	Time-dependent vertical variations in glucose metabolism along a north-south (station 32 to 24) main channel transect. Solid triangles at the top indicate cruise dates. Values on contour lines represent glucose turnover rates expressed as % of glucose pool h^{-1} .	112
62	Lateral distribution of glucose metabolism, expressed as glucose turnover rates, along transect 2 for 16 April 1985.	113
63	Lateral distribution of glucose metabolism, expressed as glucose turnover rates, along transect 2 for the period 29 Apr. - 23 May 1985.	114
64	Lateral distribution of glucose metabolism, expressed as glucose turnover rates, along transect 2 for the period 28 May - 19 June 1985.	115
65	Lateral distribution of glucose metabolism, expressed as glucose turnover rates, along transect 2 for the period 11 Jul. - 19 Jul. 1986.	116
66	Lateral distribution of glucose metabolism, expressed as glucose turnover rates, along transect 2 for the period 11 Sep. - 10 Oct. 1985.	117
67	Mean glucose metabolism, expressed as glucose turnover rates, within (\bullet) and below (O) the euphotic zone for transects 1-3 during 1985.	120
68	Mean glucose metabolism, expressed as glucose turnover rates, within the euphotic zone along transects 1 (Δ), 2 (O), and 3 (\square) during 1985.	121
69	Mean glucose metabolism, expressed as glucose turnover rates, below the euphotic zone along transects 1 (Δ), 2 (O), and 3 (\square) during 1985.	122

<u>Number</u>		<u>Page</u>
70	Mean glucose metabolism, expressed as glucose turnover rates, along the west flank (Δ), main channel (O), and east flank (\square) of Chesapeake Bay during 1985. Values are means of data from all three lateral transects.	123
71	Mean oxygen consumption within the euphotic zone (\bullet), beneath the euphotic zone to the benthos (O), and beneath the euphotic zone to 15m depth (Δ) during 1985. Values are means of data from all three lateral transects.	125
72	Mean oxygen consumption beneath the euphotic zone along transects 1 (Δ), 2 (O), and 3 (\square) during 1985.	126
73	Linear regression of mean oxygen consumption on bacterial abundance. Symbols: (\blacktriangle) euphotic zone means for the time periods 20 Aug. - 11 Sep., 14 Sep. - 3 Oct., and 5 Oct. - 2 Nov. 1984; (\bullet) beneath euphotic zone means for 1984 data collected in the time periods given above; (Δ) euphotic zone means for the time periods 12 Feb. - 17 Apr., 29 Apr. - 7 June, and 19 June - 12 Sep. 1985; (O) beneath euphotic zone means for 1985 data collected in the time periods given above. Means were calculated using data from all transects.	128
74	Mean chlorophyll <u>a</u> concentrations within (\bullet) and below (O) the euphotic zone during 1985. Values are means of data from all three lateral transects.	130
75	Mean chlorophyll <u>a</u> concentrations within (A) and below (B) the euphotic zone across transects 1 (Δ), 2 (O), and 3 (\square) during 1985.	131
76	Mean chlorophyll <u>a</u> concentrations along the west flank (Δ), main channel (O), and east flank (\square) of Chesapeake Bay during 1985. Values are means of data from all three lateral transects.	132
77	Mean phaeopigment concentrations within (\bullet) and below (O) the euphotic zone during 1985. Values are means of data from all three lateral transects.	134
78	Mean PON concentrations within (\bullet) and below (O) the euphotic zone during 1985. Values are means of data from all three lateral transects.	135

<u>Number</u>		<u>Page</u>
79	Mean PON concentrations along transects 1 (Δ), 2 (O), and 3 (\square) during 1985. Means include data from within and below the euphotic zone.	137
80	Mean PON concentrations along the west flank (Δ), main channel (O), and east flank (\square) of Chesapeake Bay during 1985. Values are means of data from all three lateral transects.	138
81	Mean POC concentrations within (\bullet) and below (O) the euphotic zone during 1985. Values are means of data from all three lateral transects.	139
82	Mean POC concentrations along transects 1 (Δ), 2 (O), and 3 (\square) during 1985. Means include data from within and below the euphotic zone.	140
83	Mean POC concentrations along the west flank (Δ), main channel (O), and east flank (\square) of Chesapeake Bay during 1985. Values are means of data from all three lateral transects.	142
84	Mean total BOD-5 along transects 1 (Δ), 2 (O), and 3 (\square) during 1985. Means include data from within and below the euphotic zone.	143
85	Mean total BOD-5 within the euphotic zone along transects 1 (Δ), 2 (O), and 3 (\square) during 1985.	144
86	Mean total BOD-5 below the euphotic zone along transects 1 (Δ), 2 (O), and 3 (\square) during 1985.	145
87	Mean total BOD-5 along the west flank (Δ), main channel (O), and east flank (\square) of Chesapeake Bay during 1985. Means include data from within and below the euphotic zone.	147
88	Mean total BOD-5 (closed symbols) and particulate BOD-5 (open symbols) in the mesohaline portion of Chesapeake Bay during 1985. Circles represent values within the euphotic zone and triangles represent values beneath the euphotic zone. Means include data from all three lateral transects.	148

- 89 Comparisons of mean particulate BOD-5 with mean filterable BOD-5 (A) and % of total BOD-5 comprised of particulate BOD-5 (B) in the mesohaline portion of Chesapeake Bay during 1985. Values are means of data from all three lateral transects. Symbols:
- (●) particulate BOD-5 within the euphotic zone;
 - (▲) filterable BOD within the euphotic zone;
 - (○) particulate BOD-5 beneath the euphotic zone;
 - (△) filterable BOD-5 beneath the euphotic zone;
 - (■) % particulate BOD-5 within the euphotic zone;
 - (□) % particulate BOD-5 beneath the euphotic zone.

TABLES

<u>Number</u>		<u>Page</u>
1	Station locations for 1985 Sea Grant/EPA Chesapeake Bay study.	18
2	Cruise dates and descriptions for 1985 Sea Grant/EPA Chesapeake Bay study.	19
3	Euphotic zone chlorophyll <u>a</u> (mg m^{-2}) at stations along the mainstem of the Bay from north (station 32) to south (station 24).	41
4	Primary productivity ($\text{mg C m}^{-2} \text{ d}^{-1}$) and chlorophyll specific [$\text{mg C}(\text{mg Chl} \cdot \text{d})^{-1}$] at stations 1, 3, and 5 of the CHOP-PAX transect.	42
5	Exponential relationships between POC and Chl where r = correlation coefficient and $\text{POC} = a(e)^b \text{chl}$.	44
6	Coefficient of determination (r^2) for power curve fits of C/Chl on Chl where $\text{C/Chl} = a(\text{Chl})^b$.	46
7	Euphotic zone chlorophyll <u>a</u> (mg m^{-2}) at stations along CHOP-PAX transect from west (station 1) to east (station 5).	51
8	Comparison of the means of key bacterial parameters measured during summer conditions in 1984 (cruises 11-18, 8/20/84 to 9/11/84) and in 1985 (cruises 10-13, 7/11/85 to 9/12/85).	152

LIST OF ABBREVIATIONS AND SYMBOLS

ABBREVIATIONS

AA _t -	Amino acid turnover rate
AODC -	Acridine orange direct count
BOD-5 -	Biochemical oxygen demand
CBI -	Chesapeake Bay Institute
Chl -	Chlorophyll a
Chop-Pax -	Choptank-Patuxent transect (transect 2)
D.O. -	Dissolved oxygen
FBOD -	Filtered (dissolved) biochemical oxygen demand
Glu _t -	Glucose turnover rate
N -	Nitrogen
N/P -	Nitrogen to phosphorus ratio
P -	Phosphorus
PBOD -	Particulate biochemical oxygen demand
Phaeop -	Phaeopigments
POC -	Particulate organic carbon
PON -	Particulate organic nitrogen
PP -	Primary production
TCA -	Trichloroacetic acid
TdR -	Thymidine incorporation rate

SYMBOLS

cm -	centimeters
Km/d -	Kilometers per day
L ⁻¹ h ⁻¹ -	Per liter per hour
mgCm ⁻³ d ⁻¹ -	Milligrams of carbon per cubic meter per day
ml -	Milliliters
pmol -	Picomoles
r, r ² -	Correlation coefficient
uCi -	Microcuries
ug/l -	Micrograms per liter
um -	Micrometers

SECTION 1

INTRODUCTION

GENERAL CONSIDERATIONS

The Environmental Protection Agency's Chesapeake Bay Program (CBP) identified oxygen depletion as a major factor contributing to a general decline in water quality and in the capacity of the Bay to support fishery resources. Results of the CBP suggest that seasonal oxygen depletion during spring-summer occurs over the mid-Chesapeake Bay as a consequence of vertical stratification and high rates of heterotrophic metabolism in bottom water and the benthos. It is generally believed that increased nutrient loading from point and nonpoint sources (D'Elia 1982; Taft 1982) has stimulated a set of ecological interactions which have to an interannual increase in the area and volume of water which is depleted in oxygen (Heinle et al. 1980; Taft et al. 1980; Officer et al. 1984). This set of ecological interactions can be summarized as follows:

- 1) the photosynthetic production of organic matter by phytoplankton has increased in response to higher nutrient inputs;
- 2) a significant fraction of this production ultimately accumulates below the pycnocline and below the euphotic zone, especially in the main channel of the Chesapeake Bay between the Chesapeake Bay Bridge and south of the Potomac River;
- 3) this increase in the supply of organic matter, of phytoplankton origin, stimulates the metabolism of heterotrophic organisms in bottom water

and the benthos; and

4) the associated increase in oxygen demand reduces dissolved oxygen levels, which depend on depth and the degree of vertical stratification of the water column.

Annual phytoplankton production has apparently increased in response to higher nutrient supply, a response that also appears to be related more to nitrogen than to phosphorus supply (Boynton et al. 1982). However, several important gaps exist in our understanding of how phytoplankton production is related to seasonal oxygen depletion. These gaps, which are basic to the development of water quality models, include:

1) a lack of understanding of the extent to which time- and space-dependent variations in phytoplankton production of the surface layer, organic input to bottom water, and oxygen depletion are related on scales of days-months and meters-kilometers,

2) how the importance of heterotrophic microorganisms as consumers of organic matter and oxygen vary over similar time and space scales, and

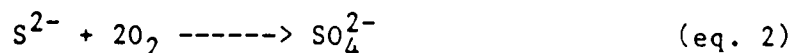
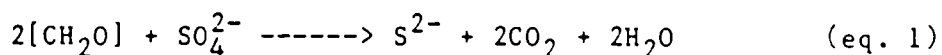
3) the influence of these relationships and environmental factors on the temporal and spatial extent of the oxygen depletion zone.

Relationships among phytoplankton production, accumulations of phytoplankton biomass in deep water, and bacterial production and respiration are of particular importance since the key parameter of oxygen depletion is a shift from phytoplankton-metazoan food webs (low oxygen demand per unit of organic matter metabolized) to phytoplankton-bacterial food webs (high oxygen demand per unit of organic matter metabolized). Naturally-occurring populations of marine bacteria were traditionally understood to be small (100's-

1000's per ml) and the main role of the bacteria was thought to be as decomposers of particulate organic detritus (POC) in sediment (Steele 1974). However, in the last ten years, as a result of several key technological advances, our understanding of the biomass, functioning and roles of marine bacterioplankton has undergone something of a revolution (Hobbie et al. 1977; Fuhrman and Azam 1980; Williams 1981; Azam et al. 1983; Ducklow 1983). It is now generally understood that bacteria constitute a sizable and dynamic pool of living carbon in marine plankton systems. This is especially true in estuarine systems, where primary production and inputs of allochthonous organic matter and inorganic nutrients are high, and where shallow depths, strong stratification and the two-layered estuarine circulation enhance regenerative functions (Ducklow 1982; Wright and Coffin 1984). Bacterioplankton are efficient producers of organic carbon whose production rates commonly range from 10 to 30% of daily photosynthetic production. Thus, in considering the production and fate of POC in marine systems, it is now important to include synoptic studies of the magnitudes and spatial/temporal variability of bacterioplankton biomass, production, and metabolic activity.

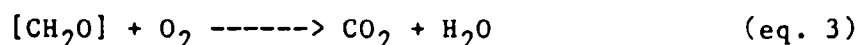
Because few such studies have been performed, we have only a sketchy understanding of the interrelationships among physical forcings, nutrient inputs, primary production, and bacterioplankton secondary production. A system like the Chesapeake Bay, in which primary production is very high, and in which nutrient inputs occur on several scales, presents a useful arena in which to evaluate these interconnections. Furthermore, it is our contention that the knowledge gained is of key significance in understanding the basic physical and biological processes generating and maintaining anoxia in the Bay.

Given that the key biological parameter of oxygen depletion is the consumption of organic material (e.g. phytoplankton carbon) by bacteria, there are two major microbiological processes which contribute to anoxia in Chesapeake Bay. One of these, sulfur cycling, is described by equations 1 and 2.



Equation 1 depicts the mineralization of organic carbon, $[\text{CH}_2\text{O}]$, by sulfate-reducing bacteria, obligately anaerobic microorganisms which use sulfate as an oxidant. The important product of this process is sulfide which is found in the anoxic portion of the water column of the mid-Bay during summer stratification. Oxygen consumption by sulfide (eq. 2) occurs abiologically, but can be microbiologically mediated by sulfur-oxidizing bacteria. The potential for carbon mineralization coupled to microbial sulfate reduction and, thus, sulfide generation and subsequent oxygen consumption is very high in marine and estuarine environments. In mid-Chesapeake Bay deep water and sediments (ca. 15 mM sulfate and 0.3 mM oxygen at saturation), sulfate would have about 100 times the oxidation capacity of oxygen at saturation. Although sulfur cycling was not a topic of investigation in the Sea Grant/EPA study reported herein, its relationship to our results will be discussed briefly in a later section of this report.

The second key microbiological process contributing to anoxia is depicted in equation 3.



This process, in which oxygen is consumed directly during the mineralization

of organic matter by microheterotrophs, has been the focus of the microbiological portion of our 1984-85 studies.

THE 1984 STUDY

In 1984 we investigated phytoplankton-bacterial interactions and distributions in time and space in the mid-Bay region during mid summer-fall when phytoplankton production and microheterotroph activity were at or near their seasonal peaks and when vertical gradients of physical and chemical properties were maximal. The spatial area covered by our 1984 study was bounded by the east and west shores of the Bay and extended about 25 km in a north-south direction centered on the mouth of the Choptank River. The emphasis of our work in 1984 was on event scale variability and on the significance of lateral variation on nutrient-phytoplankton-bacteria-oxygen relationships in the Bay during summer under high flow conditions. Specifically, we addressed the following problems:

1) Is phytoplankton production an important source of organic matter to bottom water under summer conditions?

2) How important is phytoplankton production over the shallow flanks of the main channel relative to local production in the channel per se as a source of organic matter to bottom water under summer conditions?

3) Are heterotrophic microorganisms in the water column important consumers of organic matter and dissolved oxygen and how does their importance vary in relationship to variations in phytoplankton production, organic input to bottom water, and dissolved oxygen?

4) How do variations in vertical water column stratification (mixing) influence these relationships?

Objective 3 included obtaining preliminary answers to these questions:

- 1) What are the levels of bacterial abundance/biomass and how do these vary vertically and horizontally over various time scales?
- 2) Does this variability correspond to variations in the distributions of temperature, salinity, chlorophyll, and nutrients?
- 3) What is the magnitude of bacterial production relative to primary production, and how does this vary?
- 4) Do bacterial abundance and production covary with other estimates of microheterotrophic processes (amino acid uptake and respiration and oxygen utilization)?
- 5) From the answers to these questions, what can we conclude regarding a) the mechanisms regulating variability in bacterial biomass and b) the significance of bacterioplankton metabolism in maintaining anoxia?

The major findings of our 1984 effort have been discussed in detail by Tuttle et al. (1985). These findings were as follows:

- 1) Variations in the dissolved oxygen content of mid-Chesapeake Bay bottom water were much greater than expected on the basis of vertical stratification arguments. Several east to west and west to east tilts of the halocline were observed between 1 July and 2 November. The mean cross-Bay tilt of the halocline was up to the west, resulting in the presence of nutrient-rich, oxygen-depleted water at shallower depths along the western shore than along the eastern shore. Halocline tilting events were associated in the summer with the intrusion of anoxic water and hydrogen sulfide into shallow waters of the western flank.

- 2) Low dissolved oxygen bottom water was not restricted to the well-stratified summer months. Oxygen depletion was also observed during October

due to restratification following vertical mixing events in September.

3) Variations in the particulate organic content of bottom water were largely due to inputs of phytoplankton biomass and phytodetritus. The extent and persistence of anoxia and low dissolved oxygen levels below the halocline during summer probably depends upon this input.

4) The heterotrophic bacterial response to reoxygenation of bottom water was rapid, with high rates of oxygen consumption even at low oxygen tension. The rapidity of this response likely contributes to the maintenance of low dissolved oxygen under summer conditions.

5) Phytoplankton productivity did not appear to be nutrient limited, although transient phosphorus limitation might have occurred. N:P ratios indicated that P would have been depleted before N, contrary to past observations which indicate that N is most likely to be limiting during summer.

6) Lateral variations normal to the main axis of the Bay were large and dominated the nutrient-phytoplankton-oxygen dynamics under stratified summer conditions. Thus, seasonal patterns of variation in phytoplankton productivity based on measurements over the channel down the main axis of the Bay are probably not representative of most of the Bay's area.

7) Microheterotrophs were present at the highest sustained cell densities so far observed in a marine environment throughout the study period, especially during summer stratification and following restratification of the Bay in October. Bacterial biomass appeared to be most closely coupled to chlorophyll concentrations during stratification events.

8) Bacterial production and metabolic activity were indicative of the large bacterial biomass. Thus, the bacterial population remained highly

active throughout the study period.

9) Variations in bacterial biomass, production, and metabolic activity were related to chlorophyll, particularly below the euphotic zone. This supports our hypothesis that phytoplankton or phytodetritus provide the major source of organic carbon for bacterial growth and respiration in the water column during summer and fall.

10) For a portion of the study period, especially during partial fall stratification, microheterotrophs were the dominant organisms causing oxygen depletion in the mid-Bay. Based upon direct measurement of oxygen consumption, estimates of oxygen consumption from heterotrophic bacterial production, and net rates of oxygen consumption calculated during the restratification events, water column oxygen consumption over the late summer and fall at least equals the contribution of sediment oxygen demand.

THE 1985 STUDY

In 1984 we found few differences in physical, chemical, and biological parameters within the north-south boundaries of the study area. Accordingly, we extended spatial coverage by moving the northern-most of three lateral transects to just south of the Chesapeake Bay Bridge at Annapolis and the southern-most of the transects to just north of the mouth of the Patuxent River. The locations of these transects are shown in Figure 1. In addition, we added several deep channel stations between the transects. These changes provided north to south coverage of about 80 km and afforded us the opportunity to follow the development of low oxygen conditions in the north-south direction. The cross-Bay transect off the mouth of the Choptank was retained for the purpose of comparisons between 1984 and 1985. Assessment of

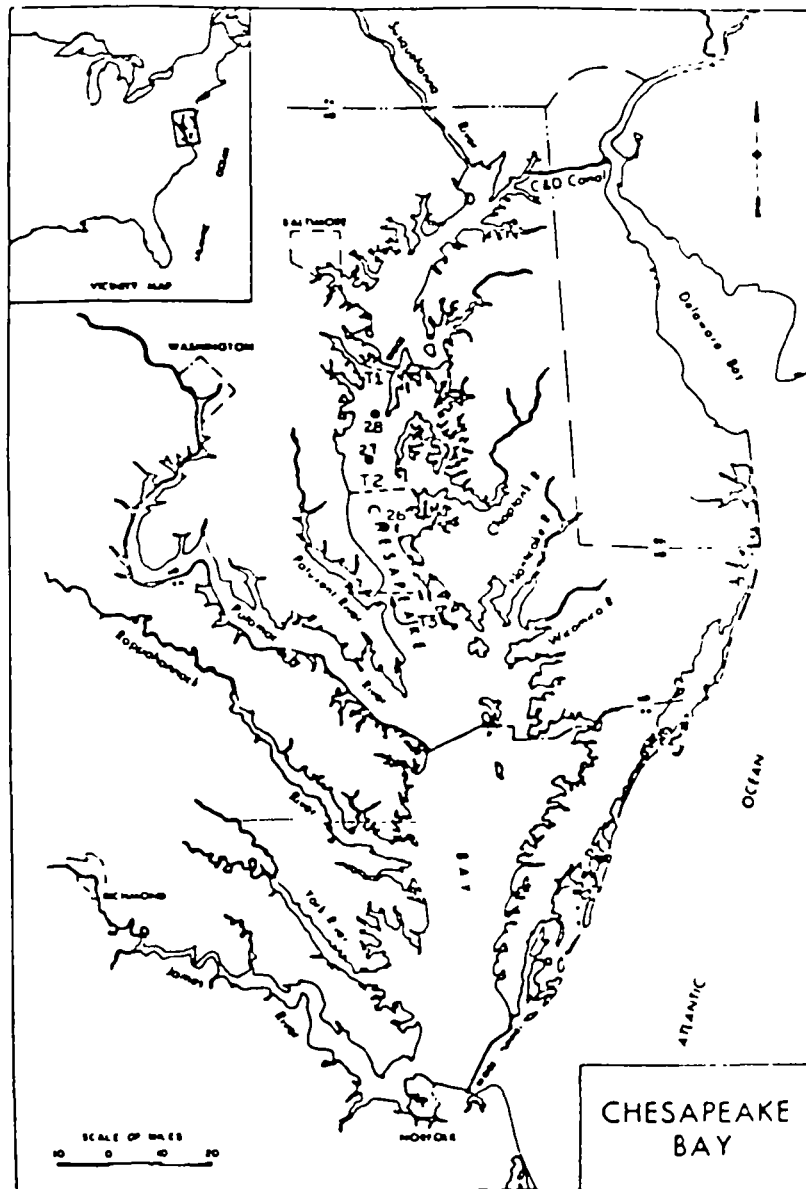


Figure 1. Site map of Chesapeake Bay illustrating transect (T1, T2, T3) locations (---) and additional deep channel stations (●) occupied during the 1985 study.

cross-Bay variability was enhanced in that stations at all three transects were occupied on every cruise.

Due to funding limitations, however, the frequency of cruises had to be limited in 1985. Whereas our 1984 work emphasized event scale variability (many of the cruises were spaced 3-4 days apart), our 1985 study focused on seasonal variations over the period February to October. We placed particular emphasis on the late spring (15 May-19 June) by making five of our 14 cruises during the time period at which we expected summer conditions to become established.

The same parameters measured in 1984 were also determined in 1985. However, on many of the cruises we added measurements of BOD-5 and bacterial glucose metabolism in an effort to increase our understanding of the relationship of carbon flow from phytoplankton to microheterotrophs which results in oxygen consumption. This report also contains a comparison of 1984-1985 during summer conditions. In this comparison we emphasize interactions among freshwater flow, vertical stability, phytoplankton production, bacterial production and metabolism, oxygen consumption, and dissolved oxygen regime.

SECTION 2

CONCLUSIONS

1. Phytoplankton production during February - May generates a quantity of organic matter more than adequate to cause oxygen decline which occurs annually during the spring in mid-Bay deep waters.

2. The development of the summer maximum in phytoplankton productivity in the mesohaline region of Chesapeake Bay seems to depend upon the regeneration of nutrients based upon phytoplankton carbon produced in the spring which sinks into the deep water and is remineralized by bacteria. These nutrients are recycled into the euphotic zone as a consequence of vertical mixing and oscillations of the pycnocline. This is contrary to the hypothesis that there is an interannual carry over of phytodetritus which fuels oxygen depletion in the Bay (Taft et al. 1980).

3. Phytoplankton growth rates in 1984 and 1985 were not limited by either N or P on a seasonal time scale. This is somewhat surprising since 1985 was a low flow year which should mean that inputs of new nutrients to the Bay were lower than in high flow years such as 1984. If this is the case, substantial reductions in nutrient inputs will be required to significantly decrease phytoplankton production in the Bay.

4. Phytoplankton biomass during summer 1985 was greatly decreased compared to 1984 even though phytoplankton production was similar in both years. This suggests that phytoplankton production was more closely coupled with zooplankton grazing in 1985 than in 1984.

5. Bacterial biomass, production, and metabolism are tightly coupled to phytoplankton production in the Bay, especially during summer conditions. Phytodetritus is the source of carbon fueling bacterial oxygen consumption in Bay deep waters.

6. Carbon utilizable by bacteria, measured as biochemical oxygen demand, shifts abruptly from POC to DOC in the late spring, particularly below the euphotic zone. This condition persists throughout the summer and supports our contention that spring phytoplankton production can support summer bacterial metabolism, nutrient regeneration, and oxygen consumption in Bay deep waters.

7. Carbohydrates rather than amino acids may be the preferred source of carbon and energy for bacterial metabolism and production.

8. Despite a significant reduction in phytoplankton biomass in summer 1985 compared to summer 1984, bacterial biomass and amino acid metabolism were similar both years under summer conditions and bacterial production in 1985 was higher. This and the fact the summer mean oxygen consumption rates below the euphotic zone were nearly identical in 1984 and 1985 indicate that increased reoxygenation of the deep water in 1985, not decreased bacterial activity, was responsible for the lack of widespread anoxia.

9. Very high bacterial standing crops were found during the summer in both years despite great differences in climatic conditions and water column stability. This suggests that fundamental changes have occurred in the ecosystem of mesohaline Chesapeake Bay over the years such that a significant portion of primary production is channeled into bacterial production.

10. The potential for the establishment of anoxia tends to be greatest

in the northern regions of the mesohaline Chesapeake Bay. This conclusion is supported by the findings of greater bacterial biomass and production as well as greater BOD near the Chesapeake Bay Bridge than near the mouth of the Patuxent River.

11. Biological parameters exhibit greater variation in an east to west than in a north to south direction. This implies that concentrating monitoring or research efforts in the mesohaline portion of the Bay over wide areas from north to south is unnecessary other than for the purpose of delineating the extent of anoxia in any given year.

12. Water column oxygen consumption by microheterotrophs is a major contributor to the development of anoxia, particularly during the spring and the early summer. Later in the summer, sulfur cycling becomes an important mechanism for maintaining anoxia.

SECTION 3

RECOMMENDATIONS

FURTHER RESEARCH

Our 1984 investigations focused on event scale variability with cruises spaced at 3 to 4-day intervals during the period of summer conditions. In contrast, the 1985 study emphasized seasonal differences. While the greatly different anoxic regimes which existed in 1984 and 1985 were fortuitous for comparing year to year variability, two summer seasons of research (our 1984 summer work lasted less than one month) are insufficient to fully understand the dynamics of oxygen depletion. We conclude that additional crucial information could be obtained from a spring-summer study in which measurements are made at or near the time intervals of the 1984 investigation.

Additional data are also needed to quantitatively assess the contribution of benthic and pelagic processes to oxygen depletion on both seasonal and event scales. So far there has not been close enough coordination of benthic and water column studies with relevance to the dynamics of the establishment and maintenance of anoxia. It would be particularly useful to be able to relate benthic and water column oxygen consumption and bacterial activity with phytoplankton dynamics and carbon flow over short time intervals.

Our research has demonstrated that a tight coupling exists between phytoplankton and heterotrophic bacteria (and, thus, oxygen consumption) in the mid-Chesapeake Bay. However, a major question which remains is whether

the tributaries significantly influence mainstem water quality, whether the mainstem affects the tributaries, or whether the two act independently. It is also not known whether the trophic state of the tributaries is similar to that of the mesohaline mainstem. The answer to this question is crucial to the effective apportionment of limited resources between tributary and mainstem restoration efforts. One approach to this question would be to compare water quality characteristics, phytoplankton/bacterial coupling, and sulfur cycling in one or more of the tributaries emptying into the mid-Bay with the adjacent mainstem.

The results of our work suggest that there has been a major shift in the food web structure of the Chesapeake Bay ecosystem. During spring and summer, phytoplankton production is consumed to a significant degree not by grazers or filter feeders but rather by free-living bacteria in the water column. Several factors, including nutrient enrichment, might be responsible for such a shift. However, a key one could be the decline in populations of filter feeding benthic animals such as oysters and clams caused by exposure to hypoxic or anoxic waters, other detrimental water quality conditions, disease, and over harvesting. For example, estimates suggest that the Bay's oyster population may now be four million bushels or less compared to 80 million bushes in 1985 (Schneider 1987). Thus, a major removal mechanism for phytoplankton biomass has been nearly eliminated from large areas of the Bay. If it can be demonstrated through additional research that increased bivalve populations could play an important role in removing phytoplankton and, by removing this organic carbon source, decrease bacterial biomass and oxygen consumption, the result could lead to major savings in the cost of restoring

Bay water quality as well as revitalizing the shellfish industry.

MANAGEMENT

Our findings impact the design of monitoring regimes to evaluate the influence of abatement procedures on the health of the Bay in general and on anoxia in particular. During the summer, biological parameters are surprisingly consistent over the 80 km north to south boundaries of the 1985 study area. We conclude that monitoring efforts, at least during the summer period, could be restricted to very few sampling stations with emphasis placed on event scale changes and east to west variability. The latter is particularly important with regard to assessment of phytoplankton production.

Secondly, we have demonstrated that a key feature of summer conditions in the mesohaline portion of Chesapeake Bay is the establishment of large standing crops of bacteria. We have further shown that the magnitude of bacterial abundance can be used to predict oxygen consumption. Therefore, we recommend that measurements of bacterial abundance be included in the Bay monitoring program. Data gained from these measurements will not only permit a rapid and technically simple determination of oxygen consumption rates but will also provide an indicator of Bay health, i.e. decreasing bacterial abundances over the summer should be indicative of improved water quality in the Bay and a desirable change in the Bay ecosystem.

SECTION 4

MATERIALS, METHODS AND EXPERIMENTAL PROCEDURES

CRUISE SCHEDULE AND STATION DESCRIPTIONS

Sixteen stations were occupied during the course of the 1985 Maryland Sea Grant/EPA study. Transect 1 consisted of three stations extending from west to east just south of the Bay Bridge (Table 1, Fig. 1). Transects 2 and 3 consisted of five stations each extending west to east from Dares Beach to Hills Point and just north of the mouth of the Patuxent River, respectively. Three additional stations were occupied along the deep channel and formed with stations SG3, SG24, and SG32 a six-station deep channel transect in a north-south direction. The correspondence of 1985 stations with stations occupied during our 1984 EPA study is indicated in Table 1. A total of fourteen two-day cruises were conducted between 02-12-85 and 10-11-85 (Table 2). Either the RV Orion, 52-ft. overall, or the RV Aquarius, 68-ft. overall, was used for each of the cruises.

SAMPLE COLLECTION

Water samples were collected with a submersible well pump connected to a hose which was lowered to the desired sampling depth. No detectable differences in physical or biological parameters could be detected when pump supplied water was compared to in situ measurements or to water collected in submersible sample bottles. This pump system is the standard water collection procedure about the UMCEES research fleet. Use of the pump system

Table 1. Station locations for 1985 Sea Grant/EPA Chesapeake Bay study.

Corresponding 1984 station numbers in parentheses.

Station	Transect #	Latitude	Longitude	Description
SG1 (CP1)	2	38° 33.50'N	76° 29.60'W	Dares Beach
SG2 (CP2)	2	38° 33.52'N	76° 27.50'W	
SG3 (CP3)	2	38° 33.57'N	76° 26.34'W	
SG4 (CP4)	2	38° 33.54'N	76° 22.50'W	
SG5 (CP5)	2	38° 33.52'N	76° 20.50'W	Hills Point
SG21	3	38° 19.78'N	76° 24.21'W	Patuxent River
SG22	3	38° 19.94'N	76° 21.64'W	
SG23	3	38° 20.20'N	76° 20.20'W	
SG24	3	38° 20.60'N	76° 18.37'W	
SG25	3	38° 20.92'N	76° 17.86'W	Barren Island
SG26 (CP7)	-	38° 28.45'N	76° 23.25'W	
SG27 (CP13)	-	38° 41.00'N	76° 25.50'W	
SG28	-	38° 50.07'N	76° 24.20'W	
SG31	1	38° 59.25'N	76° 23.80'W	Bay Bridge
SG32	1	38° 58.85'N	76° 21.89'W	
SG33	1	38° 58.69'N	76° 21.20'W	Bay Bridge
SG24B*	3	38° 20.67'N	76° 18.40'W	
SG25B*	3	38° 20.90'N	76° 17.85'W	

*Stations replaced SG24 and SG25 on some cruises.

Table 2. Cruise dates and descriptions for Sea Grant/EPA Chesapeake Bay study.

Cruise Number	Funding Agency	Date	Stations Occupied
SGB1	NOAA	02-12&13-85	all
SGB2	NOAA	03-21&22-85	all+SG3&24 repeated
SGB3	NOAA	04-16&17-85	all+SG3&24 repeated
SGB4	NOAA	04-29&30-85	all+SG3&24 repeated
SGB5	NOAA	05-16&17-85	all+SG3&24 repeated
SGB6	NOAA	05-23&24-85	all+SG3&24 repeated
SGB7	NOAA	05-28&29-85	all+SG3&24 repeated
SGB8	NOAA	06-06&07-85	all+SG3&24 repeated
SGB9	NOAA	06-19&20-85	all+SG3&24 repeated
SGB10	NOAA	07-11&12-85	all+SG3&24 repeated
SGB11	EPA	07-19&20-85	all+SG3&24 repeated
SGB12	EPA	08-15&16-85	all+SG3&24 repeated
SGB13	EPA	09-11&12-85	all+SG3 repeated
SGB14	EPA	10-10&11-85	all+SG3&24 repeated

greatly increased the speed of sampling compared to bottle sampling methods so that more discrete samples could be taken. Thus, vertical water column profiles could be described in greater detail than otherwise possible. In addition, physical water quality parameters could be analyzed in real time so that samples for nutrients and biological measurements were taken from the most appropriate depths. As the water from a sampled depth was pumped aboard it was either collected directly into sample containers or in polypropylene buckets from which samples were taken.

DETERMINATION OF PARAMETERS

Physical Water Quality Parameters

Water depth was determined with an onboard sonar-type depth finder and was confirmed by hydrographic wire depth. Secchi disk depth was determined with a 12-inch diameter black and white, weighted disk attached to a line calibrated at 10 cm intervals. Temperature and dissolved oxygen were determined using a YSI Model 57 (Yellow Springs Instrument Co.) digital dissolved oxygen meter and salinity with a YSI Model 33 salinity meter. The dissolved oxygen and salinity probes were usually submerged in containers through which the pump Bay water circulated. At selected depths at certain stations, dissolved oxygen concentrations were also determined by the CBI microwinkler method (Carpenter 1965).

Particulate Organic Carbon (POC), Nitrogen (PON), and Nutrient Determinations

Particulate organic carbon and nitrogen were measured by combustion. Fifty to 100 ml of sample were filtered through pre-combusted GF/F glass fiber filters and frozen. Upon returning to the laboratory, the filters were thawed and analyzed with a Perkin-Elmer Model 240B elemental analyzer.

Filtrates were collected and frozen for measurements of dissolved inorganic nutrients (phosphate, nitrate, nitrite, ammonium). Nutrient concentrations were determined colorimetrically using a Technicon autoanalyzer and standard procedures.

Phytoplankton Pigments and Cell Densities

Chlorophyll a and phaeopigment concentrations were measured by fluorometry. Fifty to 100 ml of sample were filtered through GF/F glass fiber filters and frozen. Upon returning to the laboratory, the filters were thawed, and pigments were extracted by grinding the filters in 90% acetone. Fluorescence of the extracts was measured before and after acidification with 10% HCl using a Turner Designs fluorometer.

Phytoplankton cell densities were determined by the inverted microscope technique. Samples were preserved with Lugol's solution and returned to the laboratory for enumeration with an inverted microscope after concentrating cells by settling for at least 48 hours.

Photosynthetic Production

The photosynthetic production of organic matter by phytoplankton was measured by the ^{14}C technique at stations 1, 3, and 5 of transect 2. Primary productivity was calculated from ^{14}C assimilation during 24-h incubations under natural light conditions. Samples were inoculated with 5 μCi of $\text{NaH}^{14}\text{CO}_3$ and incubated at surface water temperature under light levels of 100%, 50%, 22%, and 5% of incident radiation. Incubations were terminated by filtration through a GF/F glass fiber filter. Filters were fumed over HCl, placed in scintillation vials with 10 ml of Ready-Solv and counted with a Packard Tri-Carb Model 461C liquid scintillation spectrometer. Productivity

was calculated for each light level ($\text{mg C m}^{-3} \text{ d}^{-1}$). Given the shallow depth of the euphotic zone, PP-Irradiance curves (PP vs. % light) were determined using a surface sample only. Integrated euphotic zone production was estimated from vertical Chl profiles, % light depths and PP/Chl (from the PP-Irradiance curves).

Microbial Metabolism and Secondary Production Dual Label Technique

Natural rates of microbial amino acid and glucose metabolism were determined using modifications of the methods suggested by Williams and Askew (1968) and Williams et al. (1976). A mixture of 15 carbon-14 radio-labeled amino acids (ICN Corp., product #10147), an algal protein surrogate, and tritiated glucose (ICN Corp., product #27020) were used. Bacterial production was determined using modifications of the method suggested by Fuhrman and Azam (1980, 1982). Tritiated methyl-thymidine (ICN Corp., product #24060) was used in this case. Amino acid metabolism and bacterial productions were determined simultaneously (as were amino acid metabolism and glucose metabolism) using a dual label technique in which both substrates were added to the individual samples.

The incubation containers for this determination were acid washed, all polyethylene/polypropylene 10 ml syringes (Aldrich Chemical Co.) fitted with gas-tight caps. The syringes were filled from a bucket which was continually flushed with the pumped Bay water from the sampled depth. They were then capped and transferred to a dark incubation box in which the in situ temperature was maintained. Four syringes were filled with 10 ml of water from each sampled depth. Metabolic activity in one of the four syringes was stopped by addition of 100 μl of 1.2N H_2SO_4 . This was the abiotic control.

The remaining syringes were used for triplicate live incubations.

Each of the 10-ml samples was inoculated with 56.2 nanograms (nominally) of the ^{14}C amino acid mixture, and 5 picomoles of ^3H -glucose or 50 picomoles (nominally) of ^3H methyl-thymidine, and then incubated in the dark for exactly 30 min. The samples were then filtered (0.2 μm pore size membrane) and rinsed with 4 ml of 5% ice cold TCA (trichloroacetic acid). Each membrane filter was then placed in a Filmware bag (Nalge Co.); 5 ml of Scintiverse (Fisher Chemical Co.) was added, and the bag heat sealed.

Liquid scintillation spectrometry was used to quantitate the ^{14}C and ^3H simultaneously in each of the samples. Packard Model 4430 or 4530 Scintillation counters set for $^3\text{H}/^{14}\text{C}$ dual label counting were used for this quantitation. The turnover rates for the in situ amino acid and glucose pools were calculated from the assimilation rates for ^{14}C or ^3H . Bacterioplankton production was calculated from the amount of TCA insoluble, particle-associated ^3H thymidine.

Microbial Production - Single Label Technique

^3H -thymidine incorporation was also measured according to the method described by Ducklow (1982). The concentration of added thymidine was 5 nM. This method differed from the dual label technique in the following ways: only ^3H thymidine was added to duplicate samples and 30 ml samples were incubated in plastic bottles containing an air phase. Thus, these experiments were done at air saturation whereas the dual label experiments in which the sample syringes were completely filled to exclude air were done at ambient D.O. Comparison of results obtained by both methods was intended to determine whether possible low measured incorporation rates at low ambient D.O. were due to oxygen deprivation. Comparison of results at high ambient

D.O. served as an intercalibration control. Preliminary experiments indicated that the use of dual labels had no appreciable effect upon ^3H -thymidine incorporation rates.

Bacterial Biomass

Bacterial concentration was estimated by direct microscopic observation of acridine orange-stained bacteria under epifluorescent illumination (Hobbie et al. 1977). Ten milliliter, raw water samples were collected, placed in particle-free screw-capped glass tubes, and preserved with 0.75 ml of particle-free 37% formaldehyde. These samples were held at 4°C until enumerated. The enumeration technique was essentially that of Hobbie et al. (1977). One milliliter Bay water samples were mixed with 1.0 ml of particle-free Bay water in particle-free vials. These samples were then stained with 20 μl of 0.01%, particle-free acridine orange for about 4 minutes. Particles, including the bacteria, were collected on 0.2 μ porosity, Irgalan Black (Ceiba Geigy Corp.) stained, Nuclepore polycarbonate filters. The filters were washed twice with a total of about 3 ml of particle-free Bay water, and were observed under epifluorescent illumination using a Leitz Ortholux microscope at 1562x total magnification. Five randomly selected fields were observed, and all bacterial cells within a 10x10 eyepiece grid were counted. The mean of the five counts was used to calculate the total bacterial concentration in the original water sample.

In many cases, AODC counts were also done according to the method of Ducklow (1982). This technique differed from that described above chiefly in that 10 rather than 5 fields were examined. Comparison of counts in the same samples done by both methods afforded an intercalibration control.

Microbial Oxygen Consumption

Microbial oxygen consumption rates in the water column were determined from short-term changes in the oxygen concentration of enclosed water samples incubated in the dark at in situ temperatures. At each depth where these samples were taken four, acid washed, 125 ml ground glass-stoppered bottles were filled with water essentially as described in the Microbial Metabolism section above. Care was taken to be sure that no air bubbles were trapped in the bottles. Oxygen in one of these bottles was immediately fixed as described in the CBI microwinkler method. The remaining three were incubated at in situ temperature in light-tight containers for 6 hours after which the oxygen in those bottles was also fixed. Oxygen concentrations were determined by the microwinkler titration as described by Carpenter (1965). Dark oxygen consumption was determined from the difference between the oxygen concentration at the time of collection and that present after 6 hours of incubation.

Biochemical Oxygen Demand (BOD-5)

Biochemical oxygen demand was determined from changes in oxygen concentration in samples incubated in the dark at 20°C for 5 days. The samples were collected and oxygen concentration determined as described in the Microbial Oxygen Consumption section. BOD-5 measurements were done in duplicate and compared to immediately fixed samples when probe-determined D.O. exceeded 4 mg/l. When D.O. was <4 mg/l, 1-liter samples were collected and shaken to increase the initial oxygen concentration. In this case, the initial D.O. of the shaken sample was determined for comparison to duplicate shaken samples incubated for 5 days.

At selected stations, filtered BOD-5 determinations were also made. In this case, freshly collected water was filtered through Gelman type A/E glass fiber filters at <7 in. Hg. The filtrates were shaken, and the water dispensed into ground, glass-stoppered bottles.

SECTION 5

RESULTS

THE 1985 ANNUAL CYCLE-HYDROGRAPHY, NUTRIENTS, PHYTOPLANKTON

Hydrography

Seasonal variations in the vertical distributions of temperature and salinity were generally typical of partially stratified estuaries located in temperate latitudes. Surface temperature increased from less than 1°C in February to 26°C in August (Fig. 2). The rate of increase was greatest in May when surface temperature increased by 8°C from ca. 11°C at the beginning of the month to ca. 19°C by the beginning of June. A thermocline developed during April and persisted through August. Vertical stratification in the salinity field was observed throughout the study period but was strongest during April-August (Fig. 3). The effect of the spring freshet was observed during April with a time lag of 1-2 weeks between the northern most deep station (32) and the southern most deep station (24) which gives a mean drift of ca. 6 km/d. Large intrusions of high salinity bottom water occurred during April-May and again during July-August.

These patterns were reflected in the density field (Fig. 4). Like salinity, density stratification was observed throughout the study period. Density gradients across the pycnocline ranged from 0.12 to 1.24 sigma-t/m and generally decreased downstream from north to south. Peaks in the density gradient across the pycnocline occurred during April and early May

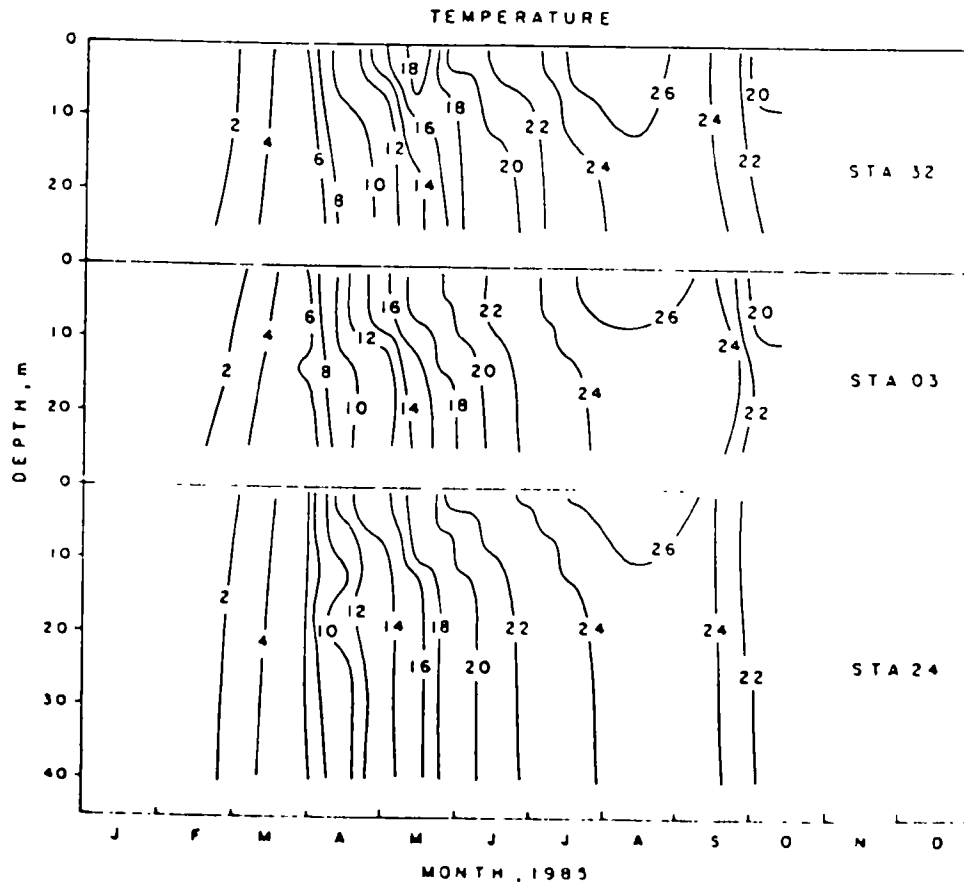


Figure 2. Temporal variations in the vertical distribution of temperature.

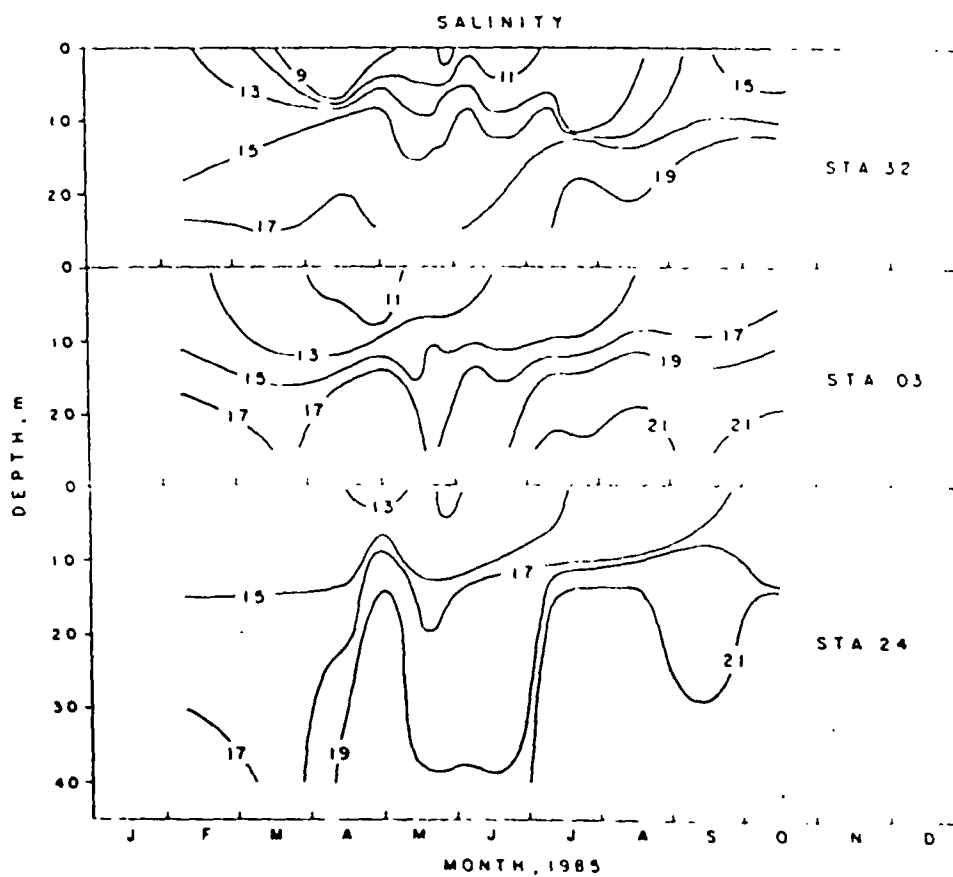


Figure 3. Temporal variations in the vertical distribution of salinity.

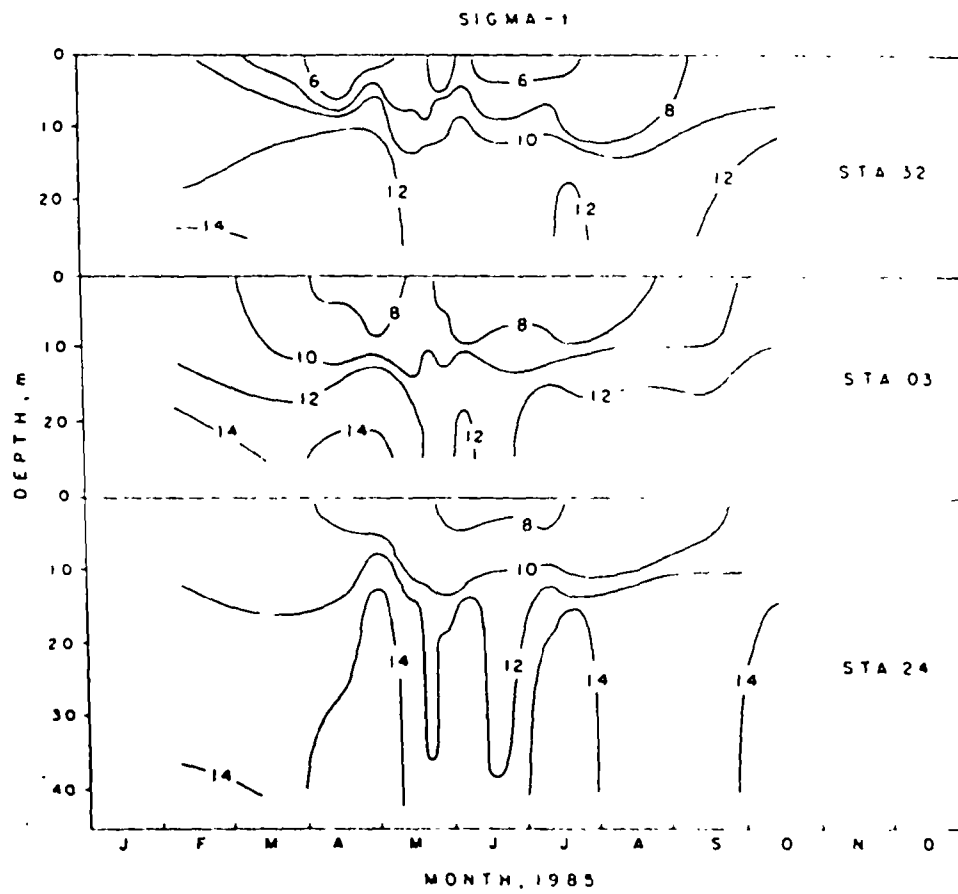


Figure 4. Temporal variations in the vertical distribution of sigma-t.

as a consequence of the spring freshet and during July-August as a consequence of surface warming and the intrusion of high salinity bottom water.

Dissolved Inorganic Nutrients

To a first approximation, distributions of nutrients were related to salinity and to vertical stratification (Figs. 5-7). Nitrate concentration was highest in the surface layer and decreased across the halocline. Maximum concentration occurred in the surface layer in association with the spring freshet. Concentration minima occurred in the bottom layer in association with intrusions of high salinity water. In contrast, ammonium and phosphate tended to increase with depth and salinity with maximum concentrations occurring in the bottom layer during late summer (Figs. 6 and 7).

N/P (nitrate + nitrite + ammonium)/phosphate) was generally high (Fig. 8), indicating that P would become limiting to phytoplankton growth before N. However, the continued presence of these nutrients in the surface layer suggest that phytoplankton growth was not nutrient limited during 1985. The shift in the frequency distribution from a peak in the 60-120 range during March-May to a peak in the 15-30 range during May-October (Fig. 8) probably reflects the combined effects of high nitrate supply during the spring freshet, low nitrate supply during summer due to low fresh water runoff, and nutrient regeneration during summer with phosphate being recycled more rapidly than ammonium.

Dissolved Oxygen

The concentration of dissolved oxygen in bottom water decreased most rapidly during winter-spring to less than 2 mg/l in May (Fig. 9). Concentrations were lowest at the northern most station and increased toward the

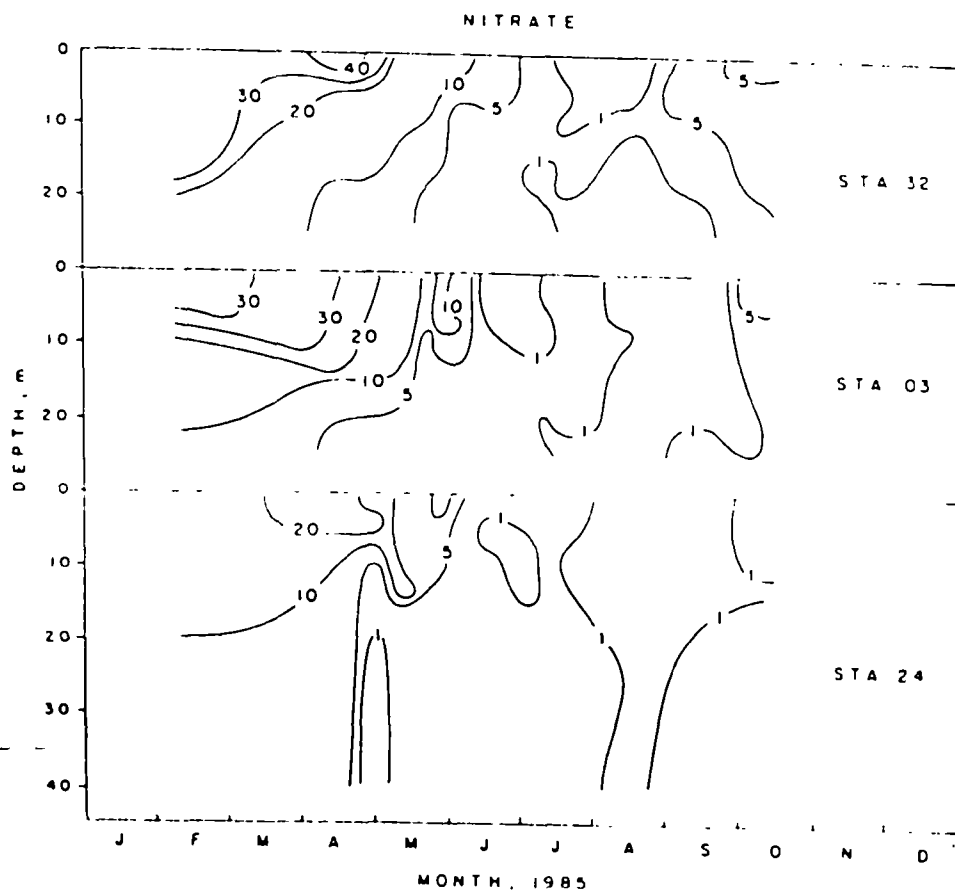


Figure 5. Temporal variations in the vertical distribution of nitrate (μM).

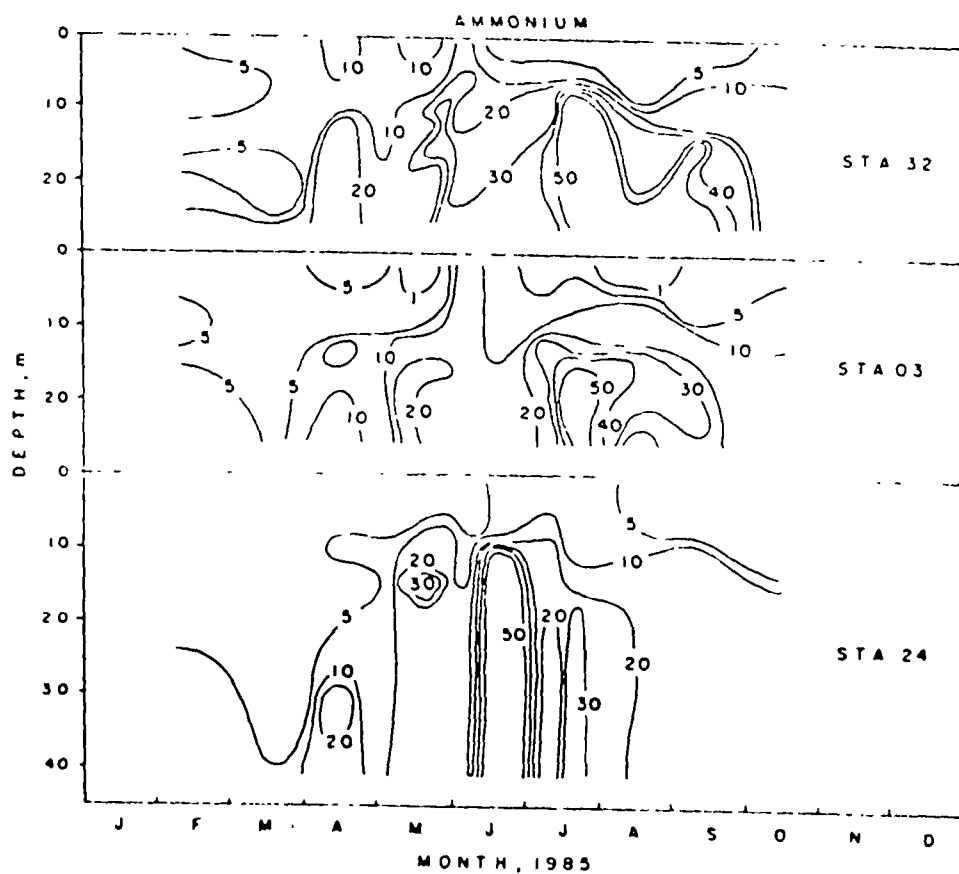


Figure 6. Temporal variations in the vertical distribution of ammonium (μM).

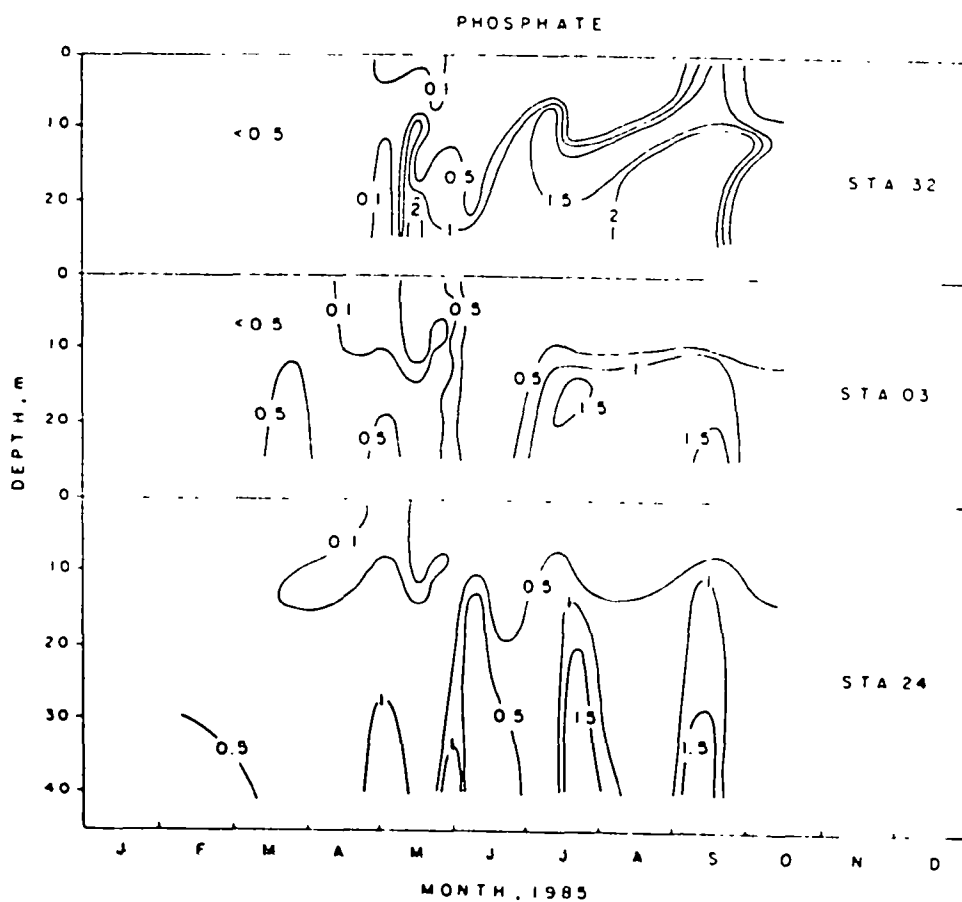


Figure 7. Temporal variations in the vertical distribution of phosphate (μM).

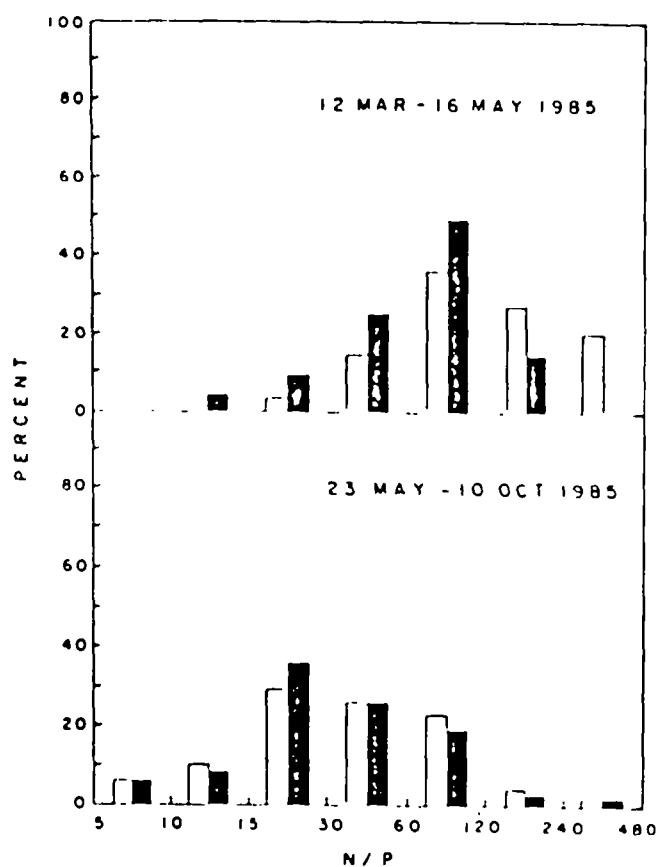


Figure 8. Frequency distributions of the atomic ratio of dissolved inorganic nitrogen (nitrate + nitrite + ammonium) to dissolved inorganic phosphorus (orthophosphate); open bars - surface, solid bars - near bottom.

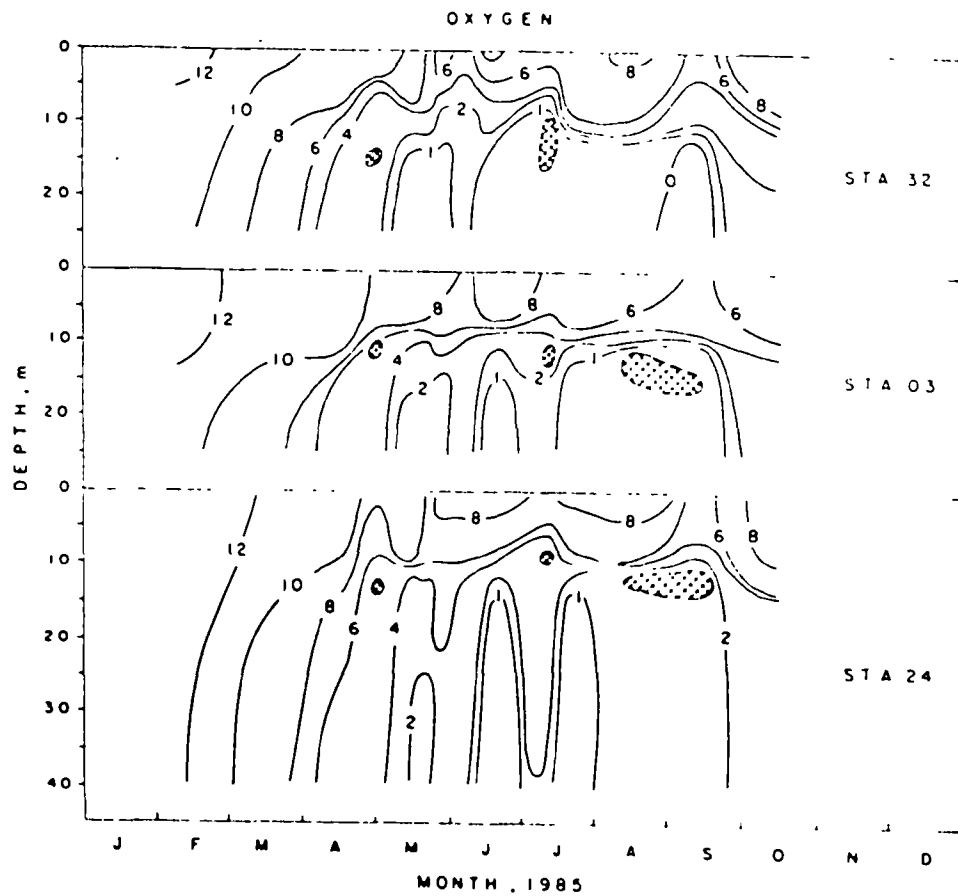


Figure 9. Temporal variations in the vertical distribution of dissolved oxygen (mg/l); hatched areas indicate locations of mid-depth oxygen minima.

mouth of the Bay. The rate of decline during February-May was 0.1 mg/l/d at all stations over the mid-Bay channel. This rate is equal to the rate of decline reported by Taft et al. (1980) and to that calculated by Officer et al. (1984). We emphasize that rate of oxygen decline determined here is the net rate of decline over a period of several weeks. It includes both oxygen consumption and re-aeration processes. Short-term oxygen consumption (respiration) measurements discussed later in this report are estimates of gross oxygen consumption and are not influenced by physical re-aeration processes. Thus, the short-term measurements will give rates of oxygen consumption higher than the net rates considered here.

Hypoxia was maintained from May through September, but anoxia was observed only during late summer at the northern most station. The oxygen content of bottom water did not remain uniformly low during this period but exhibited alternating periods of oxygen depletion and partial re-aeration, a pattern which became more pronounced with distance to the south of station 32 (Fig. 9). Distributions of the dissolved oxygen indicate that oxygen depletion occurs as bottom water moves up the Bay (e.g. Fig. 10) and that the tendency for re-aeration increases south of station 32.

Oxygen minimum zones were occasionally observed in the pycnocline (Fig. 9), a phenomenon that probably reflects the entrainment of oxygen depleted bottom water into the surface layer and subsequent transport downstream (Fig. 10). High rates of heterotrophic metabolism in the pycnocline may also contribute to the development of these oxygen minima (see section on microbial activity).

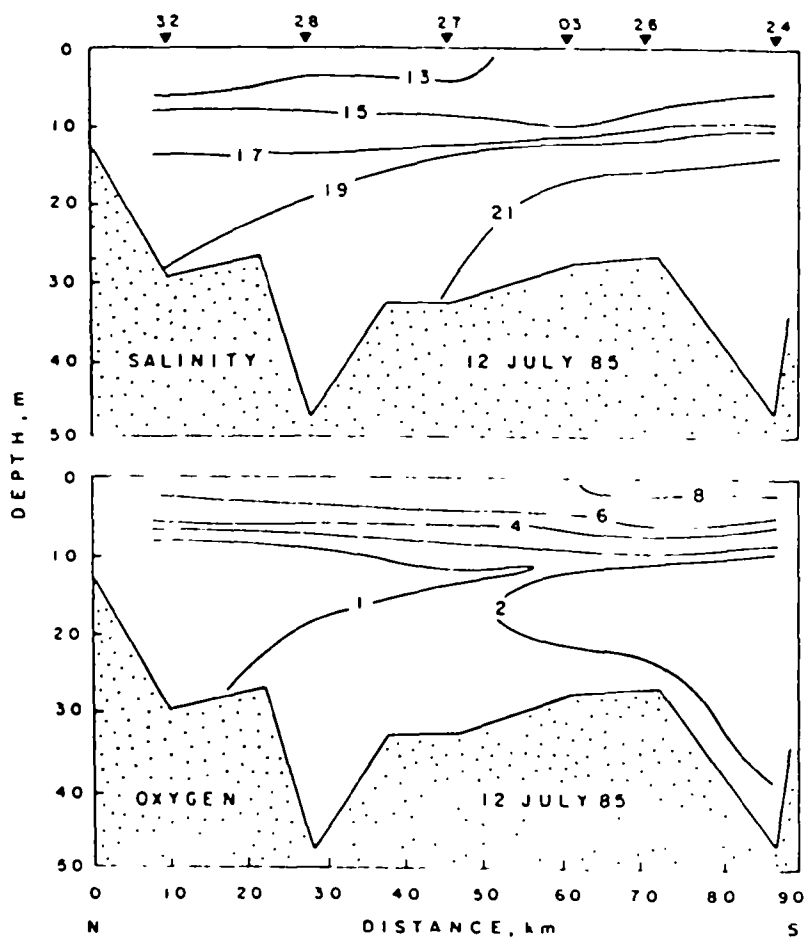


Figure 10. Variations in the vertical distributions of salinity and dissolved oxygen along the mainstem transect on cruise 10. Station numbers are indicated by closed triangles at top.

Phytoplankton Biomass and Productivity

Phytoplankton biomass, as indicated by the concentration of chlorophyll-a (Chl), was high throughout the water column during February-May (Fig. 11) when the Chl content of the euphotic zone (confined to the surface layer or the upper 3-9m of the water column at all times and places) was generally greater than 100 mg/m^2 (Table 3). The Chl content of the water column ranged between 200 and 2200 mg/m^2 and averaged 800 g/m^2 through 16 May. Within 7 days Chl decreased dramatically to a mean of 161 mg/m^2 (88 to 264 mg/m^2 on 23 May). Most Chl was confined to the surface layer during the remainder of the study.

This rapid decline in phytoplankton biomass coincided with 1) a marked decrease in the proportion of Chl accounted for by netplankton ($>20 \text{ um}$), 2) decreases in both phytoplankton productivity (PP) and chlorophyll specific productivity (PP/Chl), and 3) a decrease in the proportion of particulate organic carbon (POC) accounted for by phytoplankton. Prior to 23 May, netplankton accounted for 22 to 59% (mean=37%) of Chl compared to less than 10% after the collapse. Dominant netplankton during this period of high Chl included the diatoms Cerataulina pelagica, Leptocylindricus daquicus, Rhizosolenia fragillissima, Skeletonema costatus, Thalassionema nitzschioides, and Thalassiosira sp. and the dinoflagellates Prorocentrum spp. The nanoplankton ($<20 \text{ um}$) were dominated by cyanobacteria, microflagellates, small centric diatoms and cryptophytes throughout the study period.

Phytoplankton productivity (PP) at station 3 on the mainstem transect averaged $1200 \text{ mg C/m}^2/\text{d}$ during April and early May (Table 4). PP/Chl averaged $6 \text{ mg C}/(\text{mg Chl} \times \text{d})$ during this same period. The phytoplankton

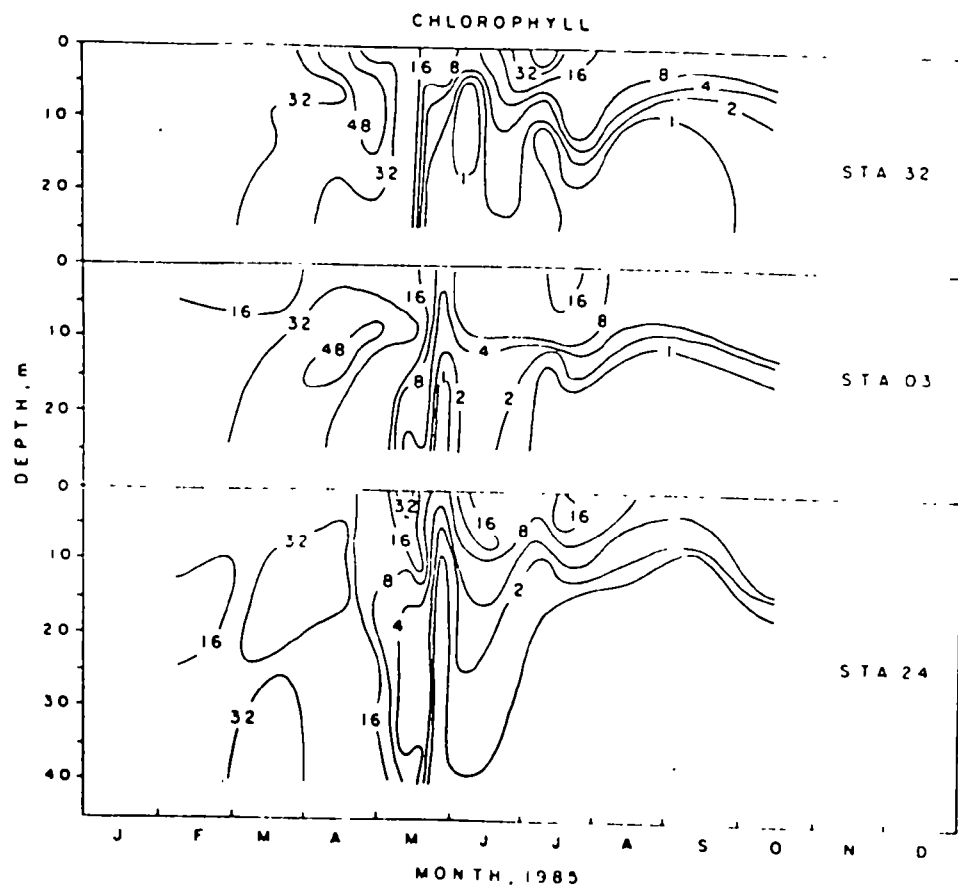


Figure 11. Temporal variations in the vertical distribution of chlorophyll ($\mu\text{g/l}$).

Table 3. Euphotic zone chlorophyll a (mg m^{-2}) at stations along the mainstem of the Bay from north (station 32) to south (station 24).

Date	32	28	27	STATION		24	Mean	C
				3	26			
12 Feb	119	193	--	146	--	181	--	--
21 Mar	176	201	167	164	167	249	187	18%
16 Apr	122	243	276	268	253	270	239	24
29 Apr	212	139	165	154	99	63	139	37
16 May	187	203	160	232	221	352	226	30
Mean	162	196	192	193	185	233		
C	25%	19%	29%	28%	36%	52%		
23 May	55	72	71	76	49	70	66	16
28 May	63	45	79	49	45	43	54	25
6 June	22	40	63	92	133	74	71	55
19 June	58	75	70	71	55	50	63	16
11 July	161	72	81	50	60	40	77	57
19 July	121	88	68	64	107	65	86	28
Mean	80	65	72	67	75	57		
C	64%	29%	9%	24%	48%	26%		
15 Aug	58	27	56	32	30	28	35	38
11 Sept	48	33	35	59	69	45	48	29
10 Oct	76	38	44	43	59	52	52	27
Mean	61	33	46	45	53	42		
C	23%	17%	25%	30%	38%	29%		

Table 4. Primary productivity ($\text{mg C m}^{-2} \text{ d}^{-1}$) and chlorophyll specific production ($\text{mg C (mg Chl} \cdot \text{d)}^{-1}$) at stations 1, 3, and 5 of the CHOP-PAZ transect.

Date	1		3		5	
	P	P/Chl	P	P/Chl	P	P/Chl
21 Mar			218	3	623	5
16 Apr	801	5	1255	8	1041	4
29 Apr	744	7	1102	6	307	3
16 May	1274	5	1230	5	465	6
23 May	87	1	329	2	227	2
28 May	475	16	263	7	272	11
11 July	1332	31	1556	26	891	22
19 July	1310	15	1301	18	1216	20
15 Aug	1969	62	1749	61	1230	51
11 Sept	789	38	1556	47	1320	44
10 Oct	1472	52	1625	45	1210	54

collapse in late May coincided with a drop in PP to 329 mg C/m²/d and a drop in PP/Chl to 2 mg C/(mg Chl x d). Following these declines, PP and PP/Chl increased to annual maxima in August, similar to the annual cycle described by Taft et al. (1980). Assuming that PP/Chl at station 3 was representative of rates at the other stations on the mainstem transect, PP averaged 1160 mg C/m²/d during February-May prior to the collapse and 1750 mg C/m²/d during June-August following the collapse. Thus, while Chl achieved its seasonal maximum during spring in conjunction with the peak in fresh water flow, PP achieved its seasonal maximum during late summer when fresh water flow (and associated nutrient inputs) was low.

The concentration of particulate organic carbon (POC) ranged from 130 to 3540 ug/l and was significantly ($P < 0.001$) correlated with Chl (Table 5). The exponential relationship between POC and Chl reflects the fact that phytoplankton constitute an increasing fraction of POC as phytoplankton biomass increases (cf. Chervin et al. 1981). As a consequence, C/Chl decreased exponentially as Chl increased (Table 6). These relationships reflect the presence of proportionately larger amounts of nonphytoplankton organic matter (mostly detritus) as phytoplankton biomass approaches zero. Linear regressions of POC on Chl when Chl exceeded 10 ug/l (the concentration about which C/Chl is relatively insensitive to variations in Chl; see Chervin et al. 1981) give C/Chl ratios for phytoplankton alone as follows:

12 Feb - 23 May	C/Chl = 30
28 May - 19 Jul	C/Chl = 40
12 Aug - 10 Oct	C/Chl = 100

Using these ratios to convert chlorophyll to phytoplankton biomass as C,

Table 5. Exponential relationships between POC and Chl where r = correlation coefficient and $POC = a (e)^{b \text{ Chl}}$.

Dates	n	r	a	b
12 Feb - 23 May	222	0.60	622	0.027
28 May - 19 June	111	0.87	516	0.085
11 July - 19 July	74	0.81	437	0.041
12 Aug - 10 Oct	115	0.88	448	0.120

Table 6. Coefficient of determination (r^2) for power curve fits of C/CHl on CHl where $C/CHl = a (CHl)^b$.

Dates	n	r^2	a	b
12 Feb - 23 May	136	0.71	301	-0.57
28 May - 19 June	77	0.85	334	-0.56
11 July - 19 July	48	0.86	292	-0.43
15 Aug	25	0.83	529	-0.43
11 Sept	24	0.75	503	-0.57
10 Oct	24	0.46	290	-0.36

phytoplankton accounted for 40-65% of total POC prior to the phytoplankton collapse in late May and for less than 20% of POC thereafter. Frequency distributions of C/Chl (Fig. 12) reflect this shift from a phytoplankton dominated system during February-May to a detrital dominated system during June-October, especially in the bottom layer where C/Chl ratios were much higher than in the surface layer during June-October.

Ratios of POC to particulate organic nitrogen (C/N) varied between 4 and 20 with most ratios less than 10 (Fig. 13). Interestingly, C/N tended to be higher during spring than during summer with little difference between the surface and bottom layers during either season. These ratios are typical of phytoplankton (Strickland 1965) and are much lower than ratios in organic matter of terrestrial origin (Muller 1977) or of material from the upper reaches of the Bay where C/N ratios exceed 20 (Flemer and Biggs 1971). Apparently, most suspended organic matter was derived from local phytoplankton production, a conclusion reached by Biggs and Flemer (1972).

Lateral Variation

During the summer of 1984 we documented time-dependent variations in density structure along the CHOP-PAX transect (Malone et al. 1986). These variations influenced lateral distributions of dissolved inorganic nutrients, oxygen, phytoplankton biomass and bacteria and appeared to be responsible for high phytoplankton production over the flanks of the main channel relative to production over the channel. Such lateral oscillations of the pycnocline were observed during summer, 1985 but were much less pronounced (Fig. 14). Likewise, while chlorophyll concentrations were higher over the flanks of the main channel in 1985 (Fig. 15), we did not observe systematic variations in the chlorophyll content of the euphotic zone (Table 7) nor in phytoplankton

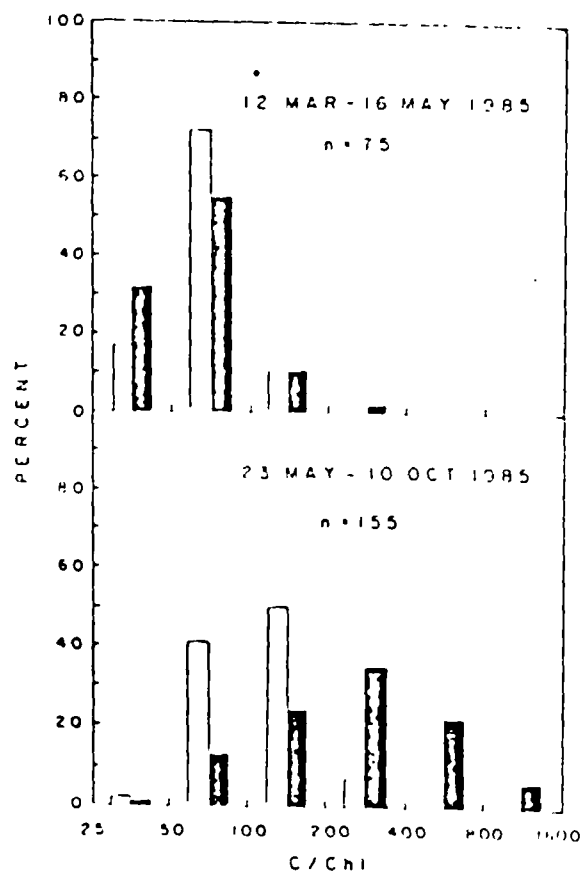


Figure 12. Frequency distributions of the ratio of particulate organic carbon ($\mu\text{g/l}$) to chlorophyll ($\mu\text{g/l}$); open bars - surface, solid bars - near bottom.

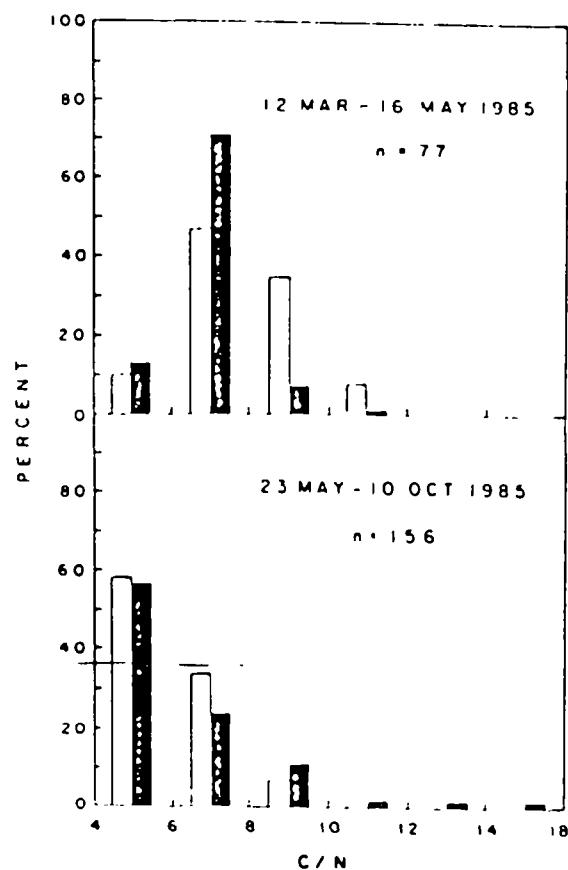


Figure 13. Frequency distributions of the ratio of particulate organic carbon (ug/l) to particulate organic nitrogen (ug/l); open bars - surface, solid bars - near bottom.

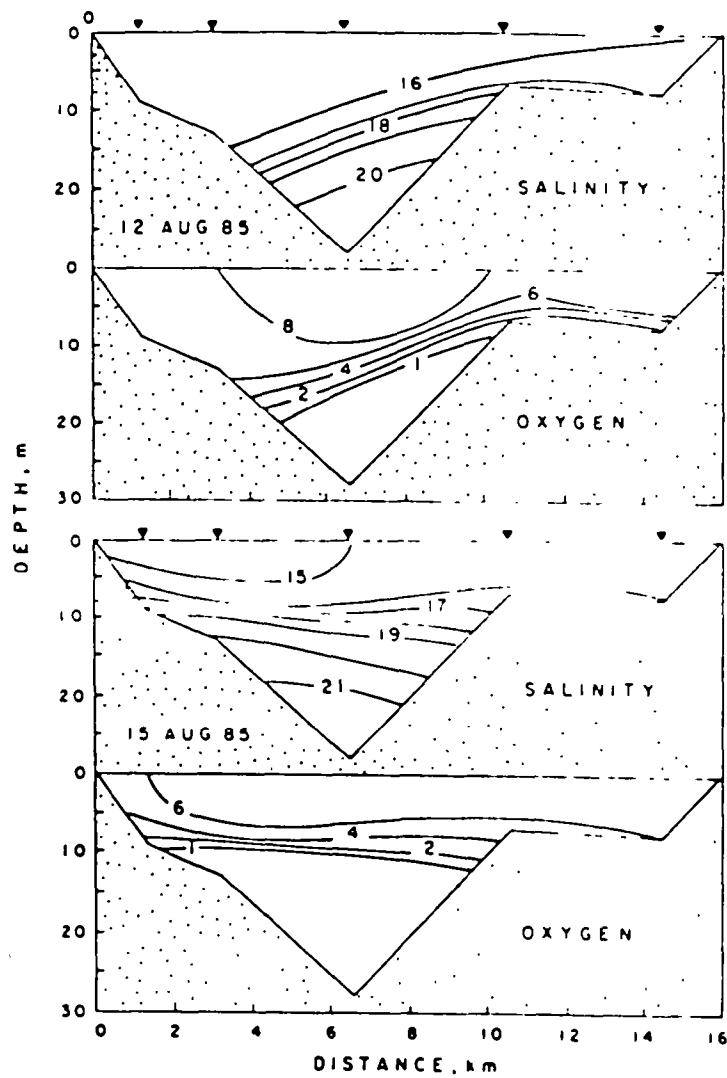


Figure 14. Lateral distributions of salinity and oxygen along the CHOP-PAX transect (from west on the left to east on the right). Solid triangles at top indicate stations along the transect.

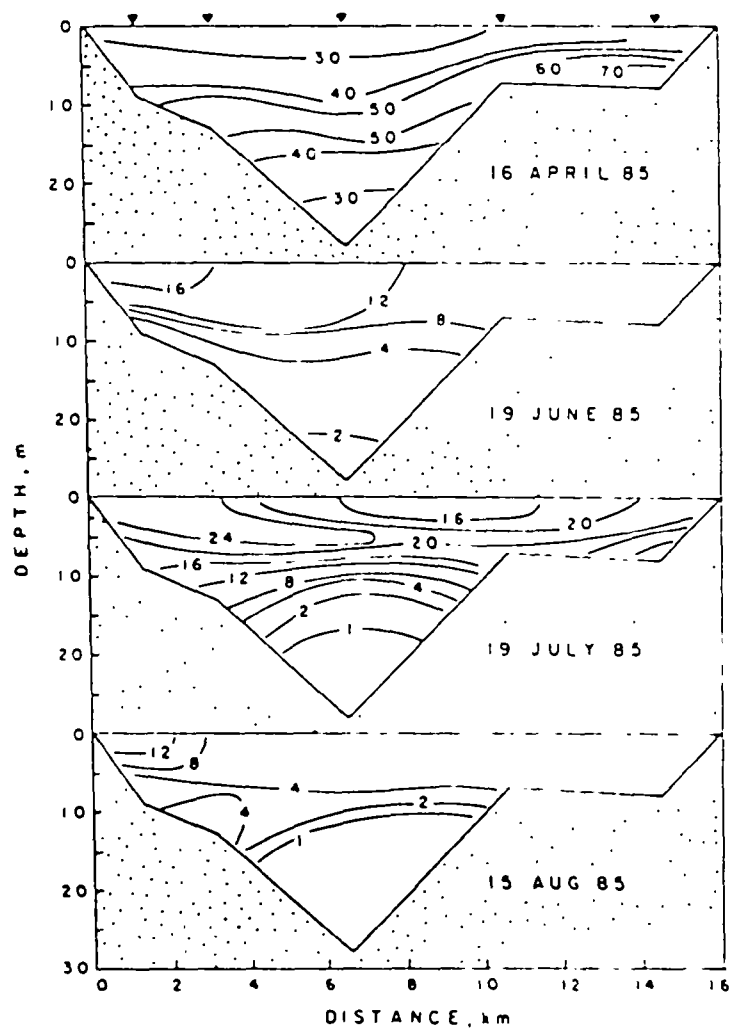


Figure 15. Lateral distributions of chlorophyll ($\mu\text{g/l}$) along the CHOP-PAX transect (from west to east). Solid triangles at top indicate stations along the transect.

Table 7. Euphotic zone chlorophyll a (mg m^{-2}) at stations along CHOP-PAJ transect from west (station 1) to east (station 5).

Date	STATION					Mean	C
	1	2	3	4	5		
12 Feb	124	131	146	93	101	119	18%
21 Mar	70	85	118	151	150	115	32
16 Apr	207	213	228	253	412	263	32
29 Apr	152	130	311	88	97	156	58
16 May	155	164	275	114	152	172	35
23 May	62	118	168	74	116	108	39
Mean	128	140	208	129	171		
C	43%	31%	37%	51%	70%		
28 May	33	31	30	21	20	27	22
3 June	29	35	47	41	31	37	20
6 June	28	58	78	60	80	61	34
14 June	37	56	46	47	38	45	17
17 July	156	43	59	46	51	51	13
19 June	177	103	93	63	62	80	23
27 June	5	48	41	23	36	31	55
3 July	52	32	32	42	38	39	21
11 July	62	62	62	59	45	58	13
18 July	26	19	14	11	10	16	41
19 July	114	124	102	89	83	102	17
Mean	47	56	55	46	45		
C	63%	56%	50%	22%	51%		
22 July	18	1	13	15	12	14	17
8 Aug	11	8	37	36	20	22	62
12 Aug	21	22	22	14	17	19	19
15 Aug	36	26	29	26	32	30	14
29 Aug	30	32	34	41	24	32	19
11 Sept	27	32	38	36	49	36	23
10 Oct	32	28	46	32	29	33	22
Mean	25	23	31	29	26		
C	35%	41%	36%	37%	47%		

productivity (Table 4). As discussed below, this contrast between 1984 and 1985 may be related to differences in vertical stratification and fresh water flow (and probably wind forcing).

1984 AND 1985 INTERANNUAL CONTRASTS - HYDROGRAPHY, NUTRIENTS, PHYTOPLANKTON

A major difference between 1984 and 1985 was the exceptionally high fresh water flow during July-August 1984 (Seliger et al. 1985). 1985 was a drought year and freshwater flow was exceptionally low. As a consequence, surface salinity was much higher and vertical stability lower during 1985 than during 1984 (Fig. 16). While this had little influence on the thickness of the hypoxic layer or on the length of time hypoxia was present (Fig. 16), it was reflected in the oxygen content of the bottom layer, i.e. anoxia was observed episodically from June through September in 1984 but not in 1985 when anoxia was only observed in September (Fig. 9). For example, compare the salinity (Fig. 17) and oxygen (Fig. 18) distributions of June 1984 with June 1985. It is likely that the lack of anoxia during 1985 was due, at least in part, to weaker stratification and stronger vertical mixing during 1985.

These differences in oxygen depletion of bottom water may also reflect differences in the production and fate of phytoplankton biomass during the summer season. The Chl content of the euphotic zone was higher and more variable during summer 1984 than summer 1985 when euphotic zone Chl was lower and relatively constant (Fig. 19). In contrast, PP/Chl was higher during 1985 than during 1984 (Fig. 19). This suggests that phytoplankton production and grazing was more closely coupled during 1985 so that phytoplankton biomass did not accumulate. As a consequence, the flux of organic matter of

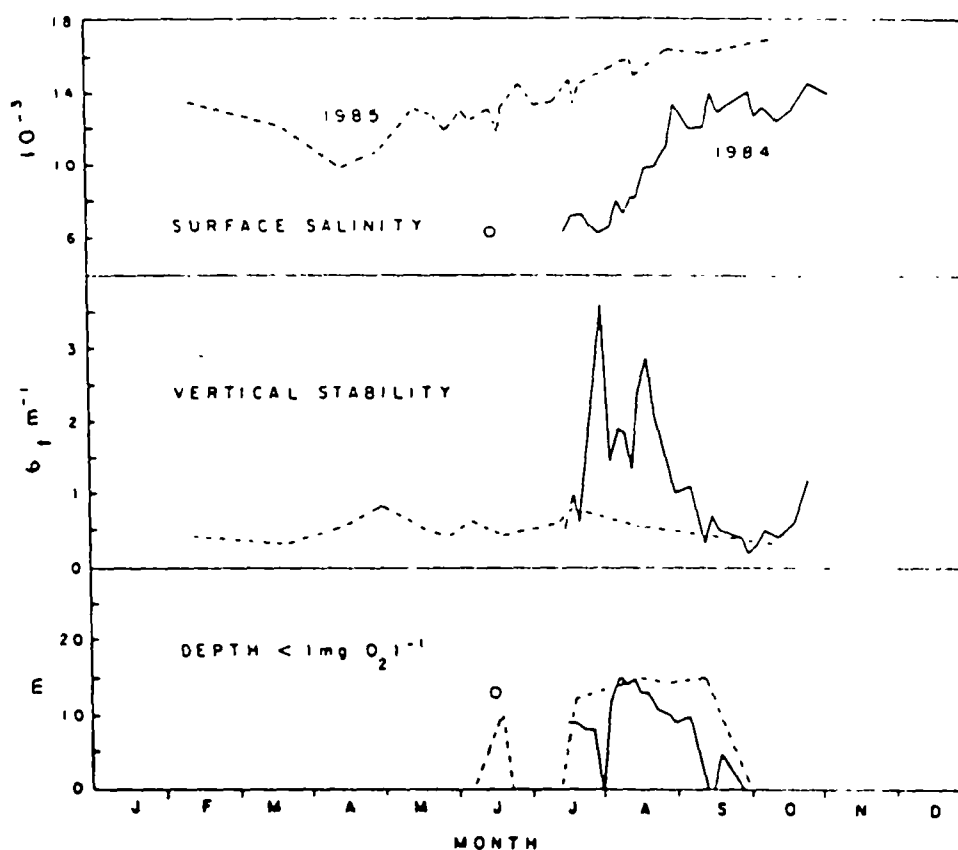


Figure 16. Temporal variations in surface salinity, vertical stability across the pycnocline, and the thickness of the hypoxic layer having oxygen concentrations less than 1 mg/l during 1984 (solid line) and 1985 (broken line); circled point is from June 1984.

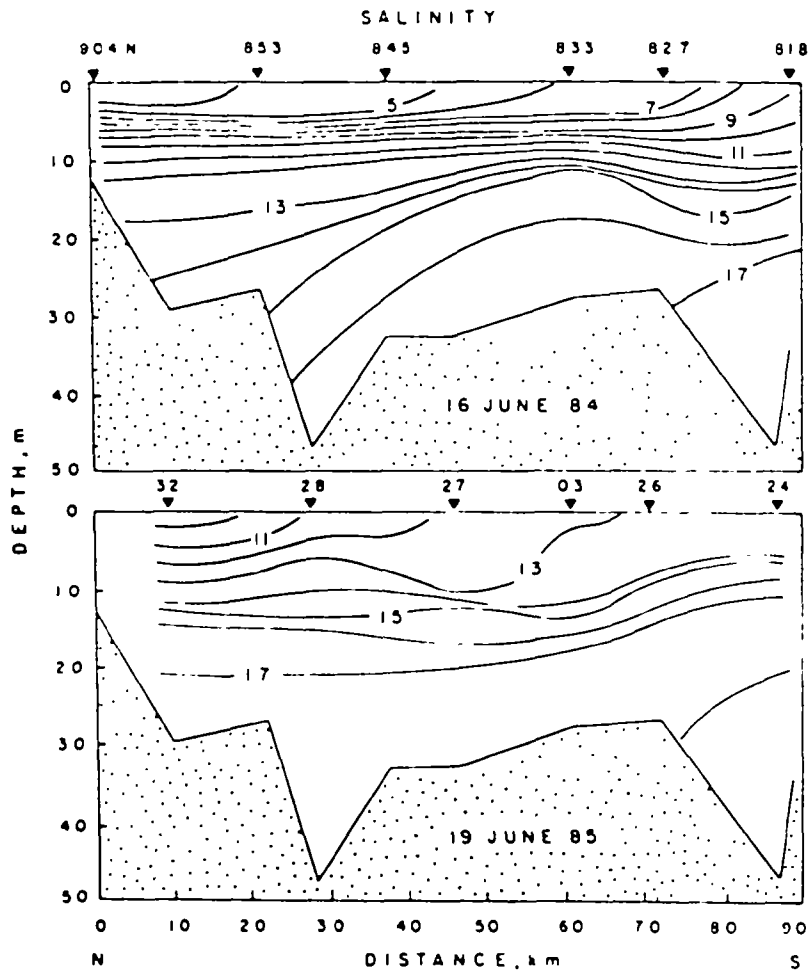


Figure 17. Variations in the vertical distribution of salinity along the mainstem transect in June of 1984 and 1985. Numbers above solid triangles indicate CBI stations (above) and stations from this study (below).

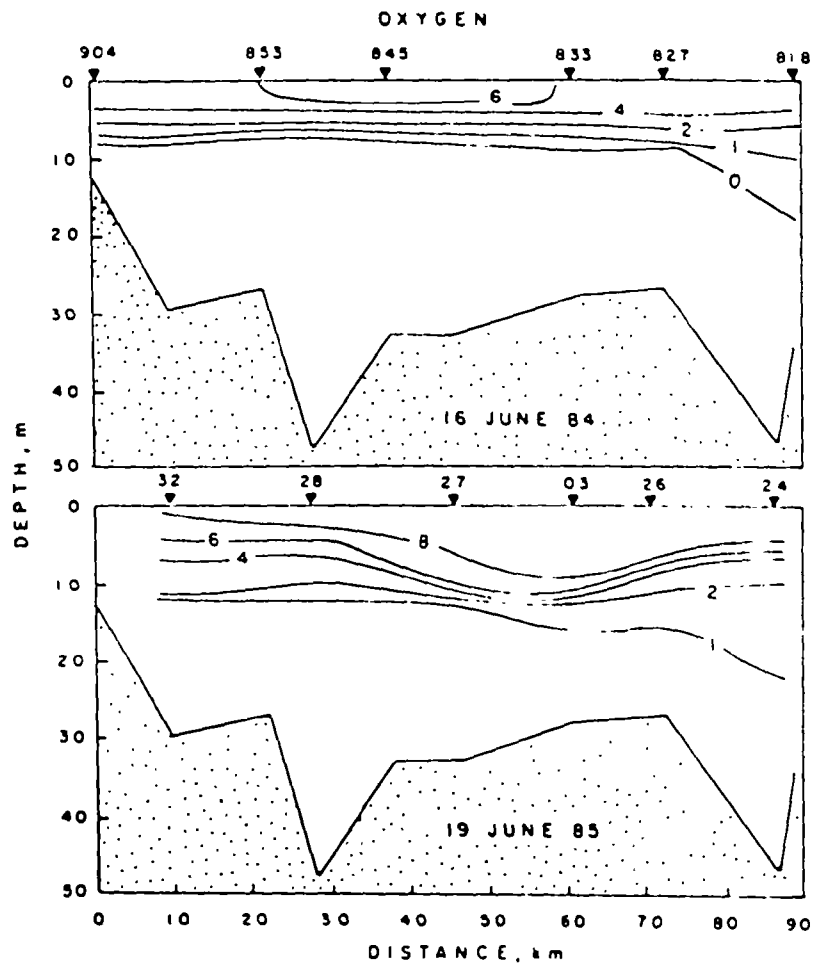


Figure 18. Variations in the vertical distribution of dissolved oxygen along the mainstem transect in June of 1984 and 1985. Stations are the same as in Figure 16.

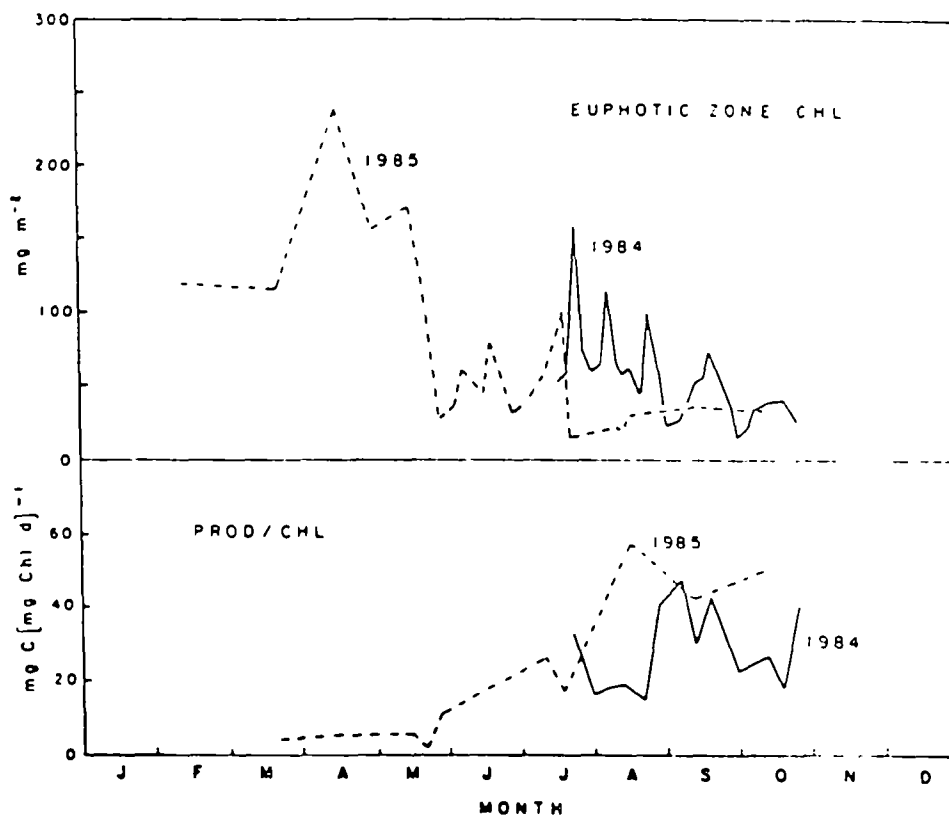


Figure 19. Temporal variations in the chlorophyll content of the euphotic zone and chlorophyll specific productivity of the euphotic zone during 1984 and 1985.

phytoplankton origin (due both to sinking of particulate organic matter and to the release of dissolved organic matter by phytoplankton in the bottom layer) into the bottom layer was probably lower during 1985. Poor coupling between zooplankton grazing and phytoplankton production during 1984 may be caused by oscillations of the pycnocline and associated variations in vertical mixing (Malone et al. 1986).

In this context, it is noteworthy that phytoplankton production showed little variation between 1984 and 1985 despite these differences in fresh water flow (and associated nutrient inputs), vertical stability, and lateral oscillations of the pycnocline. Phytoplankton production during July-October along the CHOP-PAX transect averaged $1.20 \text{ g C/m}^2/\text{d}$ in 1984 compared to $1.37 \text{ g C/m}^2/\text{d}$ in 1985. We would also like to point out that these estimates of summer production are substantially lower (and more reasonable when compared to other estuarine and coastal ecosystems) than reported by Officer et al. (1984).

Dissolved Oxygen and Vertical Stratification

While vertical stability clearly influences mixing between oxygenated surface water and oxygen depleted bottom water, variations in the oxygen content of bottom water were poorly related to variations in vertical stability during 1985 (Fig. 20). Likewise, during spring, vertical stability decreased downstream from north to south yet the rate of decrease in the oxygen content of bottom water did not vary along the mainstem transect (Fig. 21). However, bottom water oxygen concentration was strongly correlated with temperature which accounted for 88% of the variation in bottom water oxygen during the spring decline (Fig. 20). This suggests that

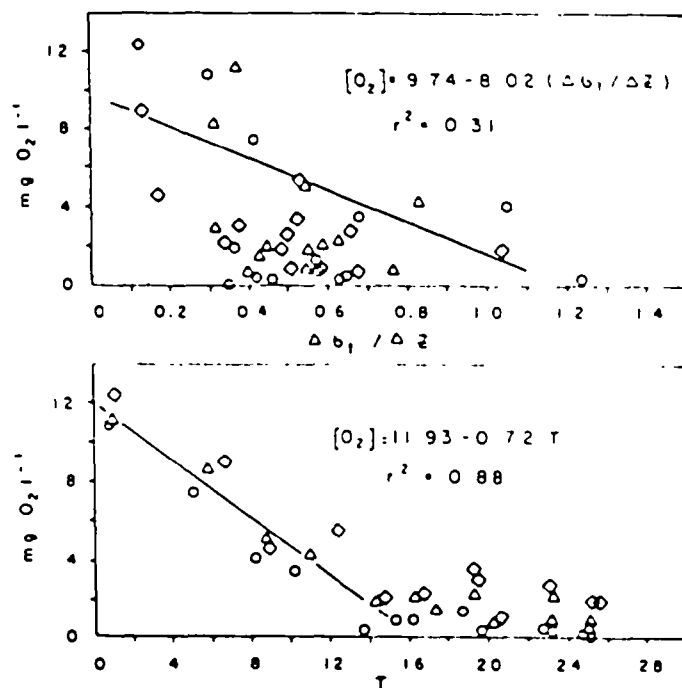


Figure 20. Mean oxygen concentration of the bottom layer in relationship to vertical stability across the pycnocline and to bottom water temperature (circle, station 32; triangle, station 3; diamond, station 24); regressions run for 12 Feb. - 16 May.

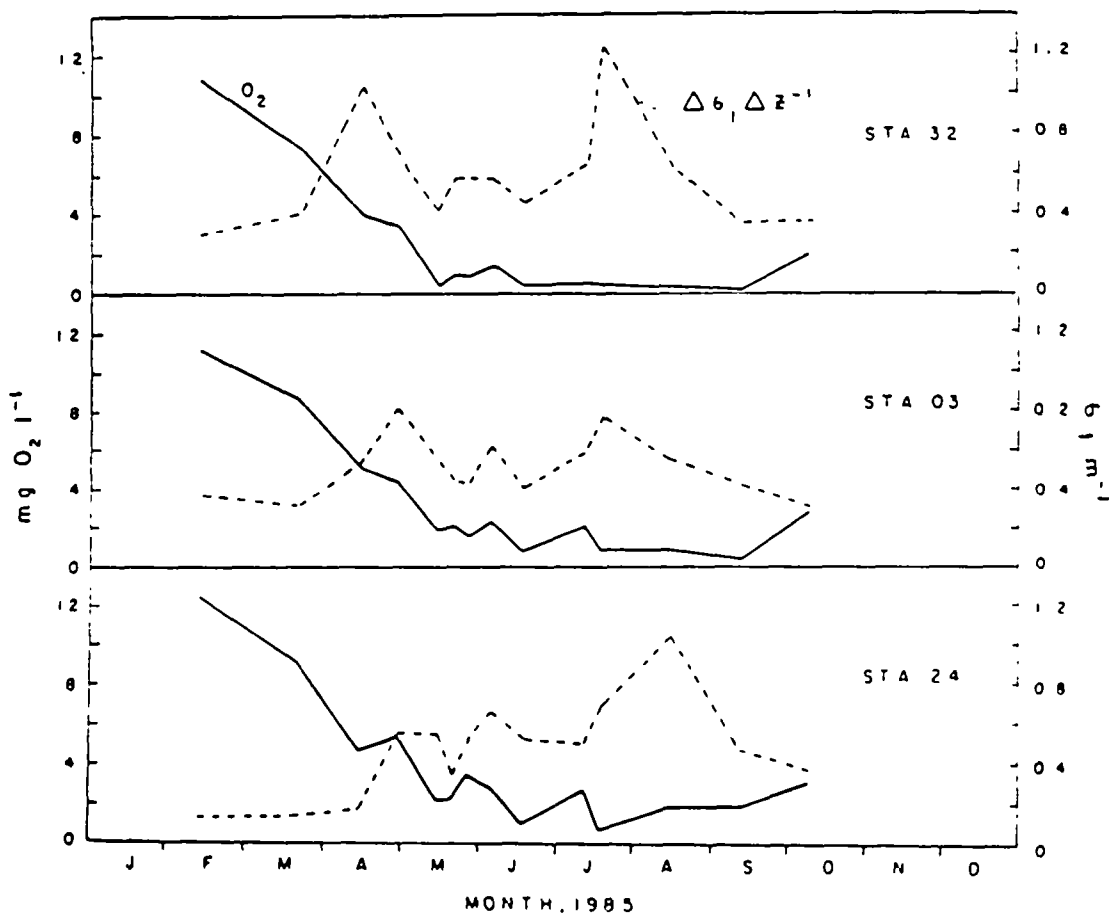


Figure 21. Temporal variations in the mean concentration of dissolved oxygen in bottom layer (solid line) and vertical stability across the pycnocline (dashed line).

heterotrophic metabolism governs the rate of decline in oxygen over the observed range of vertical stability in the Bay. The predominant effect of vertical stability appears to be on the spatial extent of anoxia during the summer.

Production and Fate of Phytoplankton Biomass

Seasonal variations in phytoplankton biomass and productivity were out of phase in the Bay with biomass peaking during spring and productivity during summer. The large accumulation of biomass during February-May suggests the possibility that the decline in dissolved oxygen during this period was a consequence of the heterotrophic metabolism of organic matter produced by phytoplankton over the same period. The rapid decline in biomass during late May may have been due to a mass mortality of phytoplankton below the euphotic zone caused by low oxygen concentrations and/or a rapid increase in grazing pressure. In either event, sinking of this organic matter into the benthos could provide a source of organic substrates for subsequent oxygen removal during summer. The development of the summer maximum in productivity would then depend on the regeneration of nutrients based on this organic matter and the recycling of these nutrients into the euphotic zone as a consequence of vertical mixing and oscillations of the pycnocline. This is contrary to the hypothesis that there is an interannual carry over of phytodetritus which fuels oxygen depletion in the Bay. However, our results do not omit the possibility that all the organic matter produced in any given year is not consumed during that year.

Nutrients and Phytoplankton Production

Our results indicate that phytoplankton growth rates (biomass specific productivity) were not limited by either P or N on a seasonal time scale.

The nutrient concentrations we observed in 1985 were simply too high to limit the rate of phytoplankton growth. This is somewhat surprising since 1985 was a low flow year which should mean that inputs of new nutrients to the Bay were lower than they would have been had fresh water runoff been greater. If this is the case, substantial reductions in nutrient inputs will be required to significantly decrease phytoplankton production in the Bay. We emphasize, however, that our results do not preclude the possibility that phytoplankton biomass yield might be nutrient limited.

In this regard, it would be a mistake to conclude that the high N/P ratios reported here and elsewhere indicate that N removal is not necessary. Differences in the cycles of N and P and in the physical chemistry of the compounds involved make interpretation of N/P ratios in terms of nutrient-limited phytoplankton growth difficult.

THE 1985 ANNUAL CYCLE - MICROBIOLOGY

Bacterial Abundance

Temporal Changes along the Main Channel

Bacterial abundance was low in late winter, averaging less than 10^6 cells/ml (Fig. 22). Bacterial numbers increased rapidly as water temperatures increased, approaching summer abundances by late April. During the period mid-February to late April, bacterial abundances exhibited little change from surface to bottom, but numbers increased earlier up Bay at stations 32 and 3 than at station 24 farther to the south.

Following a peak in late April, bacterial numbers decreased rapidly at all three stations (Fig. 22), preceding the phytoplankton decline by 1 week (Fig. 11, Tables 3 and 4). Bacterial abundance remained low, but began to

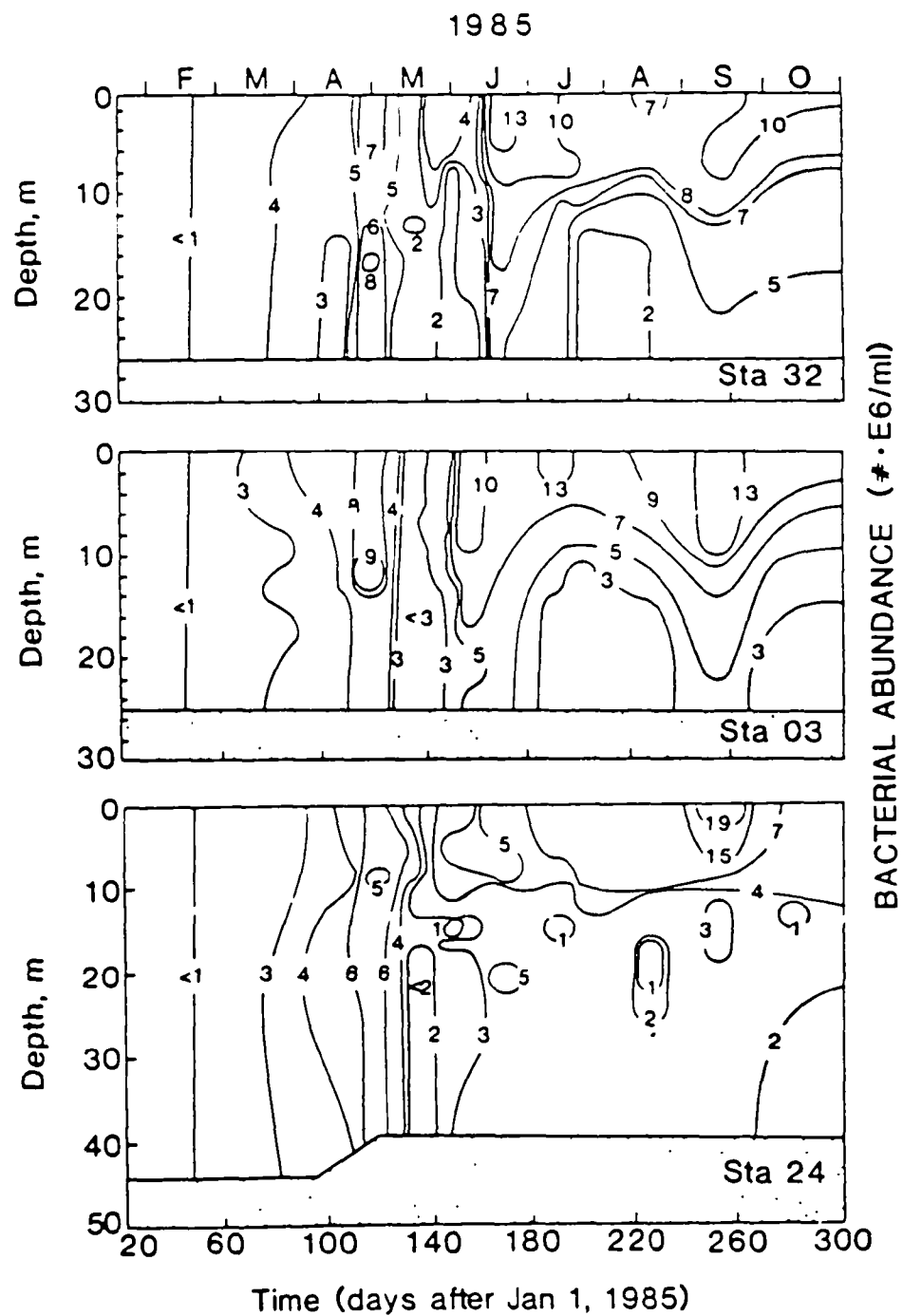


Figure 22. Time-dependent vertical variations in bacterial abundance along a north-south (station 32 to 24) main channel transect.

increase about one to two weeks after the phytoplankton decline. The increase was especially noticeable at station 3. By mid-June, summer conditions had become established, marked by higher bacterial numbers above the pycnocline and lower numbers below it. During this period, deep waters at stations 32 and 3 generally harbored larger bacterial populations than at station 24.

Temporal Changes along Transect 2

Figures 23-27 provide a synopsis of temporal changes in bacterial abundance along lateral transect 2 which was studied intensively during our 1984 investigation (Tuttle et al. 1985). Salinity contours for this transect are provided to indicate the pycnocline depth and degree of stratification (Figs. 28-32). Early cruises (Figs. 23 and 24) were often characterized by similar numbers of bacteria in surface waters, in deep waters, and from flank to flank. The presence of mid- and deep water maxima of bacterial abundance were common during the late winter and spring. Examples of this occurrence include cruises 2 and 3 (Fig. 23), cruises 4-6 (Fig. 24), and cruises 7-9 (Fig. 25). Bacterial abundance contours which were typical of summer 1984 (Tuttle et al. 1985) did not occur along transect 2 until mid-July (Fig. 16). These "typical" abundance contours, characterized by high bacterial numbers on the flanks and in surface waters and by decreasing bacterial abundances with depth, were common along transect 2 from mid-July to the end of the study period (Figs. 26 and 27).

The transect 2 series also illustrates recovery of the bacterial community following the mid-May bacterial decline (cruise 5, Fig. 24). Not until 6 June (cruise 8, Fig. 25), two weeks following the phytoplankton

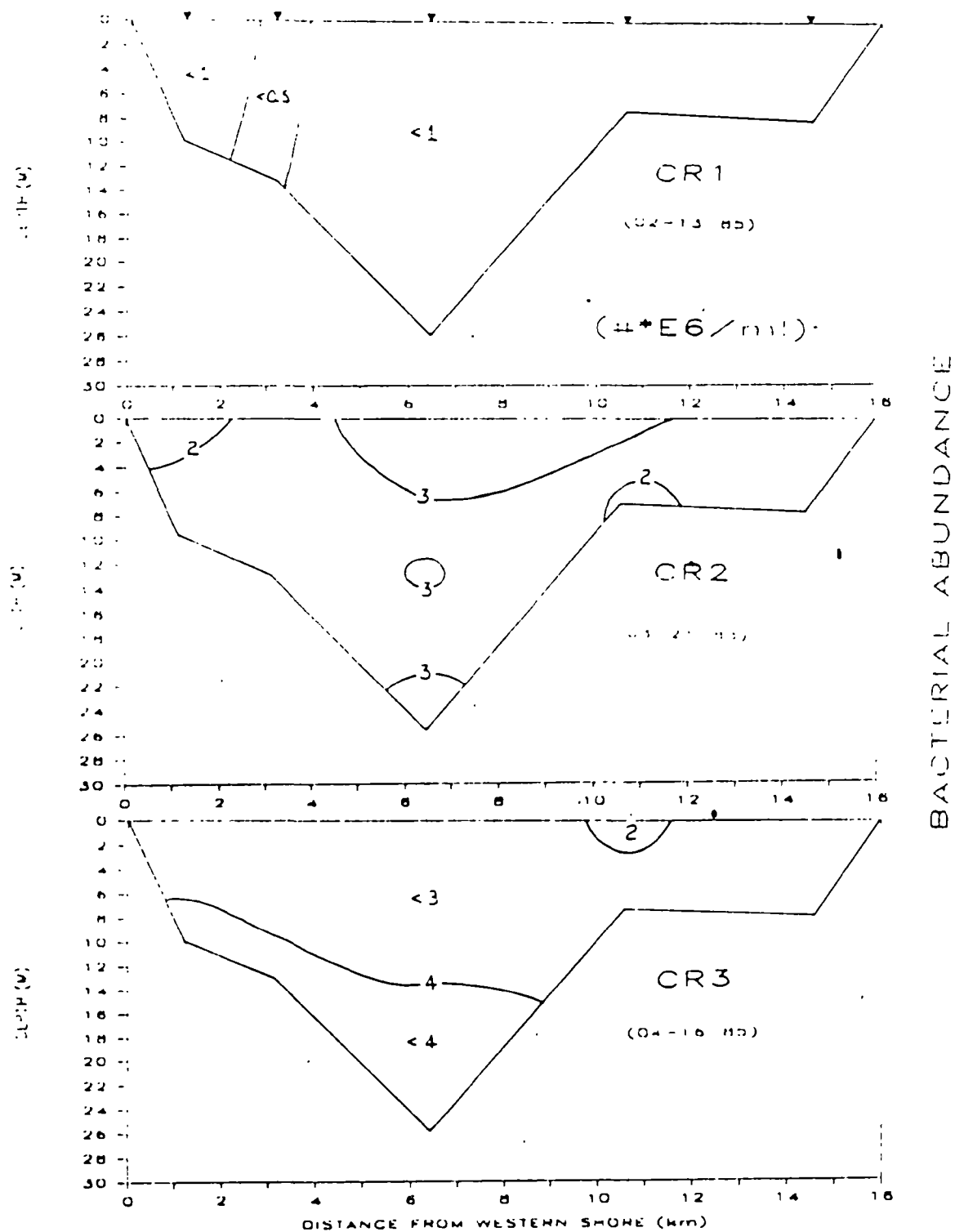


Figure 23. Lateral distributions of bacterial abundance along transect 2 for the period 13 Feb. - 16 Apr. 1985.

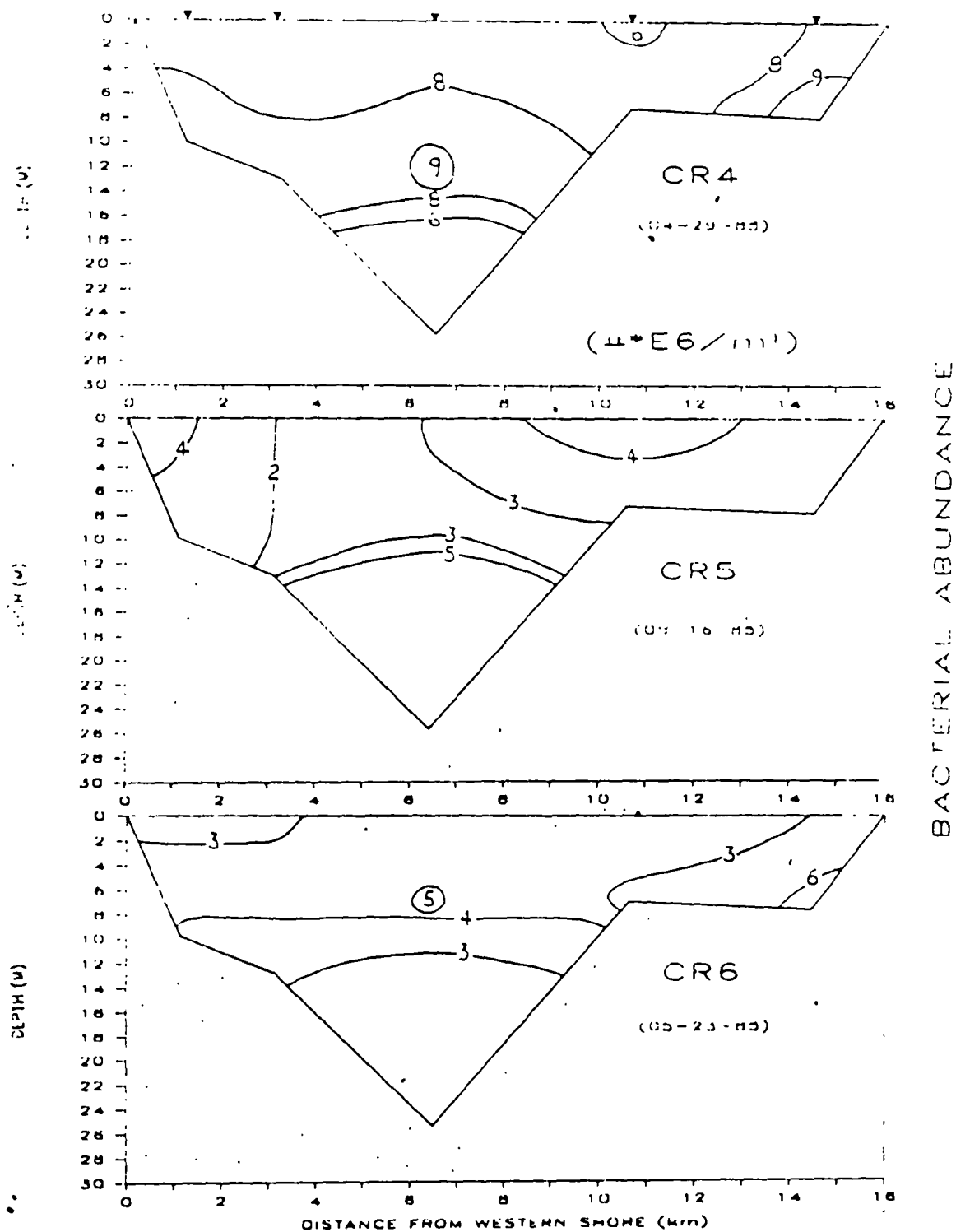


Figure 24. Lateral distributions of bacterial abundance along transect 2 for the period 29 Apr. - 23 May 1985.

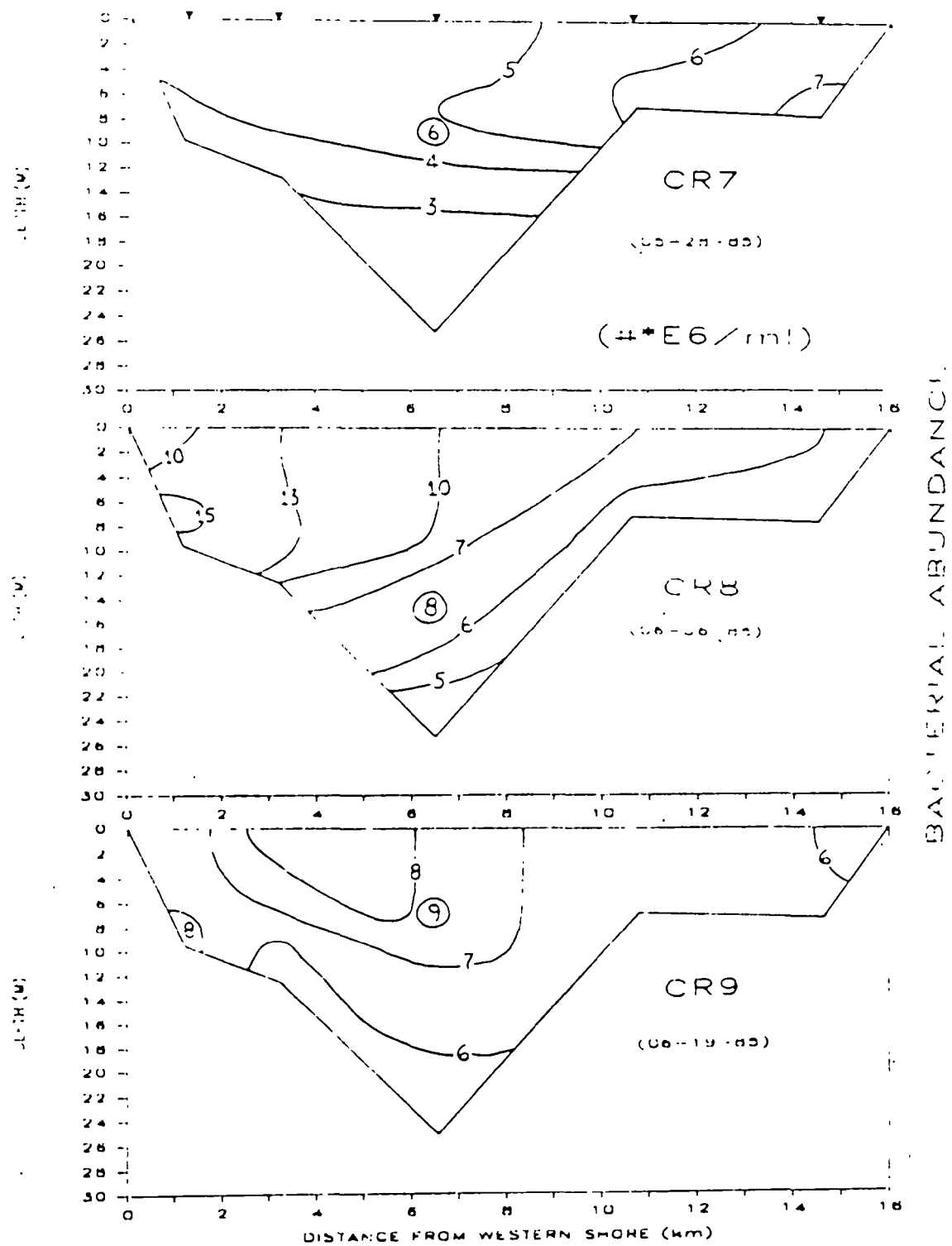


Figure 25. Lateral distributions of bacterial abundance along transect 2 for the period 28 May - 19 June 1985.

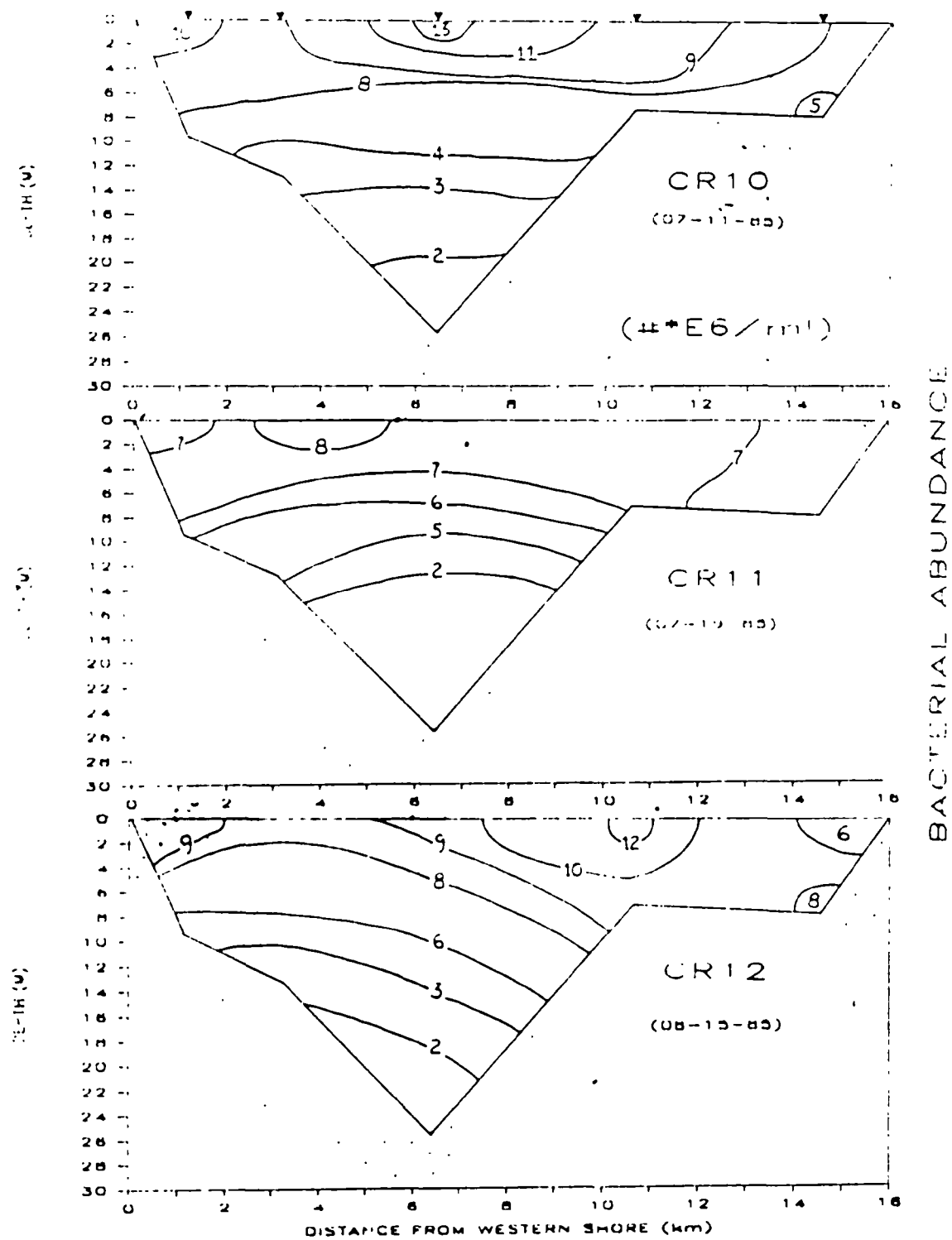


Figure 26. Lateral distributions of bacterial abundance along transect 2 for the period 11 July - 15 Aug. 1985.

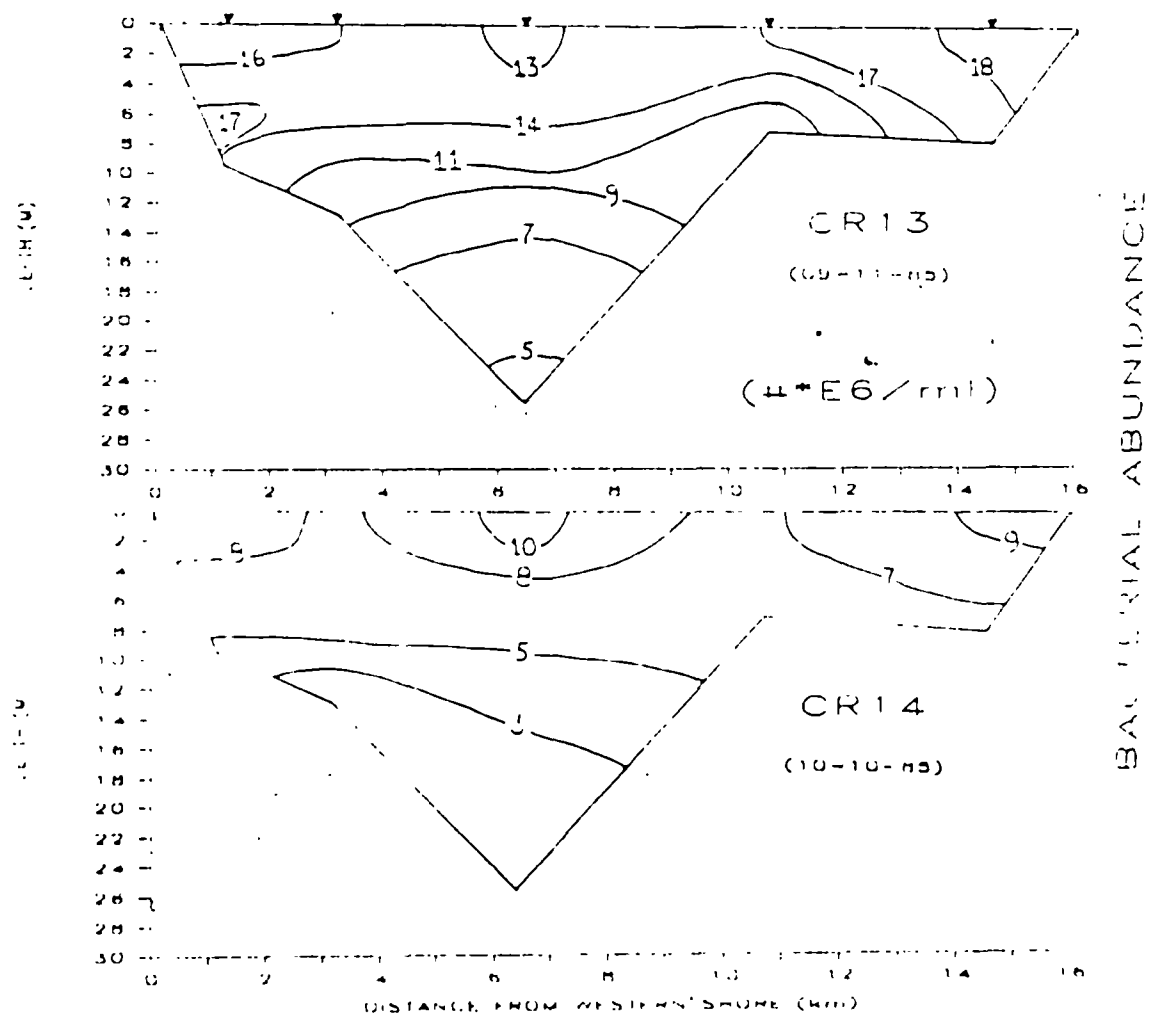


Figure 27. Lateral distributions of bacterial abundance along transect 2 for the period 11 Sep. - 10 Oct. 1985.

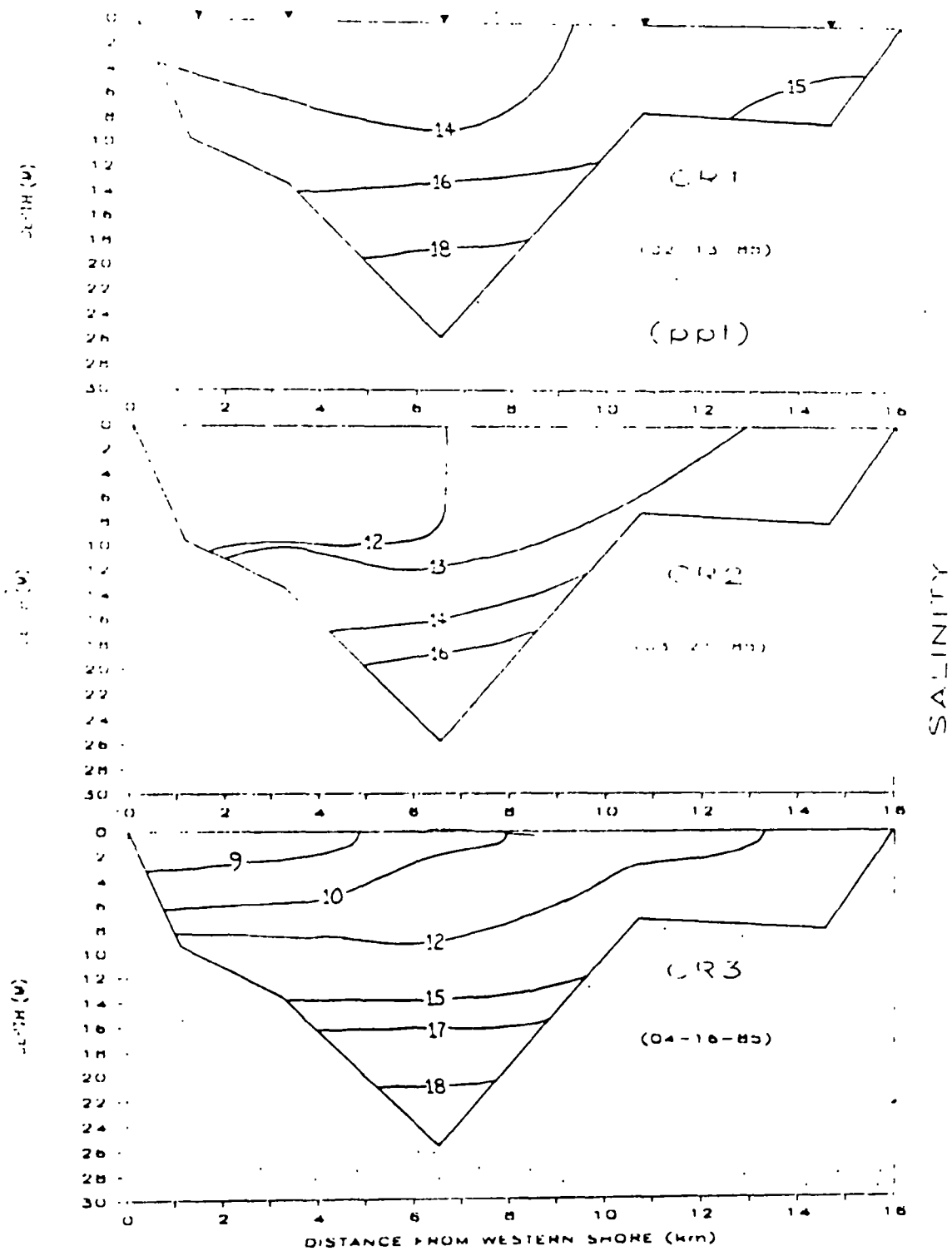


Figure 28. Variations in salinity with depth along transect 2 for the period 13 Feb. - 16 Apr. 1985.

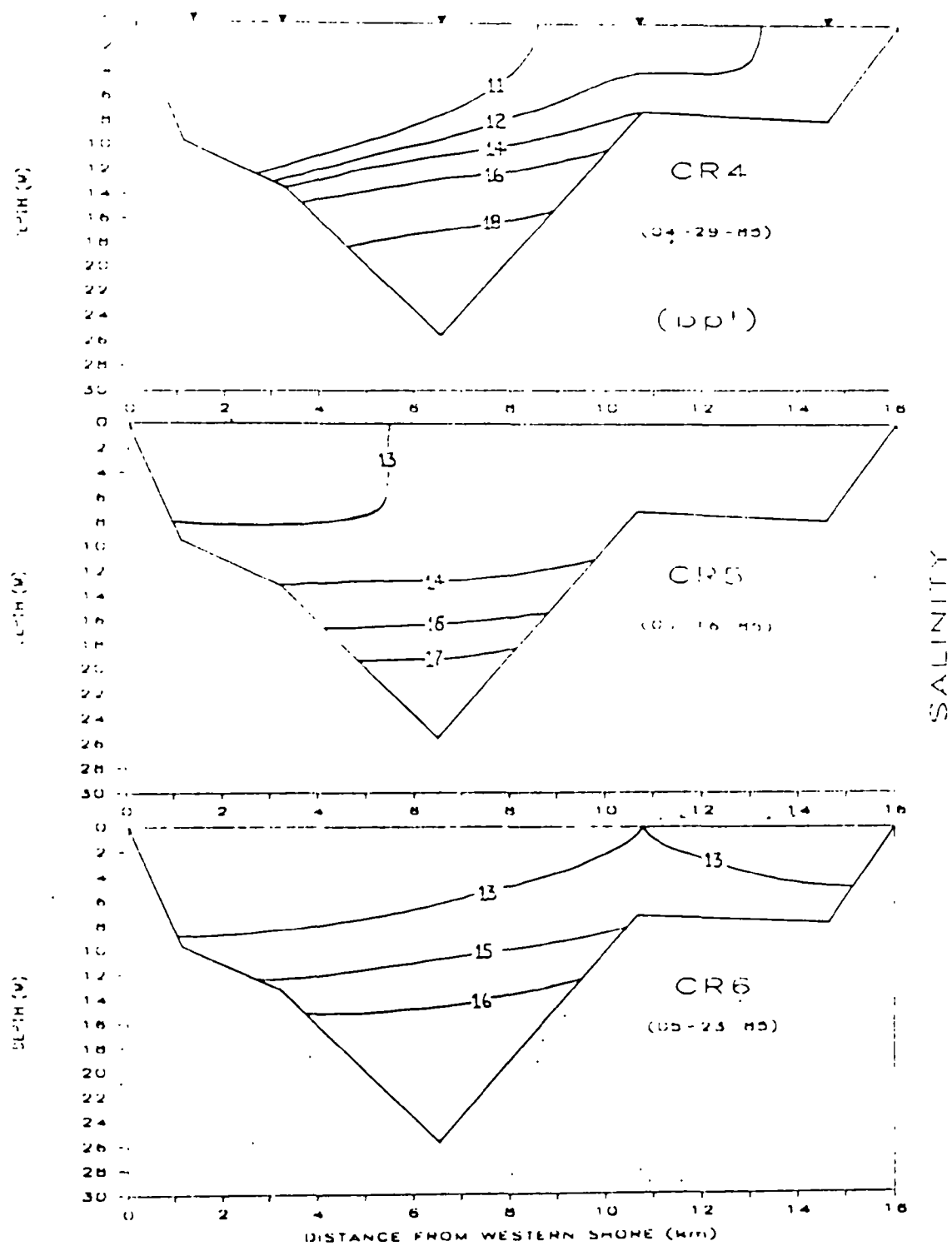


Figure 29. Variations in salinity with depth along transect 2 for the period 29 Apr. - 23 May 1985.

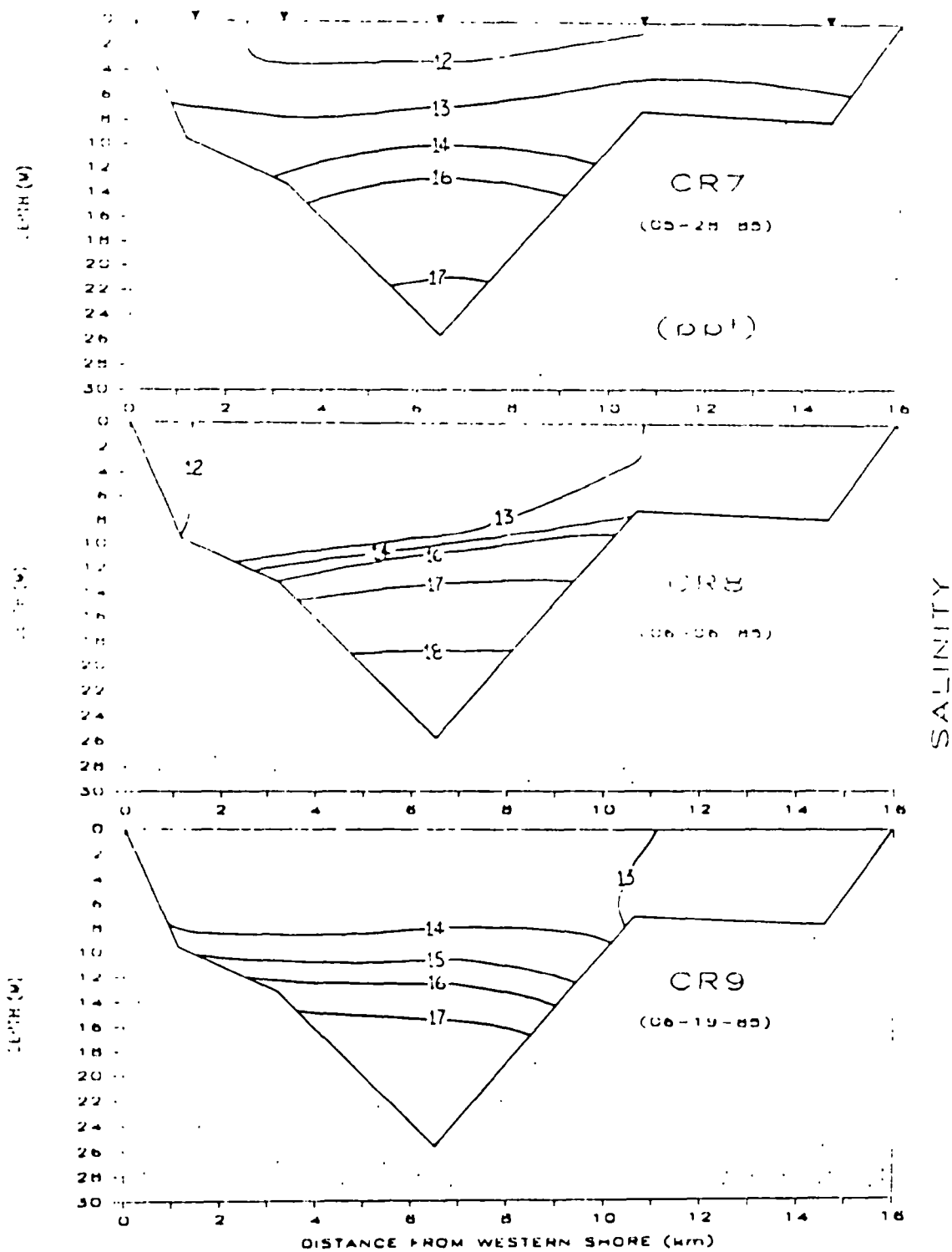


Figure 30. Variations in salinity with depth along transect 2 for the period 28 May - 19 June 1985.

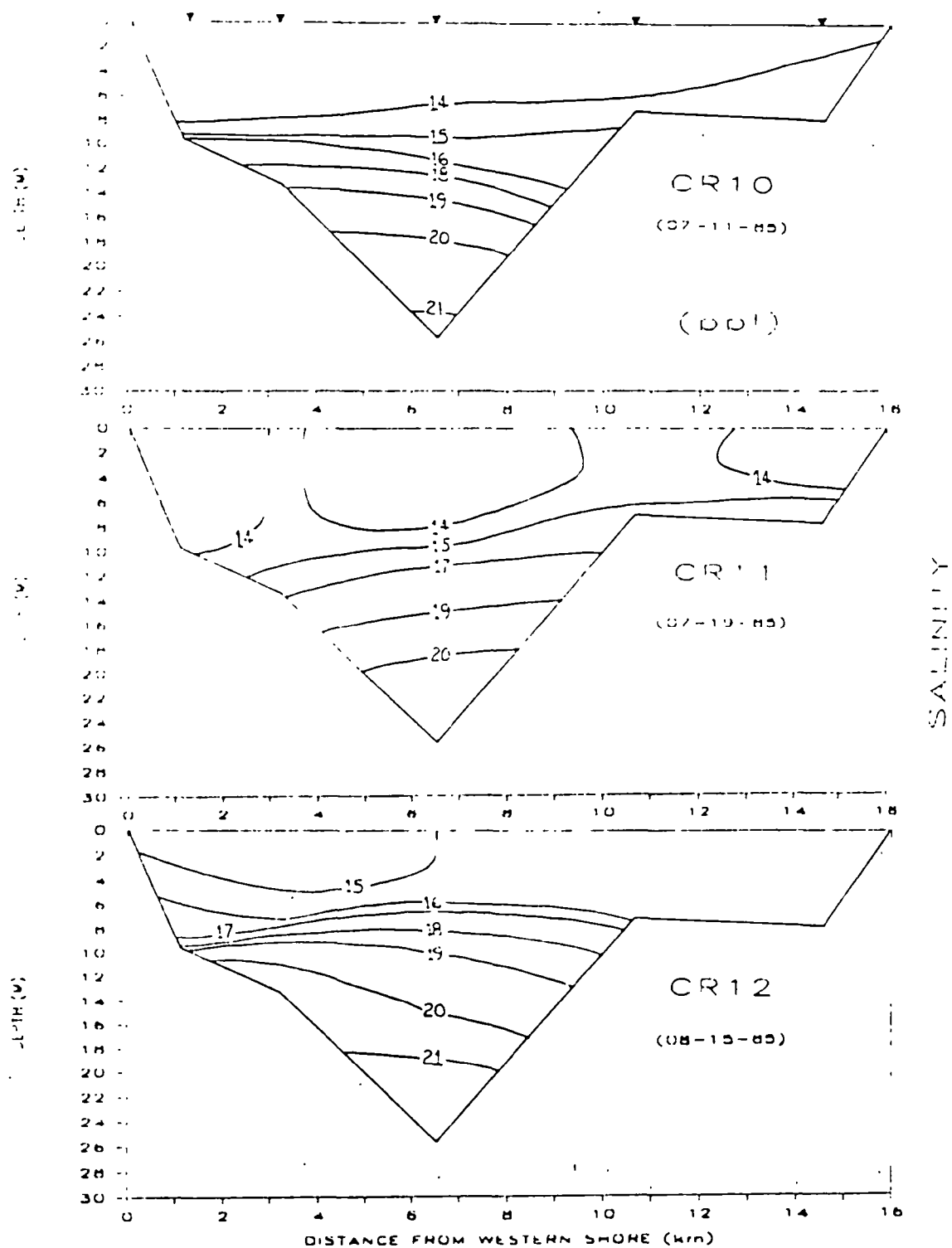


Figure 31. Variations in salinity with depth along transect 2 for the period 11 July - 15 Aug. 1985.

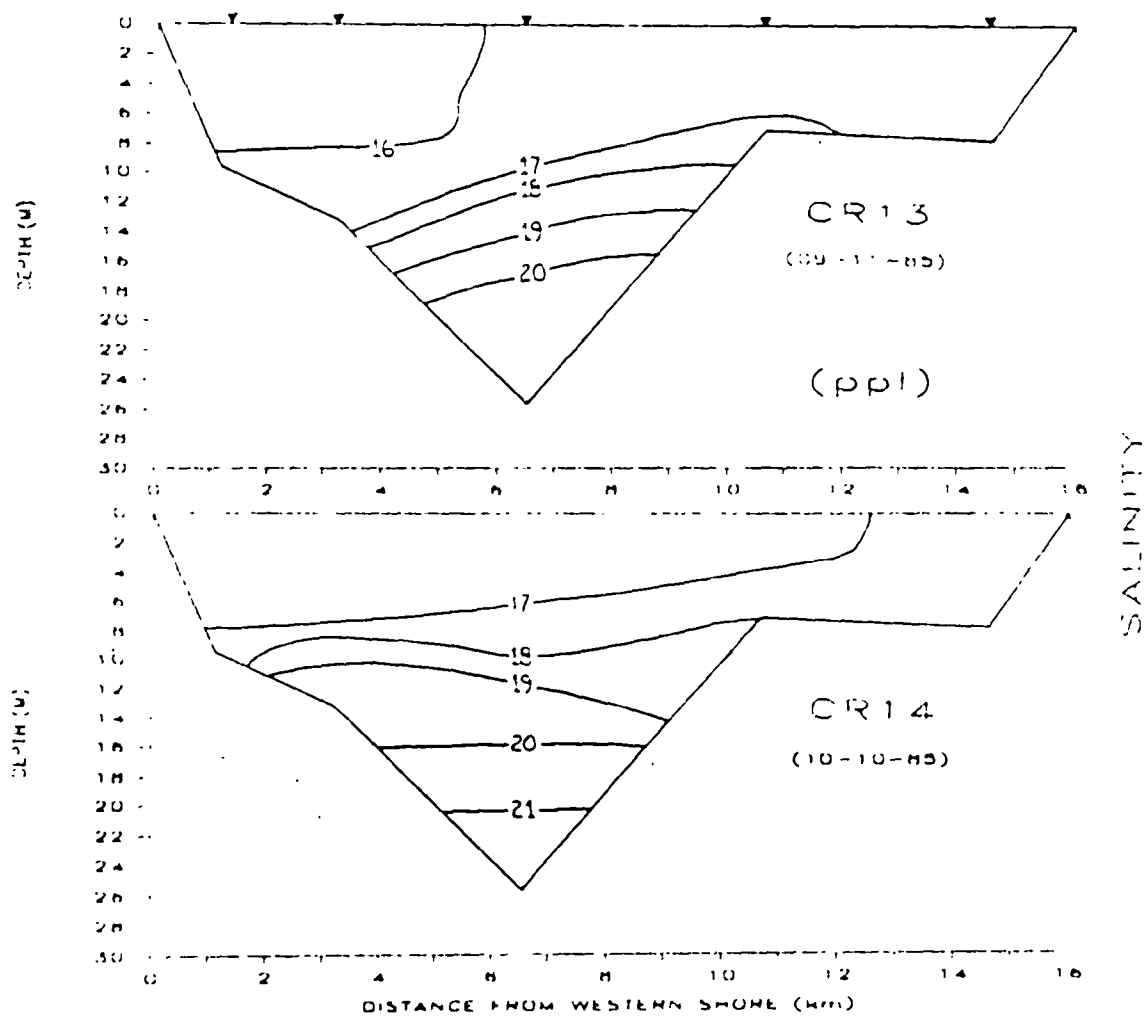


Figure 32. Variations in salinity with depth along transect 2 for the period 11 Sep. - 10 Oct. 1985.

decline, did bacterial numbers reach or exceed abundances which had been present on 29 April (cruise 4, Fig. 24). This recovery was probably fueled by dead or dying phytoplankton.

Differences with Depth

Figure 33 compares mean bacterial abundances within and below the euphotic zone. Not until the end of May, one week after the phytoplankton decline, did mean surface water abundance exceed bacterial numbers below the euphotic zone. Over the next three weeks, bacterial abundance increased in parallel within and below the euphotic zone, probably at the expense of decaying phytoplankton. Summer conditions, i.e. bacterial abundance significantly lower below the euphotic zone, were reached across the mid-Bay study area by late June and persisted throughout the remainder of the study.

North to South Differences

Mean bacterial numbers within the euphotic zone were often greater at the two more northern transects, but this was especially true from late June to mid-October (Fig. 34). Mean summer abundances often exceeded 10^7 /ml at either transect 1 or 2 on a given cruise date, but never exceeded 8×10^6 /ml at transect 3 over the time span of the last five cruises. The differences were less pronounced below the euphotic zone (Fig. 35), but mean bacterial numbers at transect 1 or 2 always exceeded mean bacterial numbers at transect 3 from early June to mid-October.

East to West Differences

In accordance with depth and with north-south transect location, mean bacterial abundance was nearly uniform laterally until late May (Fig. 36). Following the phytoplankton decline over the study area, however, mean bacterial numbers were greater over the flanks than over the deep channel.

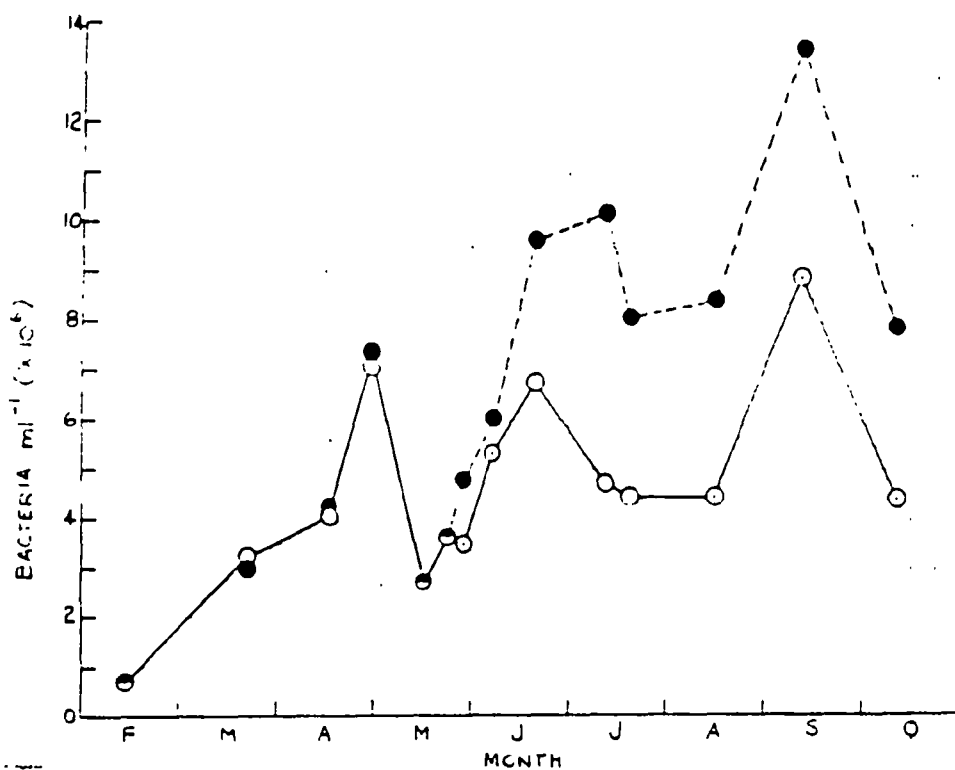


Figure 33. Mean bacterial abundances within (●) and below (○) the euphotic zone for transects 1-3 during 1985. Bacterial abundances are expressed in millions of bacterial ml⁻¹.

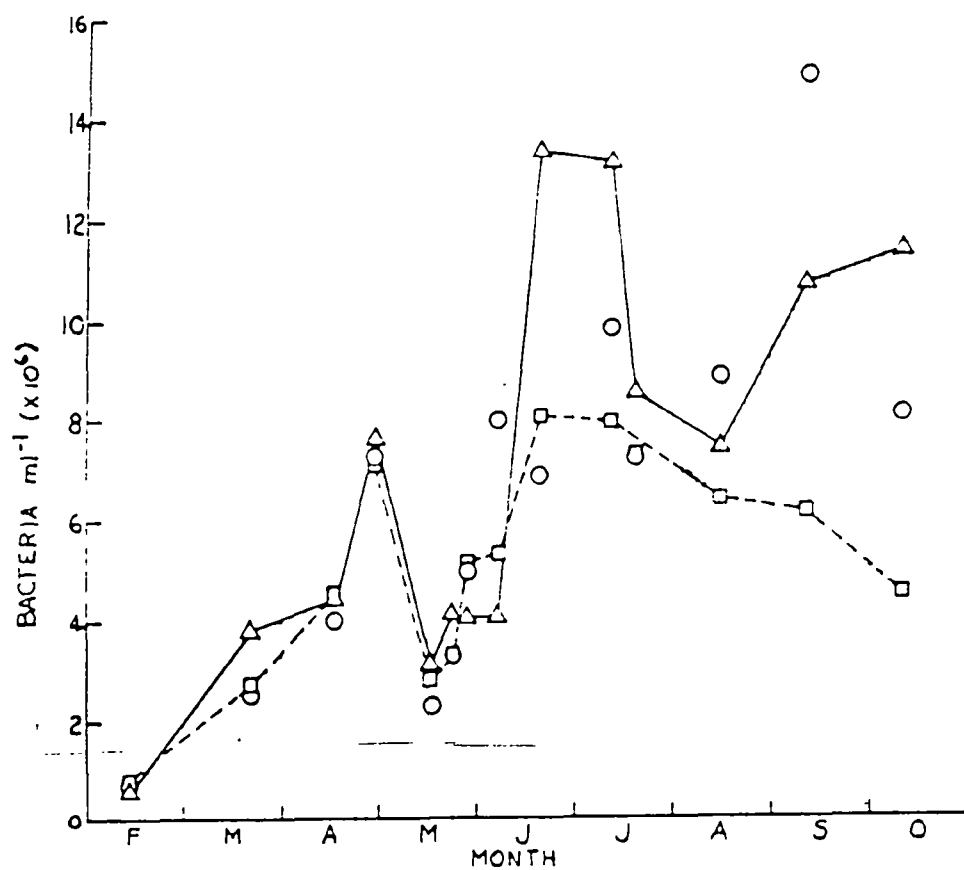


Figure 34. Mean bacterial abundances within the euphotic zone along transects 1 (Δ), 2 (O), and 3 (\square) during 1985. Bacterial abundances are expressed in millions of bacterial ml^{-1} .

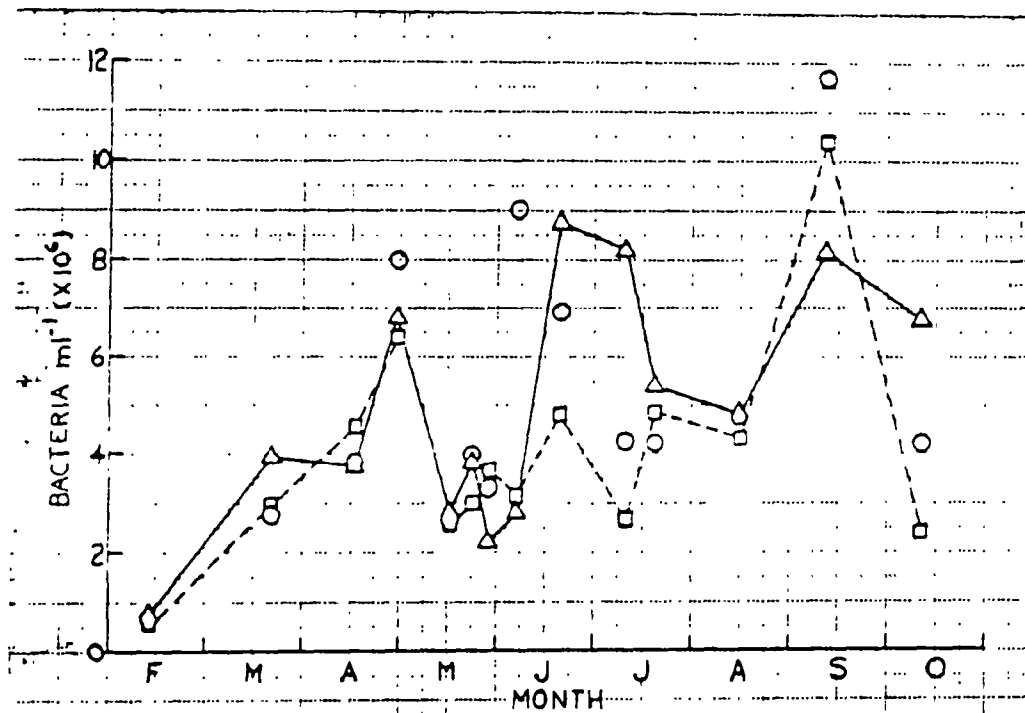


Figure 35. Mean bacterial abundances below the euphotic zone along transects 1 (Δ), 2 (\circ), and 3 (\square) during 1985. Bacterial abundances are expressed in millions of bacterial ml^{-1} .

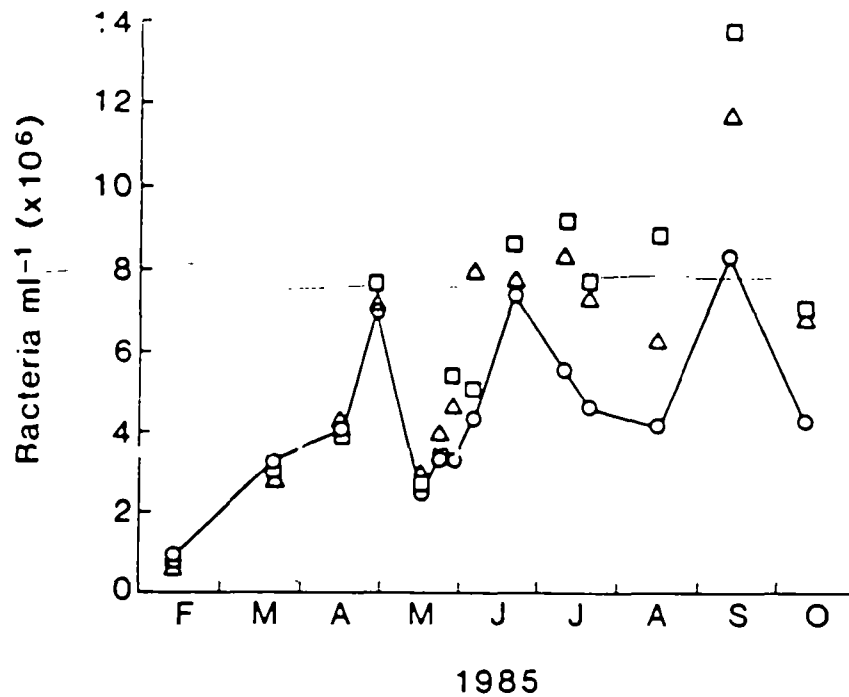


Figure 36. Mean bacterial abundances along the west flank (Δ), main channel (O), and east flank (\square) of Chesapeake Bay during 1985. Values are means of data from all three lateral transects. Bacterial abundances are expressed in millions of bacterial ml^{-1} .

From mid-June until the end of the study, abundances tended to be highest over the eastern flank.

Bacterial Size

As we counted bacteria to estimate abundance, we divided the microorganisms observed into the following size classes: $<1\text{ }\mu\text{m}$, $1\text{ to }2\text{ }\mu\text{m}$, and $>2\text{ }\mu\text{m}$. For our purposes here, we consider only two size classes, namely bacteria less than or greater than $1\text{ }\mu\text{m}$.

Early in the year significant portions of the bacterial community were $>1\text{ }\mu\text{m}$ (Figs. 37 and 38). The proportion of these larger bacteria decreased until by mid-May, most of the bacteria observed were smaller than $1\text{ }\mu\text{m}$. This pattern of size distribution was consistent for northerly and southerly transects and within and below the euphotic zone (Figs. 37 and 38). The proportion of larger bacteria was greatest at transect 2. The proportion of larger to smaller bacteria at transect 2 increased as bacterial abundances increased following the phytoplankton decline in late May. This change in size proportions was independent of depth (Figs. 37 and 38). A similar but smaller change occurred at transect 3.

During summer conditions, bacteria $<1\text{ }\mu\text{m}$ consistently comprised 85 to 95% of the bacterial community. Except in early June when the proportion of larger bacteria increased from east to west, little difference in bacterial size was observed from flank to flank (Fig. 39). The reason for these changes in bacterial size are unclear. One possible explanation is that increasing bacterial growth rates throughout the spring as water temperature increases select for smaller sized bacteria. On the other hand, we may simply have observed shifts in the bacterial species composition.

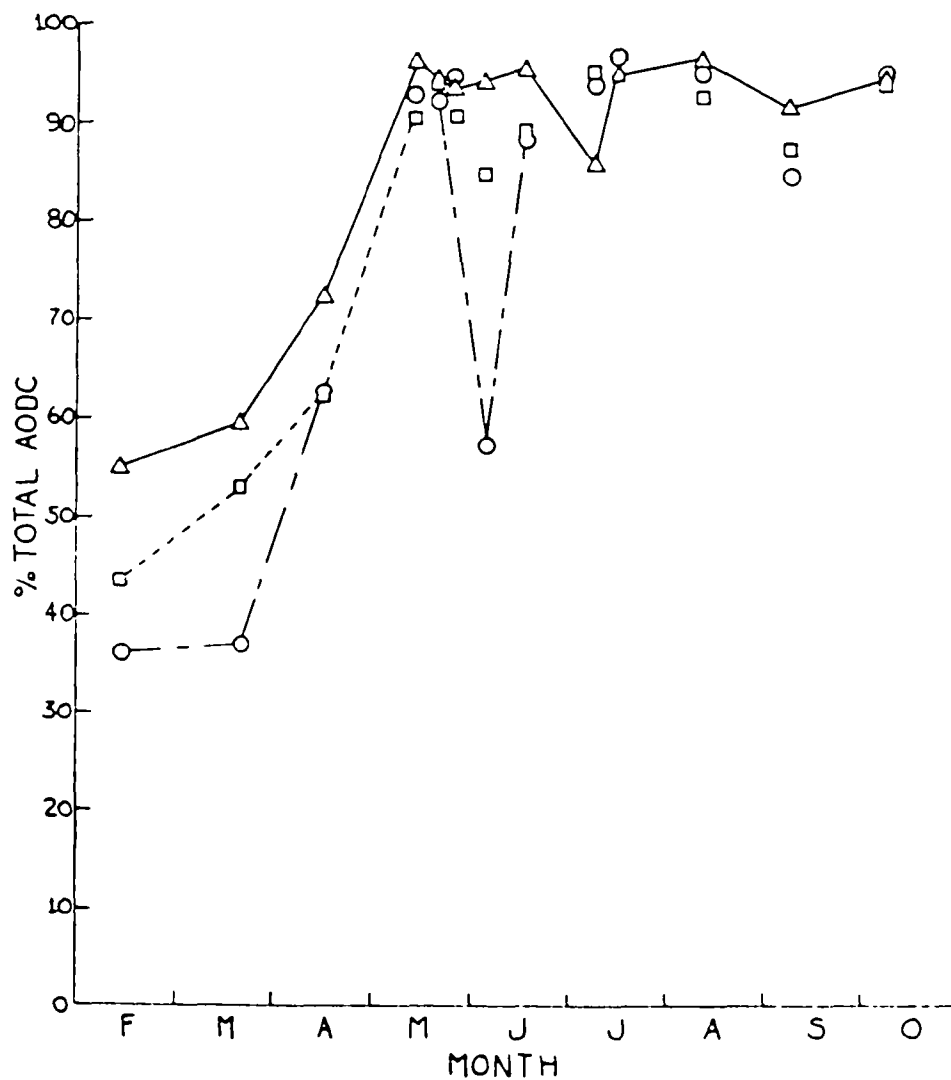


Figure 37. The percent of total bacterial abundance within the euphotic zone attributable to bacteria smaller than 1 μ m along transects 1 (Δ), 2 (\circ), and 3 (\square) during 1985.

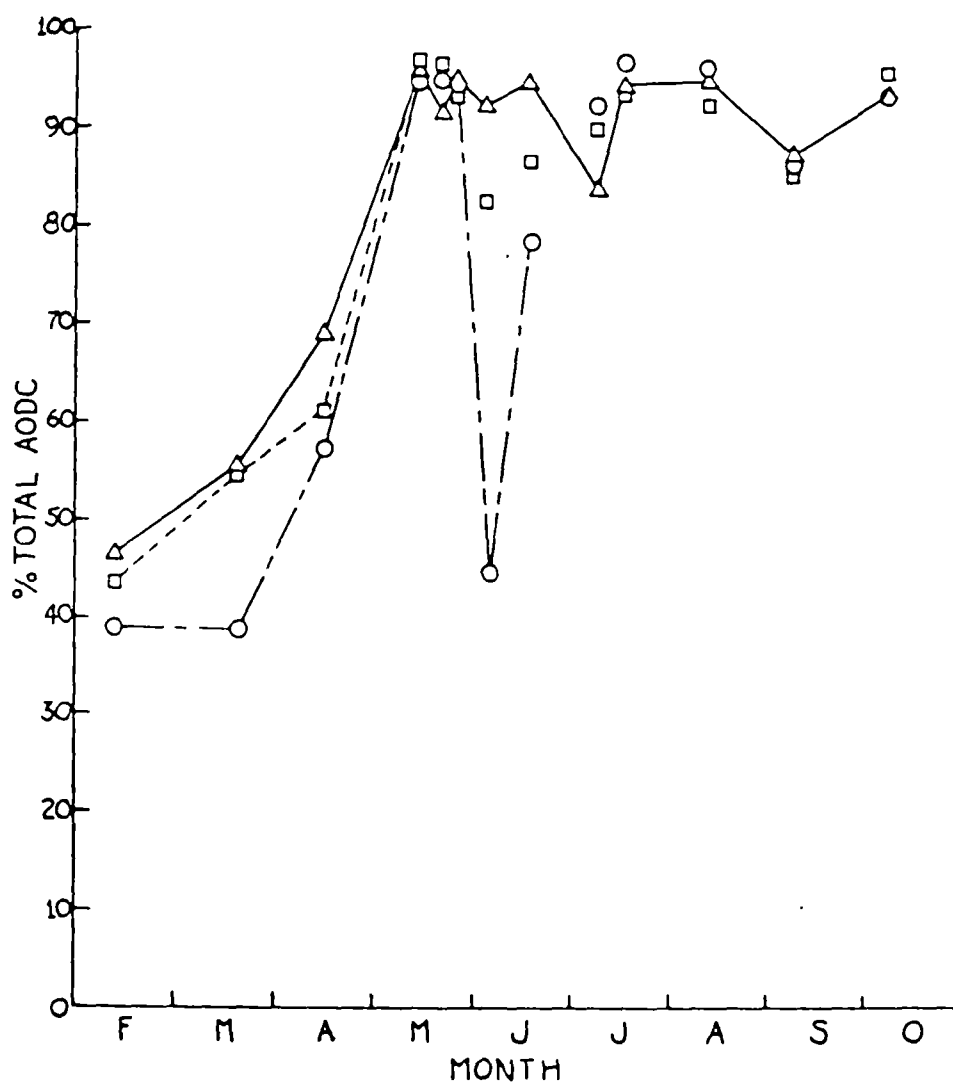


Figure 38. The percent of total bacterial abundance below the euphotic zone attributable to bacteria smaller than 1 μ m along transects 1 (Δ), 2 (O), and 3 (\square) during 1985.

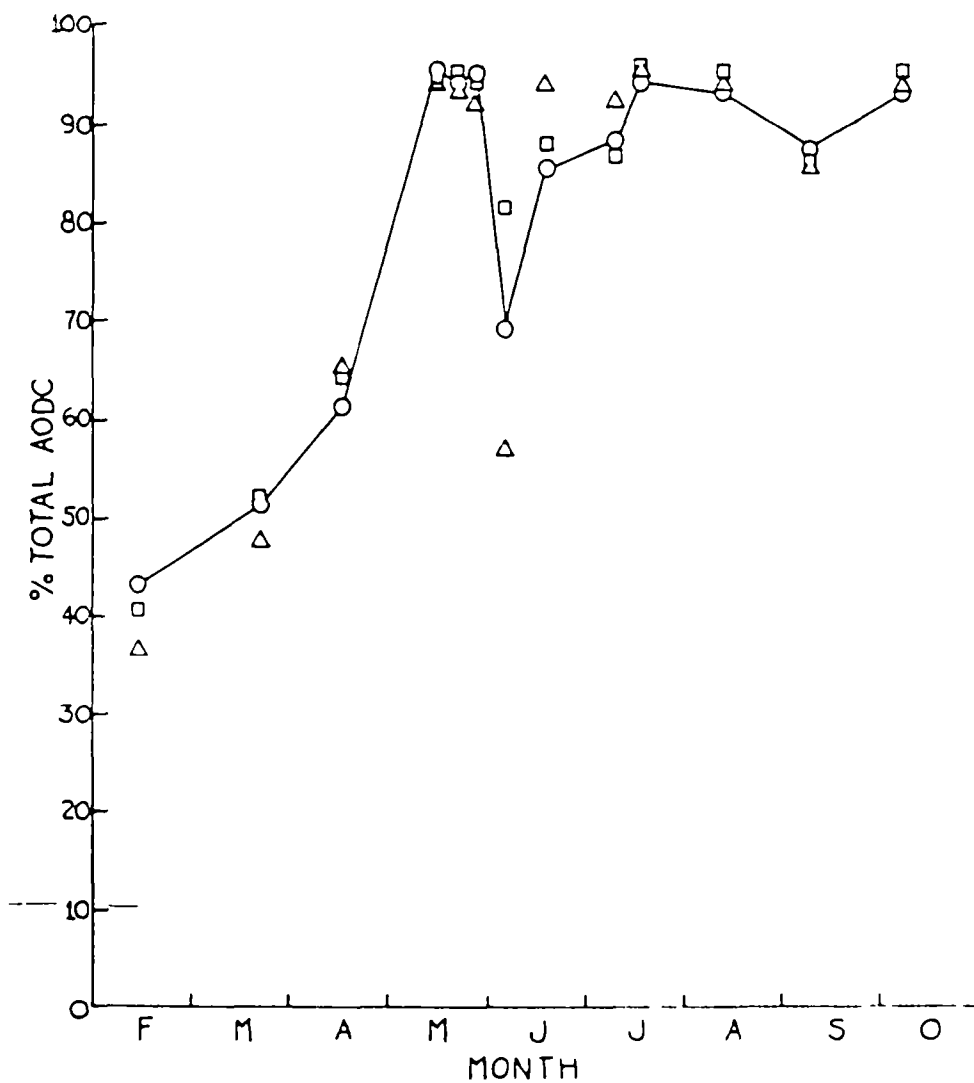


Figure 39. The percent of total bacterial abundance attributable to bacteria smaller than 1 μ m along the west flank (Δ), main channel (O), and east flank (\square) of Chesapeake Bay during 1985. Percentages are calculated from means of data from all three lateral transects.

Bacterial Production

Temporal Changes along the Main Channel

In agreement with bacterial abundance, bacterial production was low in late winter with TdR averaging about 10 pmol/l/h (Fig. 40). Production increased rapidly in the spring with increasing water temperatures, almost reaching summer levels by late April. At this time, mid and bottom water TdR often equaled or exceeded summer values. Bacterial production decreased abruptly in mid-May at all three deep stations, coincident with decreases in bacterial abundance and one week before the rapid reduction in phytoplankton biomass and production over the entire study area. The decreases in bacterial production were greater at station 24 than at either of the more northern stations.

Rapid recovery of bacterial production followed the phytoplankton decline, particularly in near surface waters at station 32 (Fig. 40). High surface water production (TdR >200 pmol/l/h) was characteristic of station 32 from late May to mid-July and from late August to late September. Farther south at station 3, high surface water production extended from early June to late August. High production in surface waters was less frequent at station 24. Episodes of very high, near surface water production occurred at all three deep stations, but were not necessarily coincident along the main axis of the Bay.

Bacterial production in deep water was usually highest to the north at station 32 where TdR often equaled or exceeded 100 pmol/l/h from mid-April to mid-September (Fig. 40). A notable exception to this pattern occurred during July and early August just before the onset of anoxia (Fig. 9). Deep water bacterial production at station 3 was similar to station 32 except that

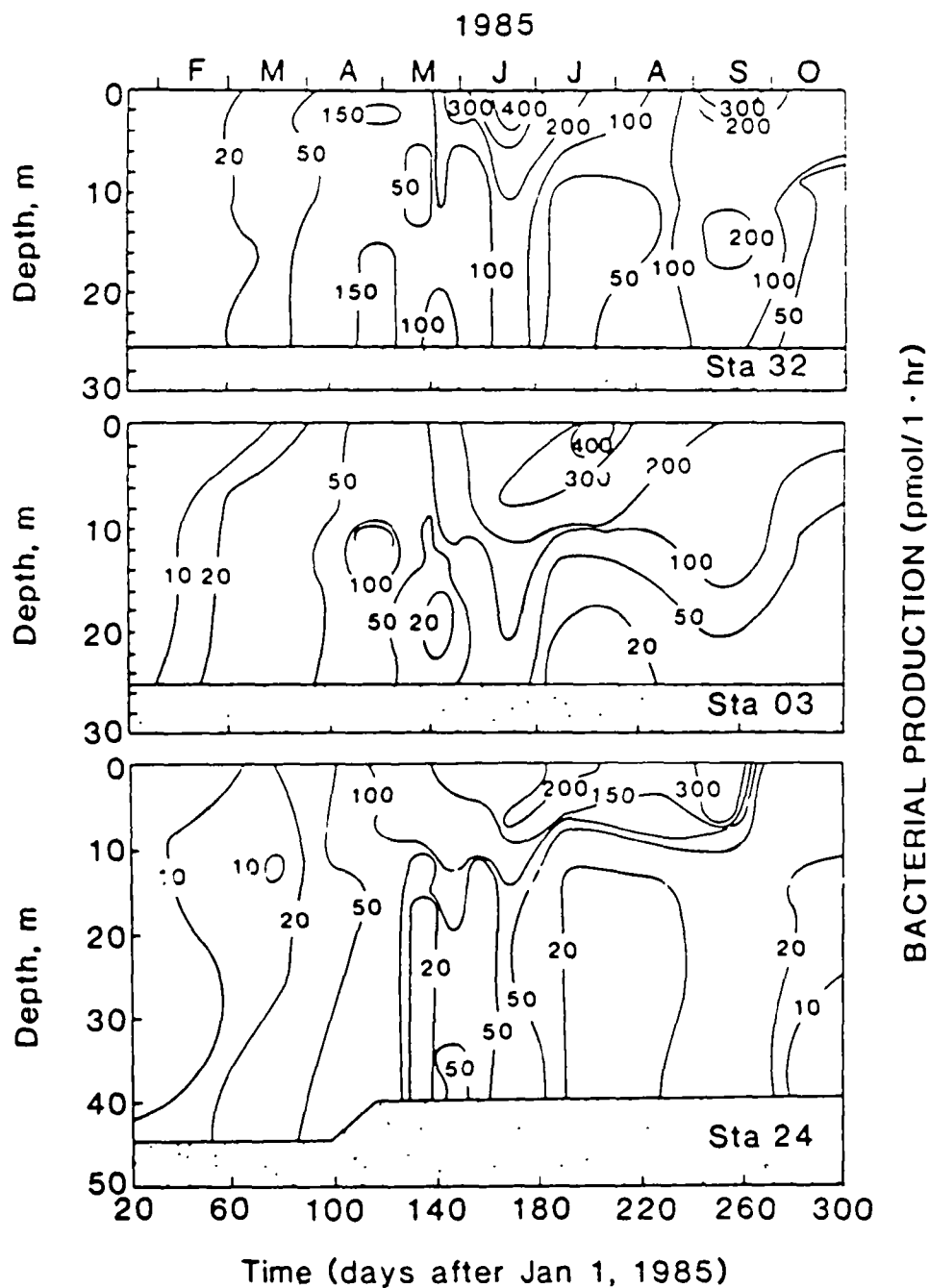


Figure 40. Time-dependent vertical variations in bacterial production along a north-south (station 32 to 24) main channel transect. Values on contour lines represent TdR in $\text{p mol L}^{-1} \text{ h}^{-1}$.

production in near bottom water was usually lower farther north (i.e. at station 32) and TdR isoclines closely followed salinity contours (Fig. 3) during the summer. At station 24, bacterial production below the pycnocline (10-12 m depth) never exceeded TdR values of 50 pmol/l/h.

A synopsis of bacterial production profiles across lateral transect 2 is shown in Figures 41-45. Early in the year bacterial production exhibited little in the way of a pattern with TdR in deep channel water likely to be as high as in surface water on the flanks (Fig. 41). Later in the spring the response of bacterial production to the spring phytoplankton bloom and the subsequent reduction in bacterial production are clearly evident (Fig. 42). Within 12 days after the bacterial decline and within 7 days after the phytoplankton decline (cruise 7, Fig. 43), bacterial production had recovered to spring bloom levels and thereafter continued to increase into the summer. By early July (Fig. 44) summer conditions had become established, marked by high bacterial production in surface waters and on the flanks and much lower production in the deep waters, decreasing with depth at deep channel stations. From late April (Fig. 42) on, bacterial production isoclines followed salinity contours (Figs. 29-32, 42-45). A noticeable decrease of bacterial production was observed from mid-September to mid-October (Fig. 45), signaling the end of summer conditions.

Differences with Depth

As we observed with bacterial abundances (Fig. 33), mean bacterial production early in the year was similar within and beneath the euphotic zone (Fig. 46). However, mean bacterial production within the euphotic zone began to exceed production below the euphotic zone nearly two weeks before

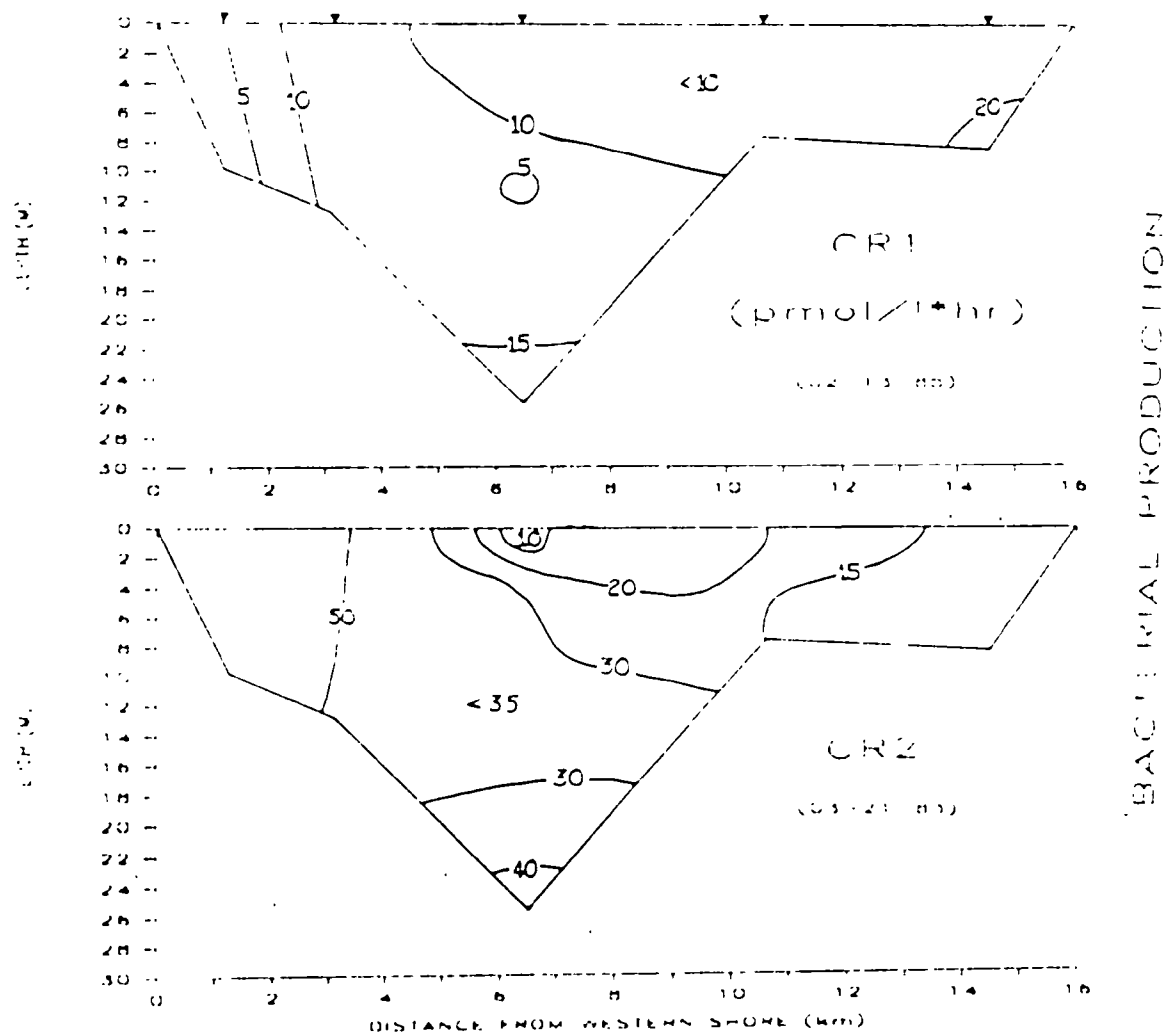


Figure 41. Lateral distribution of bacterial production along transect 2 for the period 13 Feb. - 21 Mar. 1985.

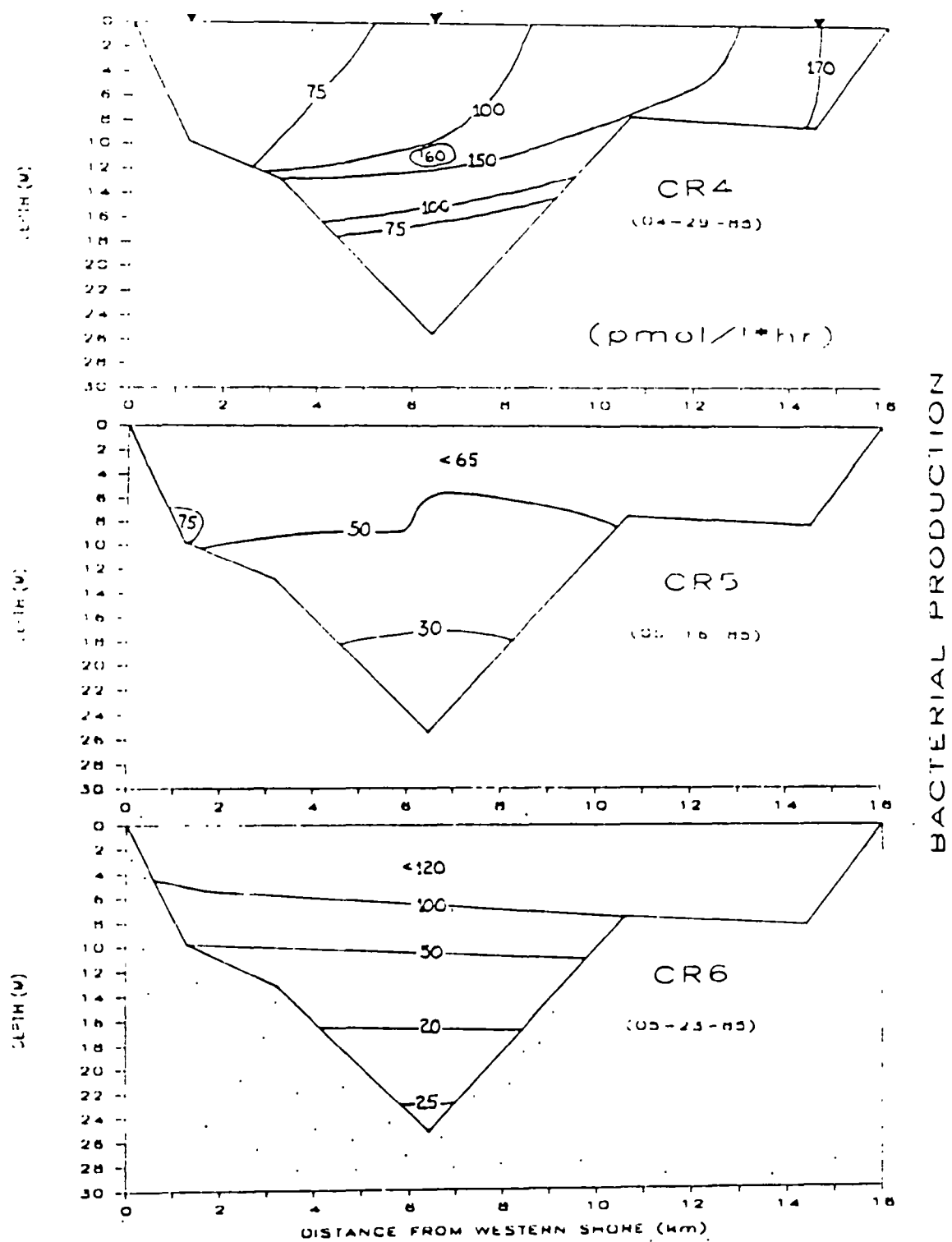


Figure 42. Lateral distribution of bacterial production along transect 2 for the period 29 Apr. - 23 May 1985.

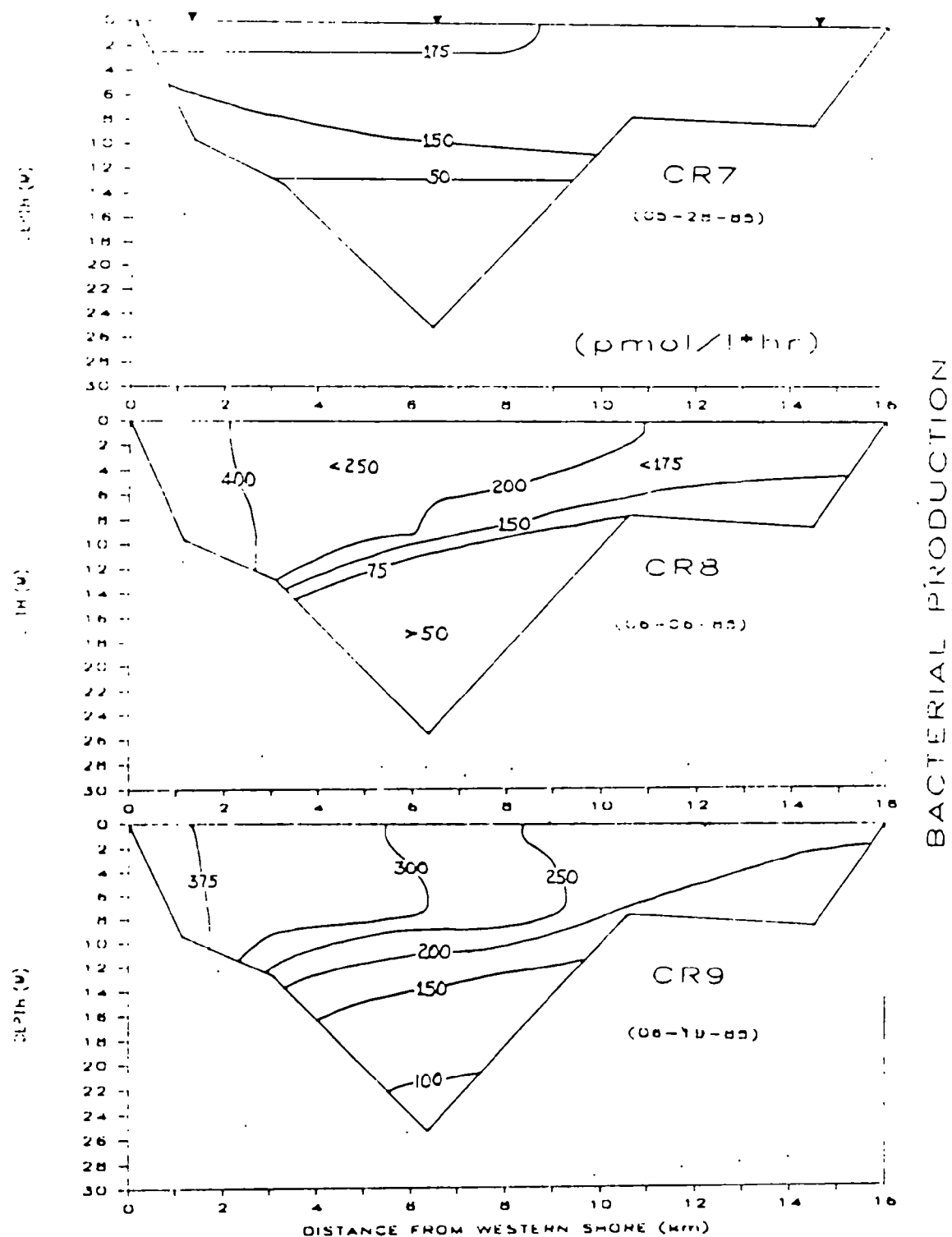


Figure 43. Lateral distribution of bacterial production along transect 2 for the period 28 May - 19 June 1985.

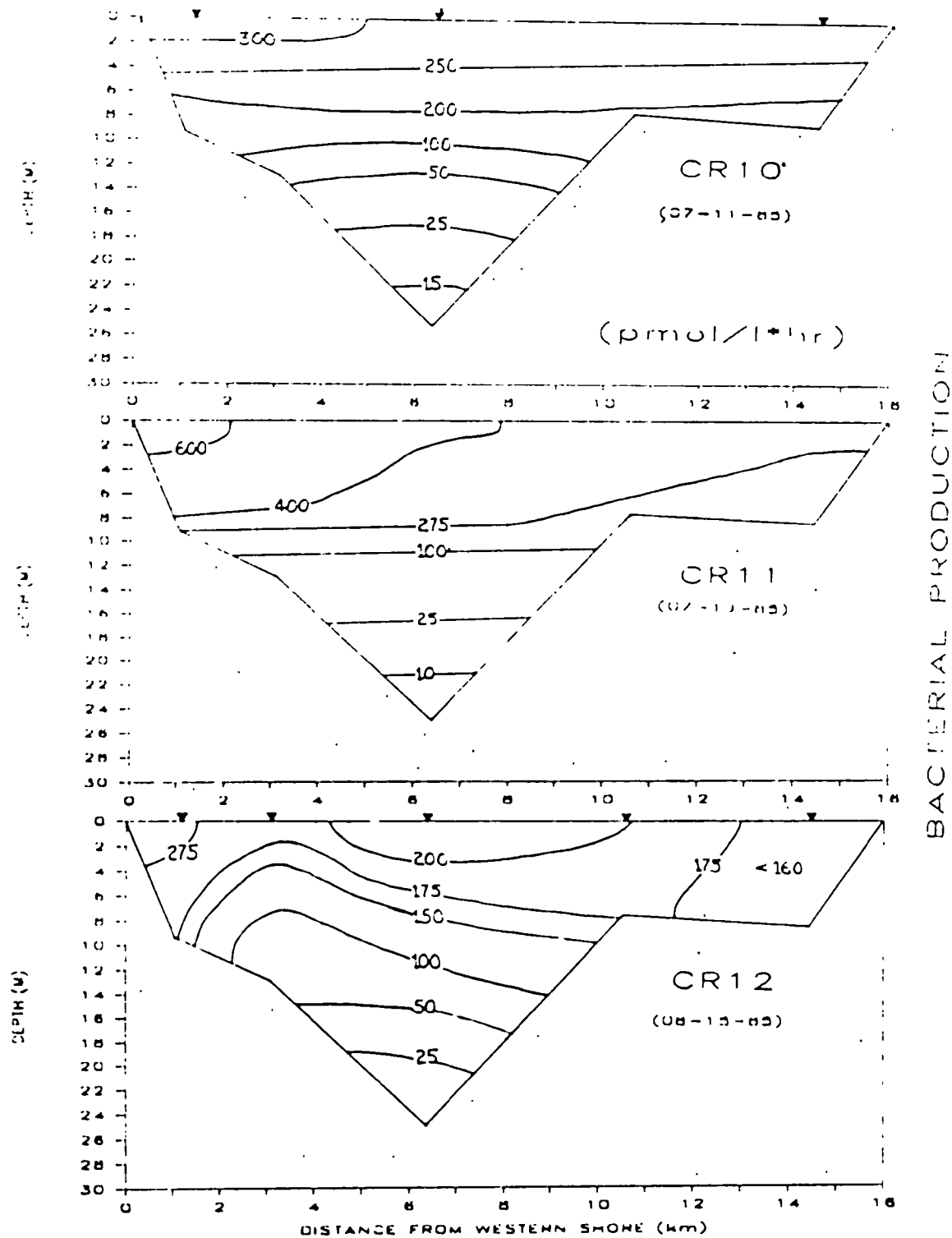


Figure 44. Lateral distribution of bacterial production along transect 2 for the period 11 July - 15 Aug. 1985.

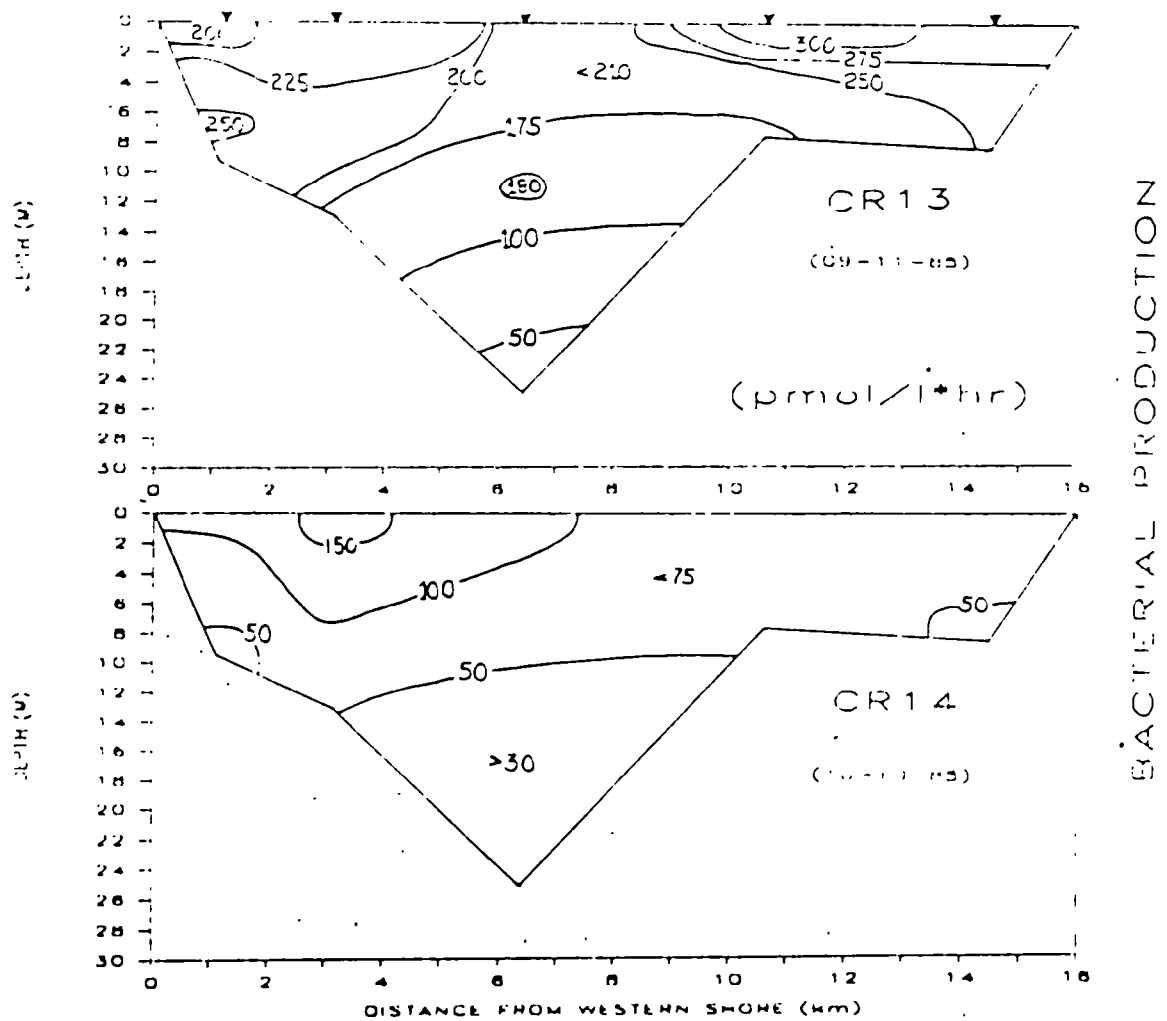


Figure 45. Lateral distribution of bacterial production along transect 2 for the period 11 Sep. - 10 Oct. 1985.

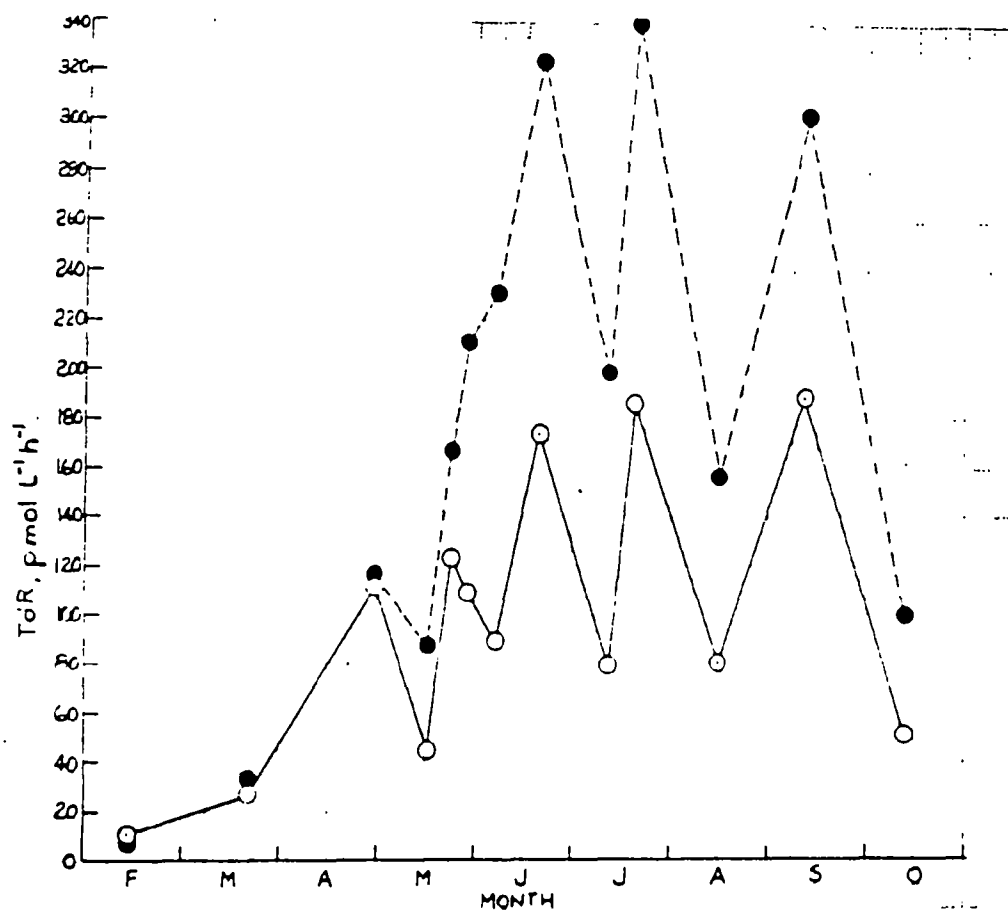


Figure 46. Mean bacterial production, expressed as TdR, within (●) and below (○) the euphotic zone for transects 1-3 during 1985.

bacterial abundances exhibited the same pattern. The time difference between the changes in within and beneath euphotic zone ratios of bacterial biomass and production may be indicative of an increase in the biomass specific growth rate of euphotic zone bacteria. Alternatively, bacteria below the euphotic zone may have been subjected to increased removal pressure (e.g. predation).

Following the mid-May decline of bacterial production, euphotic zone production oscillated throughout the remainder of the study (Fig. 46). Peaks of production occurred in late June, late July and mid-September. Four peaks were found below the euphotic zone, three of which were coincident with euphotic zone maxima and a fourth which occurred in late May during the phytoplankton decline (Tables 3 and 4). The frequency of oscillation and/or timing of actual peaks may have been different than the data indicate. More frequent sampling intervals (such as the twice weekly sampling intervals of 1984) would have been necessary to resolve this problem.

North to South Differences

Bacterial production was generally highest farthest to the north from February to mid-July (Fig. 47). This was true both within (Fig. 48) and below (Fig. 49) the euphotic zone. Mean bacterial production below the euphotic zone was greater at either transect 1 or 2 than at the southern-most transect 3. When expressed as transect means (Figs. 48 and 49), the production data from mid-May to mid-October indicate three coincident peaks within and below the euphotic zone at transect 1, two of which (mid-June and mid-September) also occurred along transects 2 and 3. The third peak in late May occurred only below the euphotic zone at the two southern-most transects (Fig. 49).

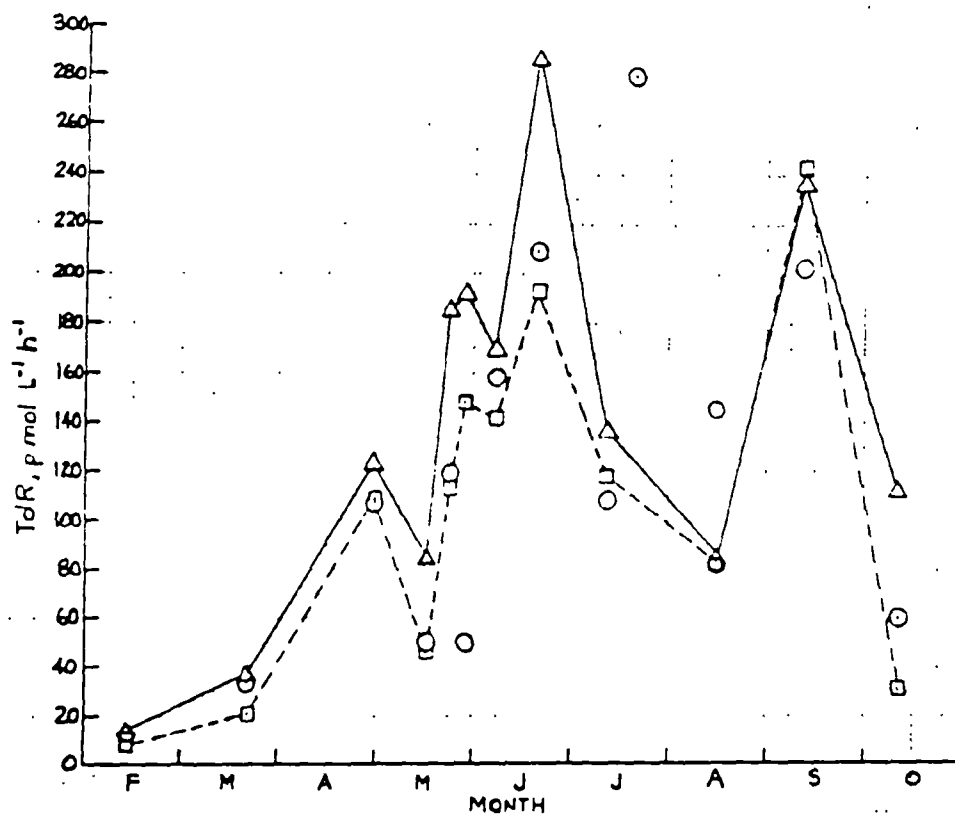


Figure 47. Mean bacterial production, expressed as TdR, along transects 1 (Δ), 2 (○), and 3 (□) during 1985.

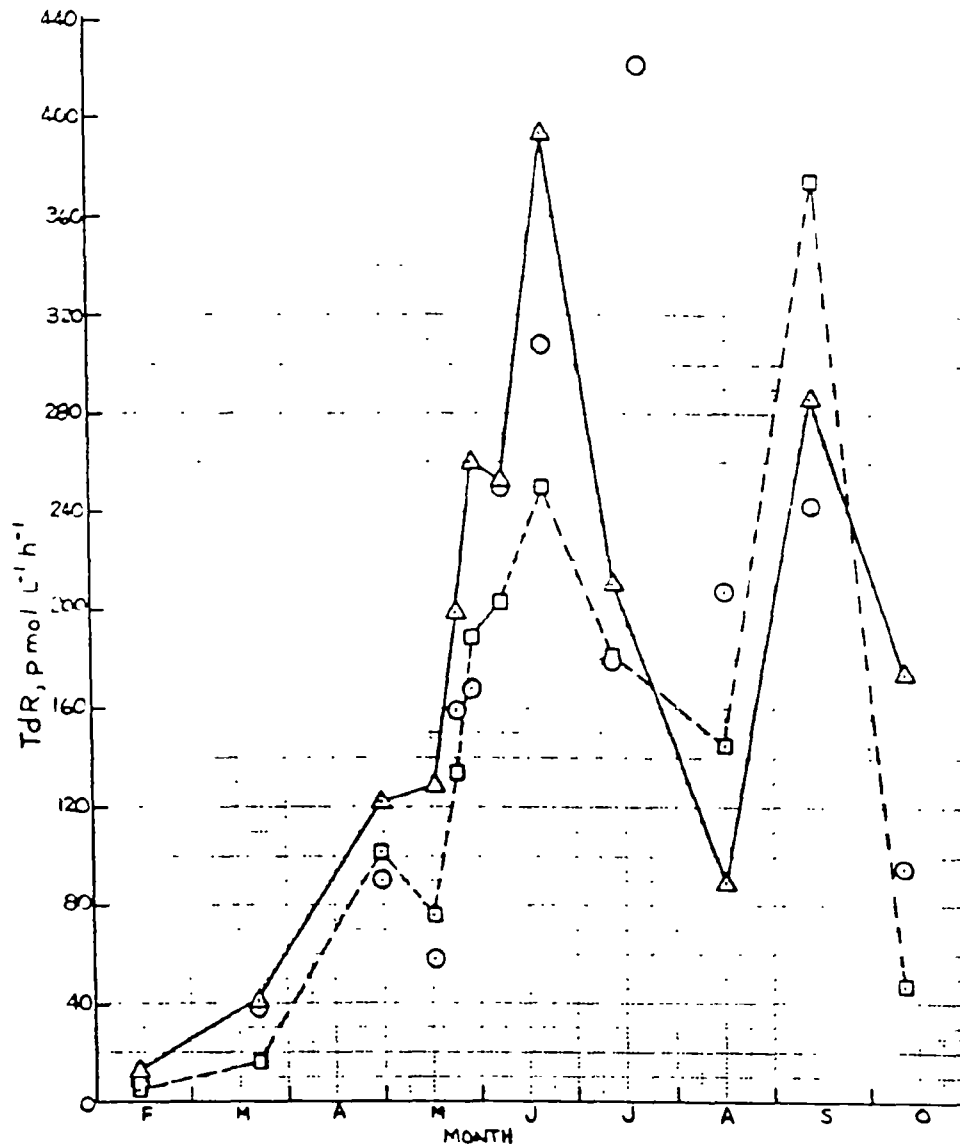


Figure 48. Mean bacterial production, expressed as TdR, within the euphotic zone along transects 1 (Δ), 2 (\circ), and 3 (\square) during 1985.

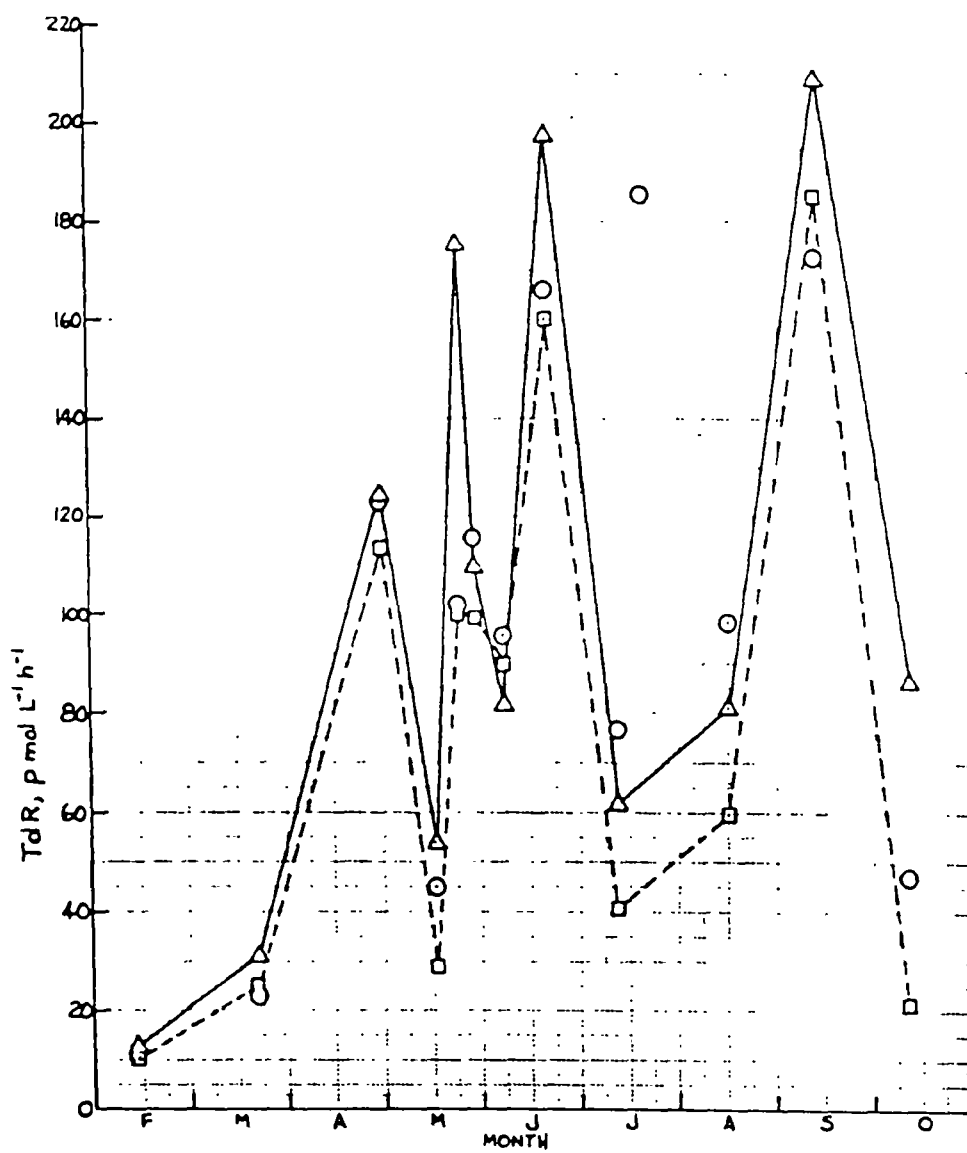


Figure 49. Mean bacterial production, expressed as TdR, below the euphotic zone along transects 1 (Δ), 2 (○), and 3 (□) during 1985.

East to West Differences

Mean bacterial production was relatively constant across the Bay until the spring phytoplankton bloom in late April to mid-May when production was greatest along the eastern flank (Fig. 50). Following the mid-May bacterial decline, however, bacterial production tended to be much greater over both flanks than over the deep channel (with the exception of the east flank along transect 2 in late July). Unlike bacterial abundance (Fig. 36), bacterial production in the late spring to mid-summer was often greater to the west than to the east (Fig. 50). During mid-August to mid-September, however, production to the east exceeded production to the west, consistent with the same time period in 1984 (Tuttle et al. 1985). In contrast to 1984, bacterial abundance was also higher to the east than to the west in the late summer (Fig. 36).

Amino Acid Metabolism

Temporal Changes along the Main Channel

Amino acid metabolism (expressed as turnover rate) was low in late winter but began to increase rapidly in the spring (Fig. 51) in a pattern similar to bacterial abundance (Fig. 22) and production (Fig. 40). This increase was most rapid at station 32 until mid-April when contours were similar for station 24. High amino acid turnover rates accompanied the spring phytoplankton maximum with the greatest responses in mid and deep waters at stations 3 and 24. Turnover rates observed at these stations were the maximum values measured during the study. While amino acid metabolism at station 32 also increased, the response was less than at the more southerly mainstem stations except in surface waters. The bacterial decline in mid-May

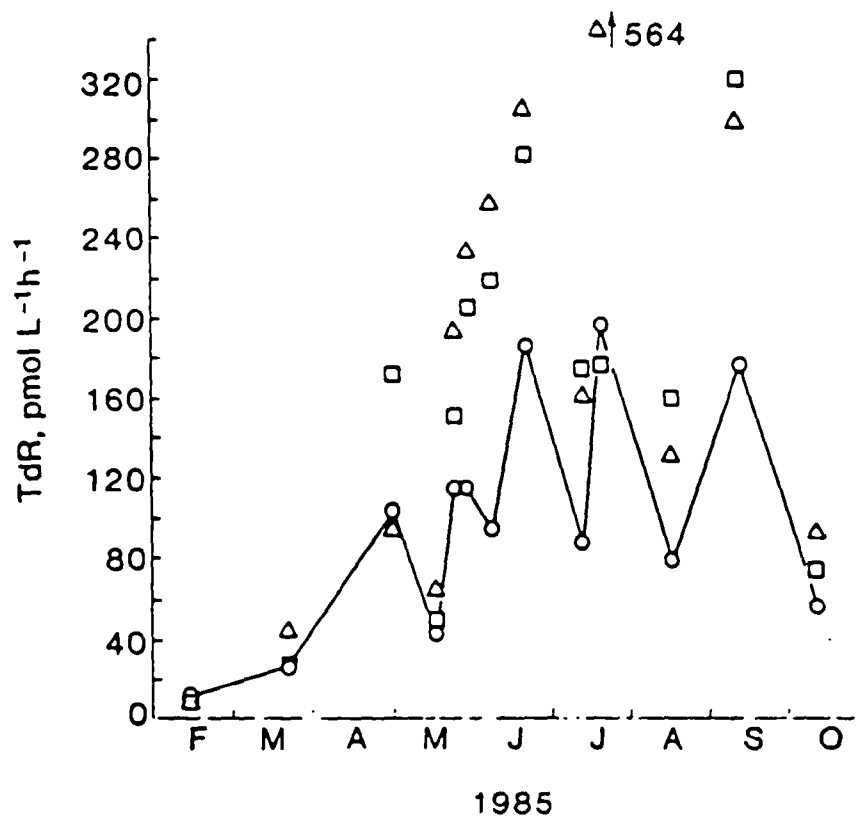


Figure 50. Mean bacterial production, expressed as TdR, along the west flank (△), main channel (○), and east flank (□) of Chesapeake Bay during 1985. Values are means of data from all three lateral transects.

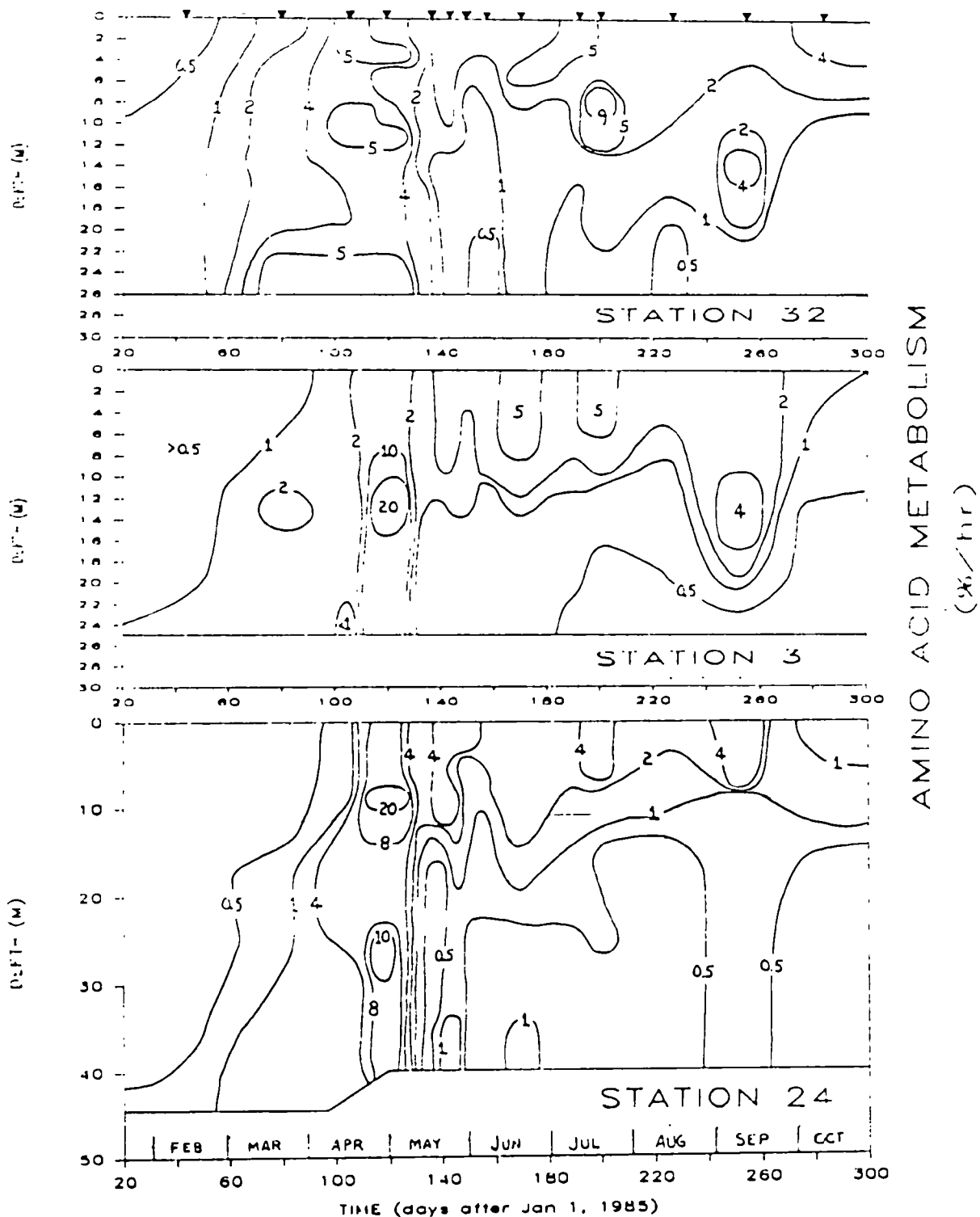


Figure 51. Time-dependent vertical variations in amino acid metabolism along a north-south (station 32 to 24) main channel transect. Solid triangles at the top indicate cruise dates. Values on contour lines represent amino acid turnover rates expressed as % of amino acid pool h^{-1} .

was accompanied by greatly decreased amino acid metabolism all along the north-south transect. Unlike bacterial production (Fig. 40), amino acid metabolism failed to recover to levels measured during the spring phytoplankton bloom except at station 32, and only there in surface waters or near the pycnocline. During summer conditions, subpycnocline amino acid metabolism did not exceed 1 to 2%/h except in mid-September at stations 32 and 3. The mid-water maxima found then at these stations were not observed at station 24.

Amino acid metabolism across transect 2 increased from February to March, decreased in mid-April and then increased to maximum levels in late April during the spring phytoplankton maximum (Figs. 52 and 53). The highest turnover rates were measured in mid and deep water, but rapid metabolism also occurred near the western shore and across the eastern flank (Fig. 53). The yearly maximum in metabolic rates measured on 29 April were followed by a sharp decline of amino acid metabolism on 16 May during the decline in bacterial abundance (Fig. 24) and production (Fig. 42). Within one week (cruise 6, Fig. 53), amino acid metabolism increased in surface and mid-waters coincident with the dramatic phytoplankton decline observed on the same day. However, turnover rates on this and on subsequent cruises throughout the remainder of spring and summer (Figs. 54-56) never reached values measured on 29 April.

The relationship of amino acid metabolism (Figs. 52-56) to salinity (Figs. 28-32) was irregular. On cruises 4 (Figs. 29 and 53), 9 (Figs. 30 and 54), 10 (Figs. 31 and 55), 13 and 14 (Figs. 32 and 56), amino acid metabolism tended to follow salinity contours. On cruises 8 (Figs. 30 and 54) and 11 (Figs. 31 and 55) amino acid metabolism isoclines appeared to be in opposi-

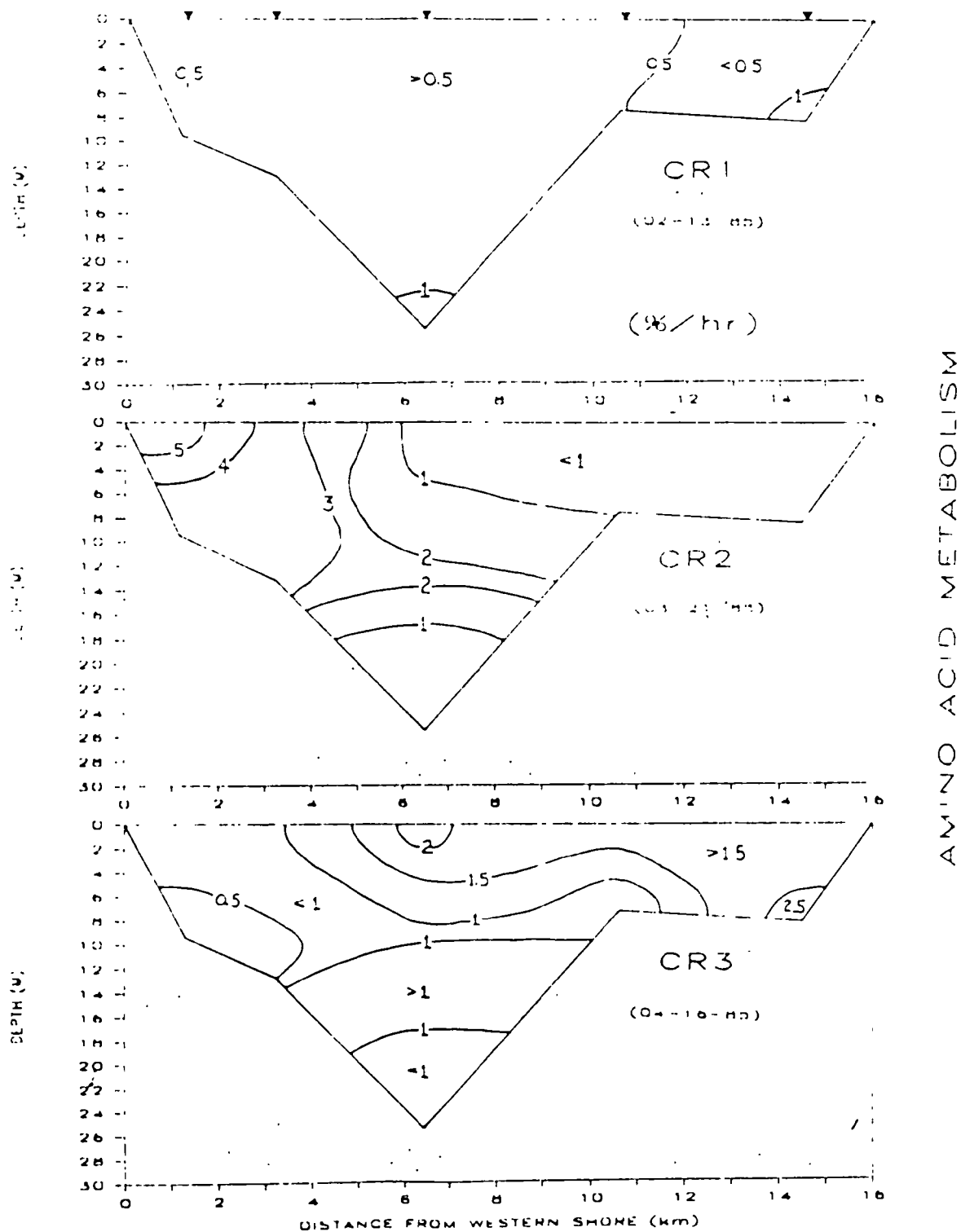


Figure 52. Lateral distribution of amino acid metabolism, expressed as amino acid turnover rates, along transect 2 for the period 15 Feb. - 21 Mar. 1985.

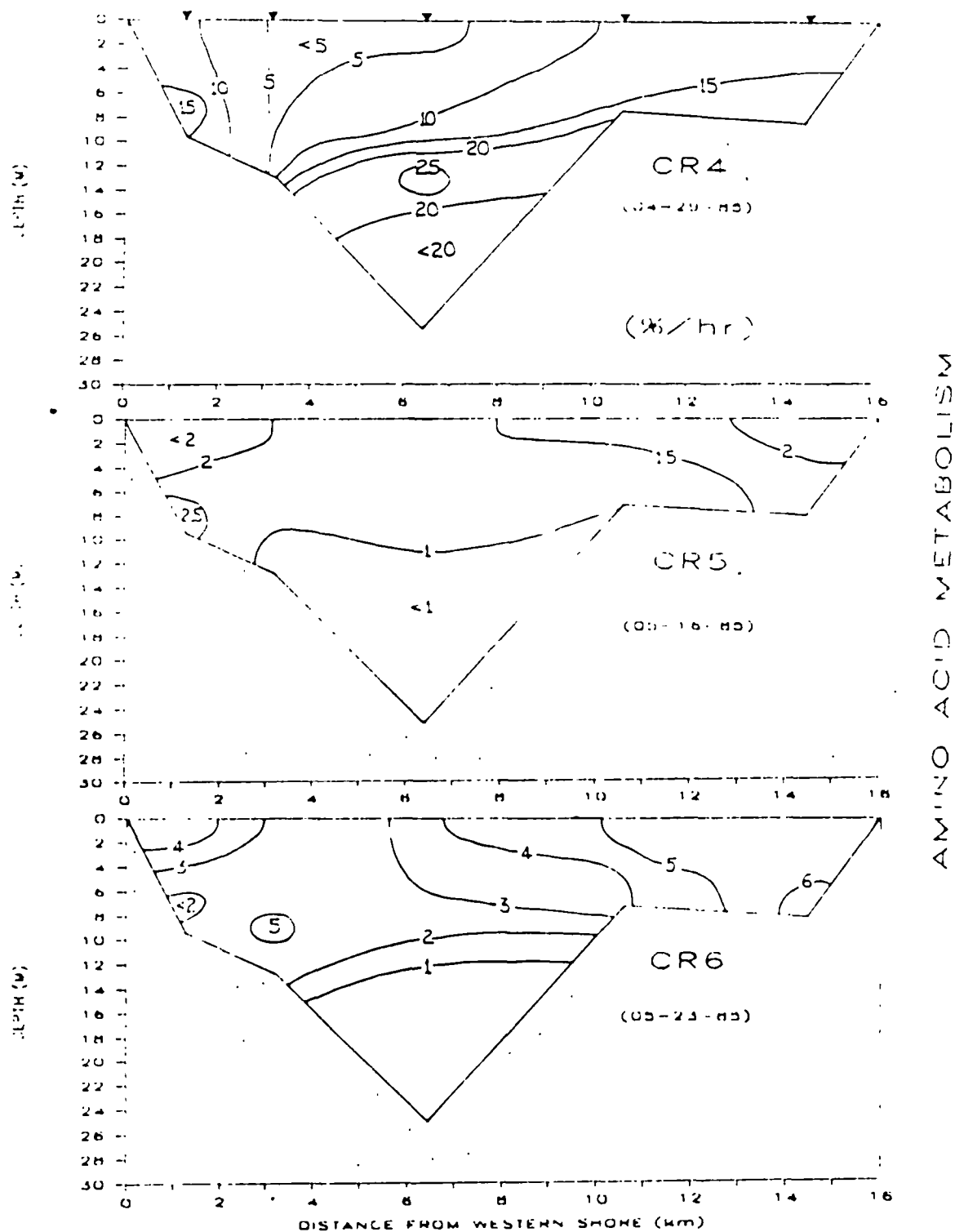


Figure 53. Lateral distribution of amino acid metabolism, expressed as amino acid turnover rates, along transect 2 for the period 29 Apr. - 23 May 1985.

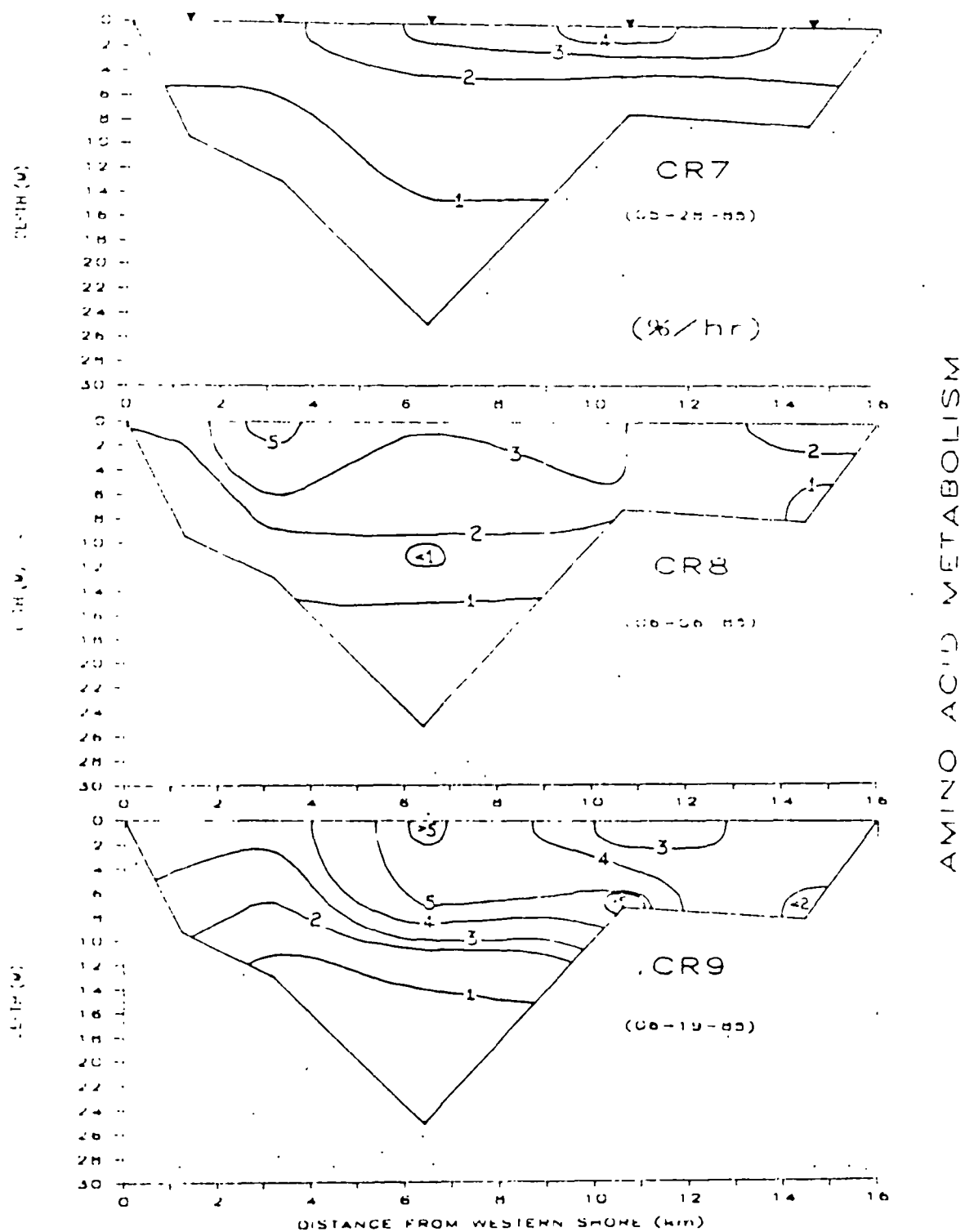


Figure 54. Lateral distribution of amino acid metabolism, expressed as amino acid turnover rates, along transect 2 for the period 28 May - 19 June 1985.

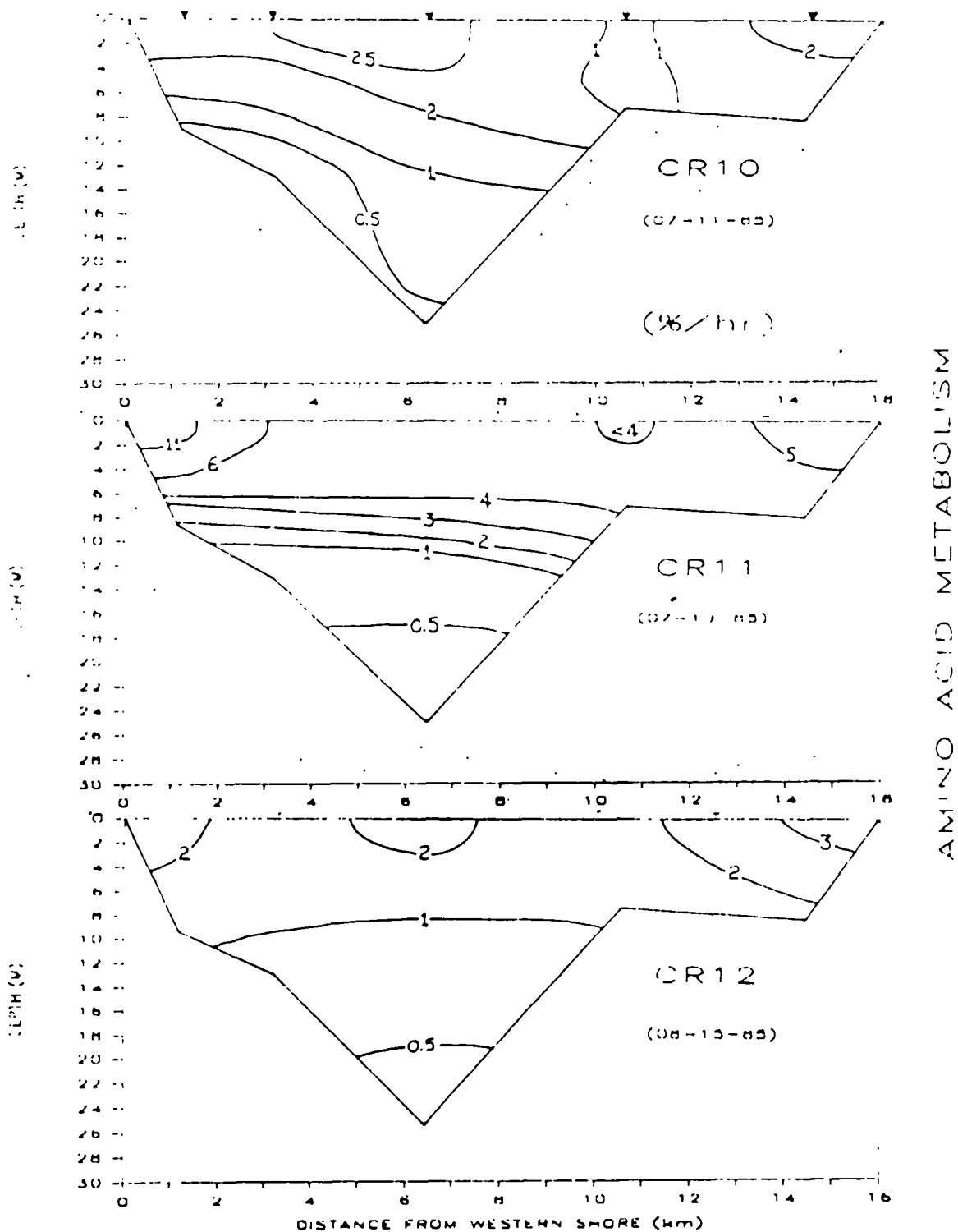


Figure 55. Lateral distribution of amino acid metabolism, expressed as amino acid turnover rates, along transect 2 for the period 11 July to 15 Aug. 1985.

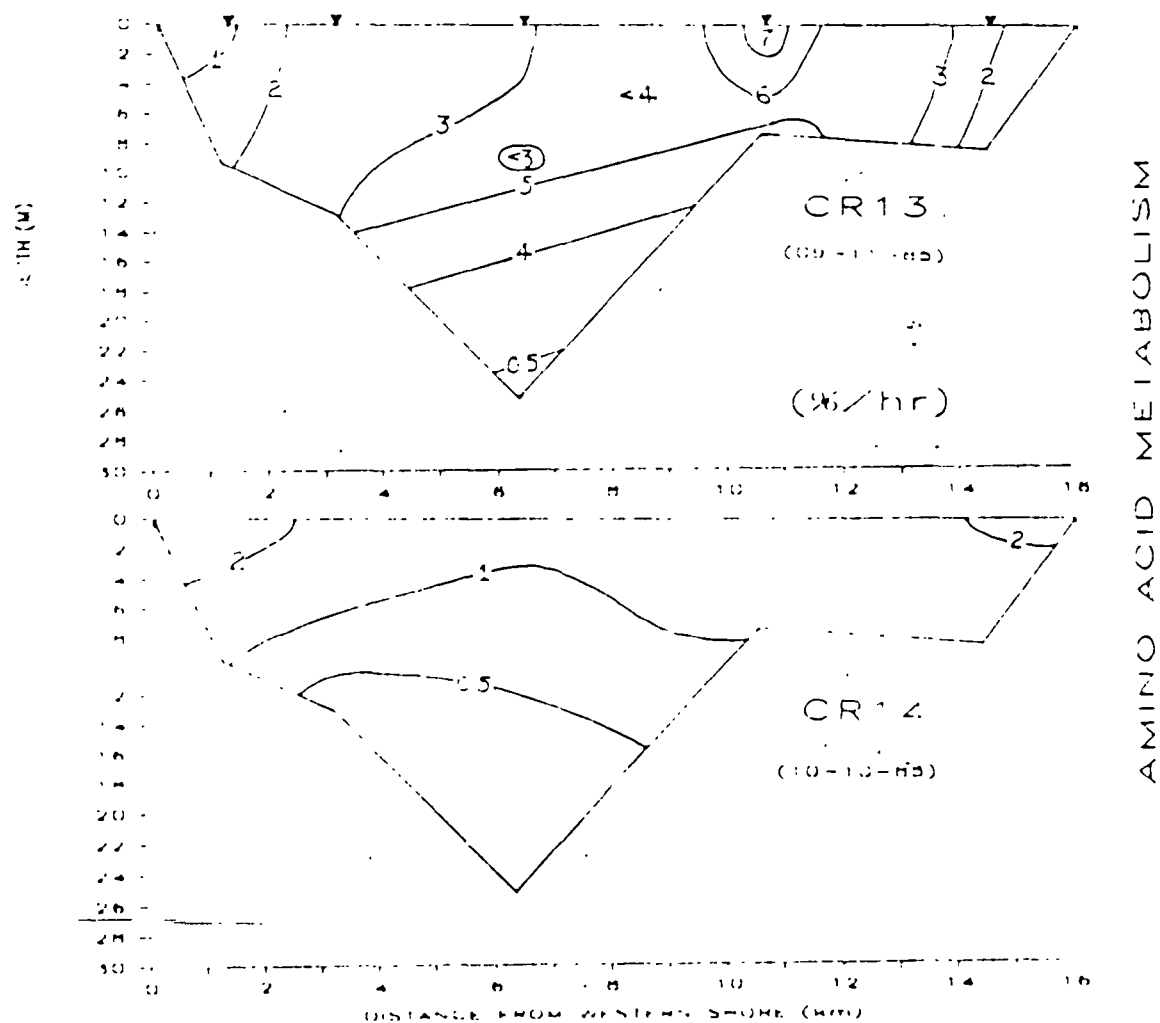


Figure 56. Lateral distribution of amino acid metabolism, expressed as amino acid turnover rates, along transect 2 for the period 11 Sep. - 10 Oct. 1985.

tion to salinity contours.

Differences with Depth

Mean amino acid turnover rates for the entire study area are shown in Fig. 57. In agreement with bacterial production estimates (Fig. 46), amino acid metabolism was most rapid below the euphotic zone until the mid-May bacterial decline when it became higher in the euphotic zone and remained so throughout the study period. The amino acid metabolism data were characterized by a series of oscillations with 5 peaks, the largest of which coincided with the spring phytoplankton bloom. All these peaks occurred simultaneously above and below the euphotic zone and coincided with peaks of bacterial production (Fig. 46).

North to South Differences

From February to mid-April, mean amino acid turnover rates were highest along transect 1 within and below the euphotic zone (Figs. 58 and 59). This was also true of the late June to mid-August period, but the differences between rates at transects 1 and 3 were small, particularly within the euphotic zone. All five amino acid metabolism peaks were coincident at transects 2 and 3 within and below the euphotic zone.

Mean amino acid metabolism at transect 1 did not always coincide with the two transects to the south. For example, the mid-September peak across transects 2 and 3 did not occur at all in the euphotic zone at transect 1 (Fig. 58) and was only a minor peak below the euphotic zone (Fig. 59). The late May euphotic zone peak at transect 1 occurred five days later than at transects 2 and 3 (Fig. 58).

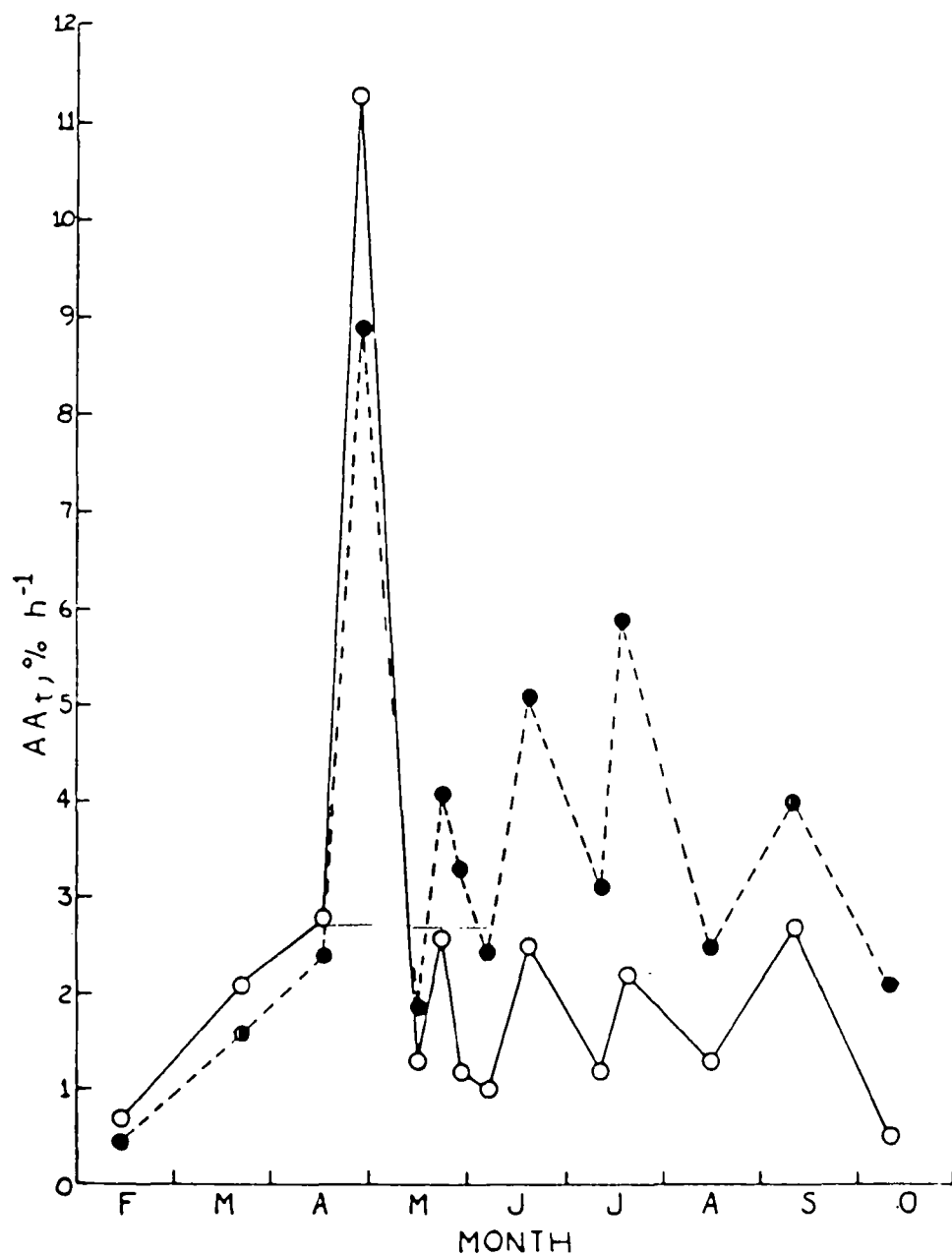


Figure 57. Mean amino acid metabolism, expressed as amino acid turnover rates, within (●) and below (○) the euphotic zone for transects 1-3 during 1985.

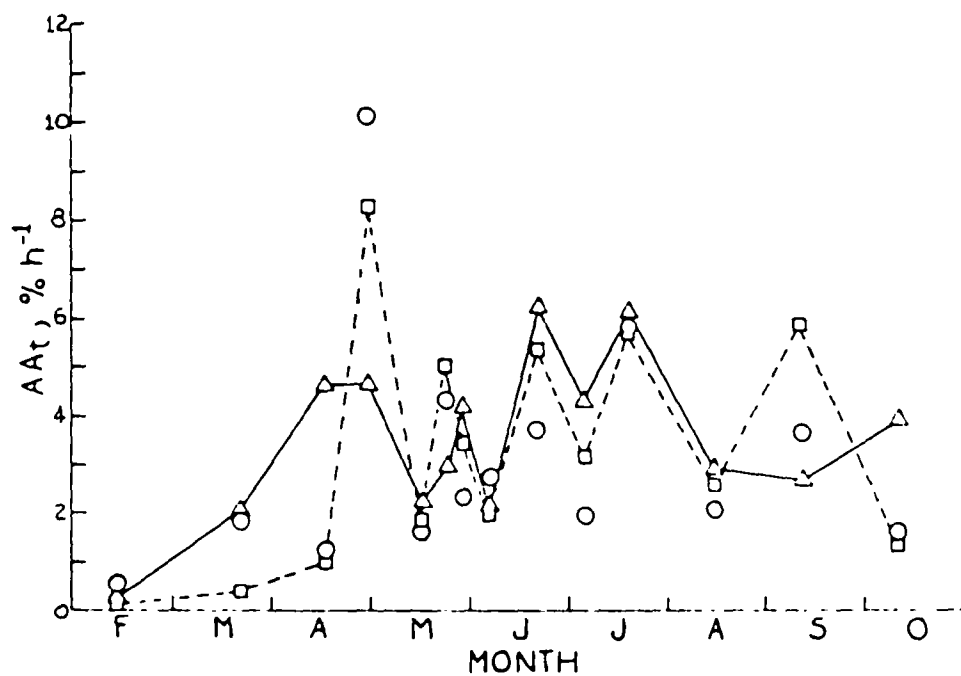


Figure 58. Mean amino acid metabolism, expressed as amino acid turnover rates, within the euphotic zone along transects 1 (Δ), 2 (\circ), and 3 (\square) during 1985.

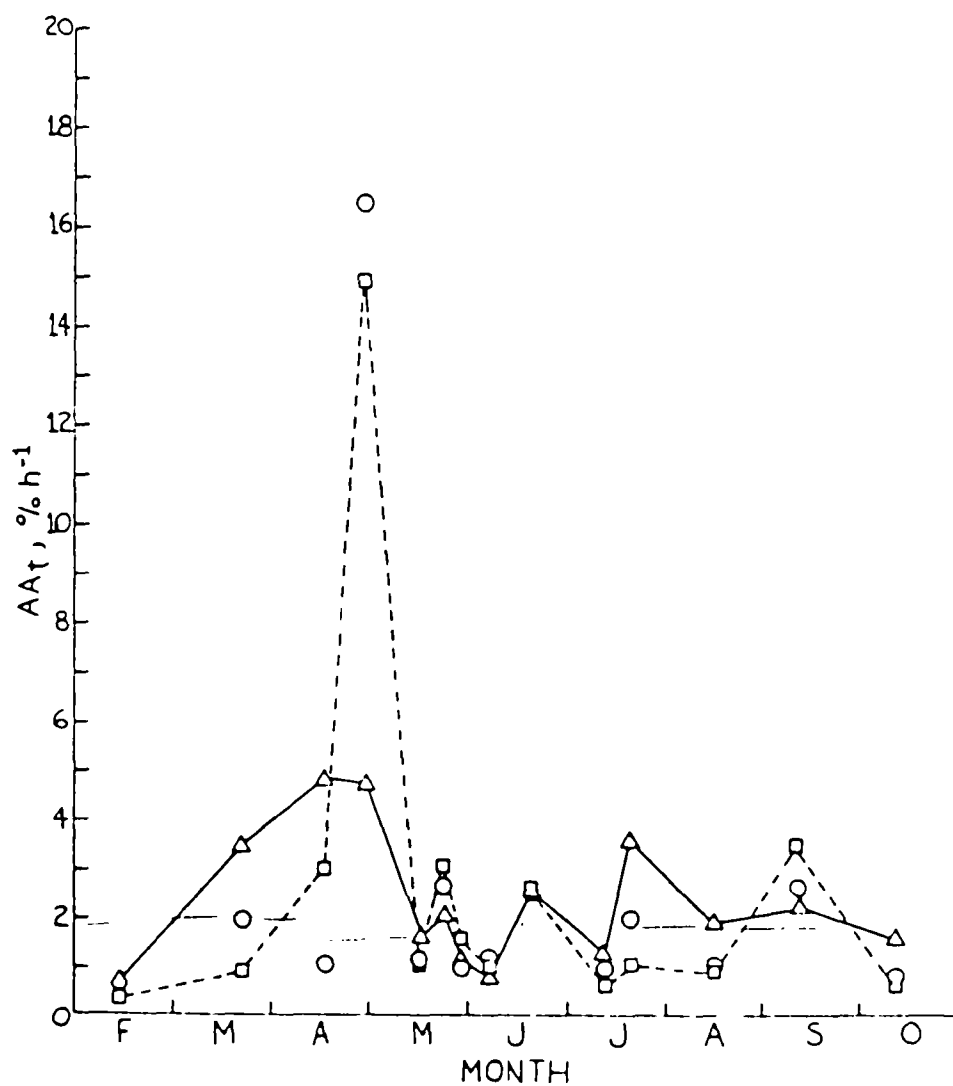


Figure 59. Mean amino acid metabolism, expressed as amino acid turnover rates, below the euphotic zone along transects 1 (Δ), 2 (○), and 3 (□) during 1985.

The fact that the 29 April peak was substantially greater at the southerly transects than at transect 1 (Figs. 58 and 59) may be significant with respect to bacterial production means measured on the same day (Figs. 48 and 49). Comparison of bacterial production with amino acid metabolism at each of the transects suggests that amino acid metabolism was uncoupled from bacterial production, especially at transects 2 and 3; that amino acid pools were lower in late April than during the summer when bacterial production was higher but amino acid turnover was lower; or that the bacterial community at transect 1 was also using carbon and energy sources other than amino acids to support growth. We have insufficient information to decide among these possibilities.

We did not measure amino acid respiration during 1985. However, respiration measurements made during summer and fall cruises in 1984 indicated the respiration accounted for 40% of total amino acid metabolism (Tuttle et al. 1985). Summer 1985 amino acid turnover rates corrected for respiration are similar to the rates found in summer 1984.

East to West Differences

From late April throughout the remainder of the study, mean amino acid metabolism along the flanks exceeded metabolism over the main channel (Fig. 60). After the mid-May bacterial decline the differences along the eastern flank compared to the western flank were small, but mean amino acid turnover to the east exceeded that to the west at each of the peak events.

Glucose Metabolism

Our 1984 amino acid metabolism data correlated well with chlorophyll a and bacterial production estimates (Tuttle et al. 1985). This suggested that amino acids were a reasonable surrogate for phytoplankton carbon capable of

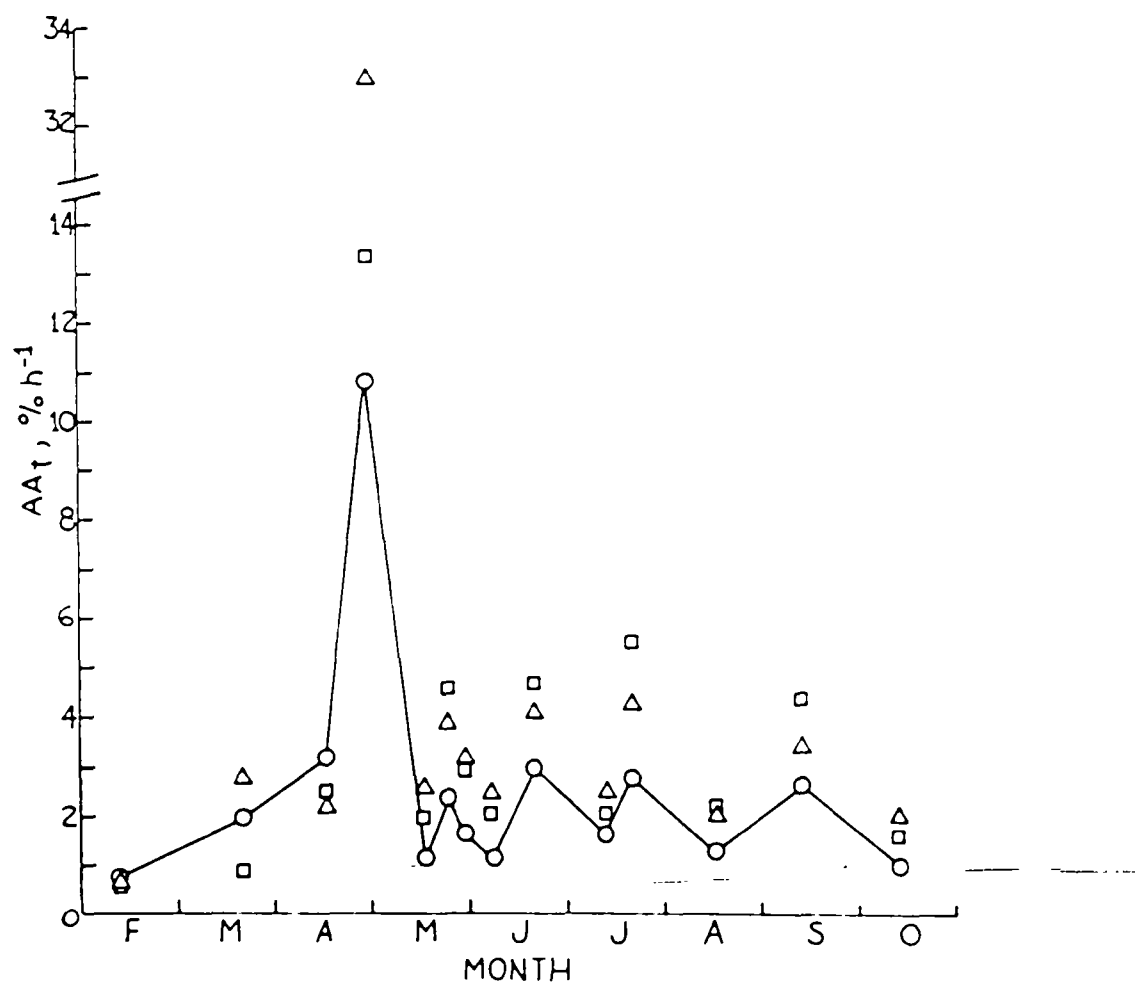


Figure 60. Mean amino acid metabolism, expressed as amino acid turnover rates, along the west flank (Δ), main channel (O), and east flank (\square) of Chesapeake Bay during 1985. Values are means of data from all three lateral transects.

being utilized for microheterotroph production during late August to early November 1984. Nevertheless, our 1985 study was conducted over a longer time period, thereby increasing the likelihood that phytoplankton community structure and thus carbon and energy sources for bacterial production could change. We added glucose metabolism determinations to our 1985 measurements to assess the possibility that bacterial growth and metabolism in Chesapeake Bay waters might be fueled by organic carbon and energy sources other than amino acids.

Temporal Changes along the Main Channel

We began measurements of glucose metabolism in mid-April (Fig. 61). Glucose turnover rates were already substantial at this time with particularly high values at station 32 at all depths and in mid-water at station 24. The spring phytoplankton maximum (Fig. 11) coincided with high glucose turnover rates—in deep water, most notably up Bay at stations 32 and 3. Deep water rates to the south at station 24 were lower, but very high rates of glucose turnover were found in surface and mid-water at this location.

Glucose metabolism decreased in concert with the bacterial decline in mid-May. Its recovery, coinciding with the phytoplankton decline, was rapid but turnover rates in deep water never again reached the values found in late April (Fig. 61). Surface and mid-water rates, however, remained high until late July (when measurements had to be discontinued at stations 32 and 3) or mid-August (station 3). Summer deep water glucose metabolism tended to be greater at stations 32 and 3 than at station 24 to the south.

A cross-Bay synopsis of glucose metabolism at transect 2 is depicted in Figures 62-66. In mid-April (Fig. 62) glucose turnover rates were highest

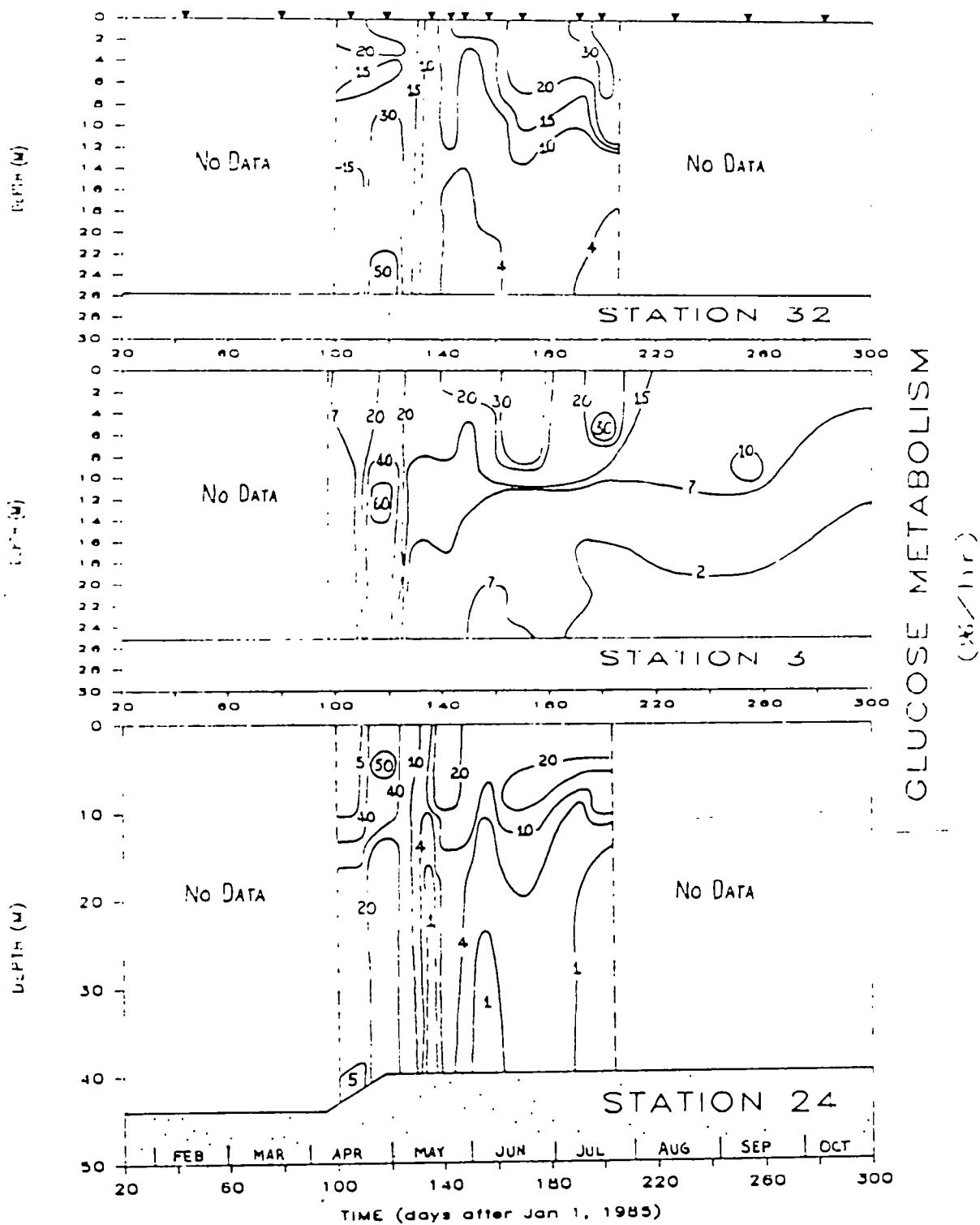


Figure 61. Time-dependent vertical variations in glucose metabolism along a north-south (station 32 to 24) main channel transect. Solid triangles at the top indicate cruise dates. Values on contour lines represent glucose turnover rates expressed as $\% \text{ of glucose pool } h^{-1}$.

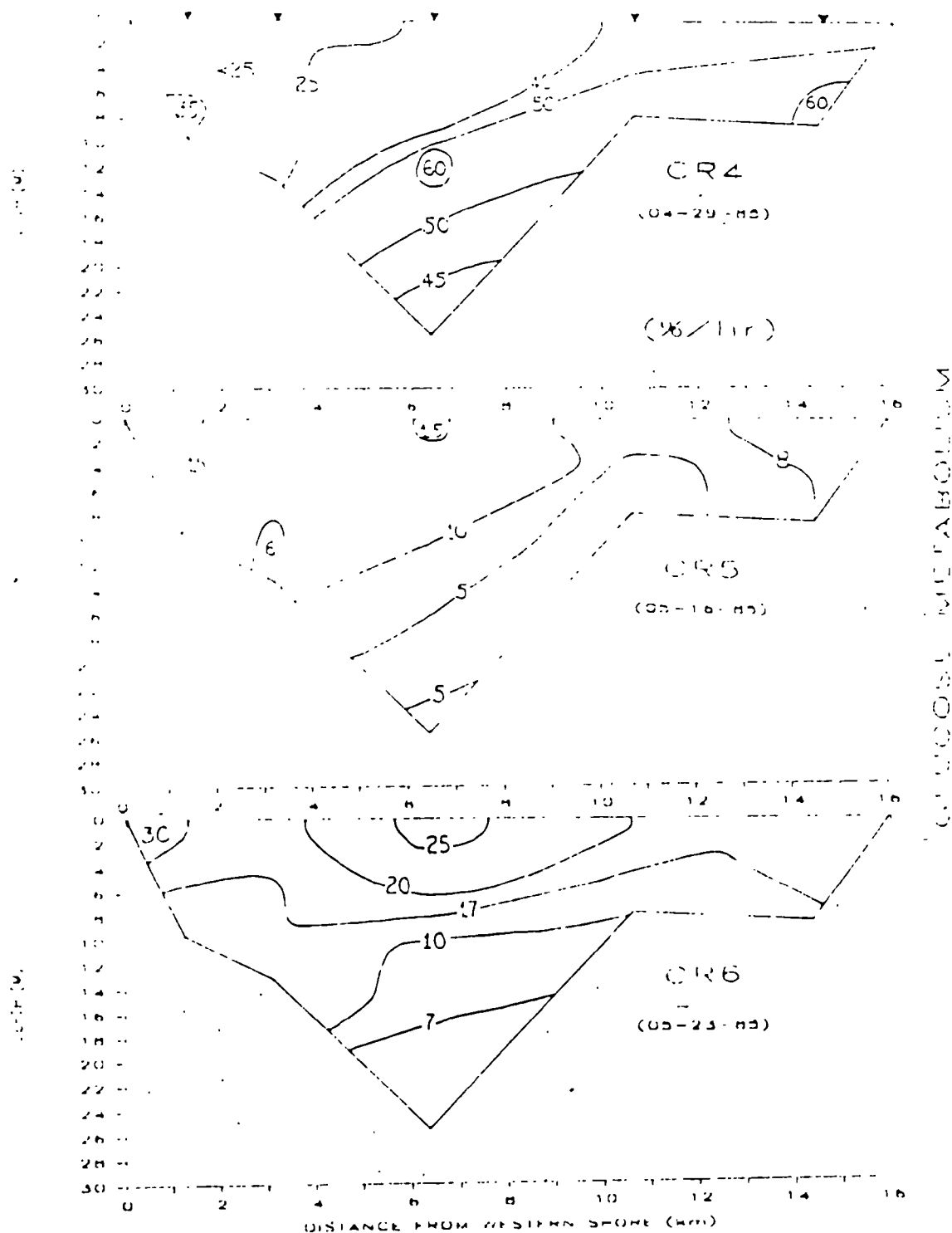


Figure 63. Lateral distribution of glucose metabolism, expressed as glucose turnover rates, along transect 2 for the period 29 Apr. - 23 May 1985.

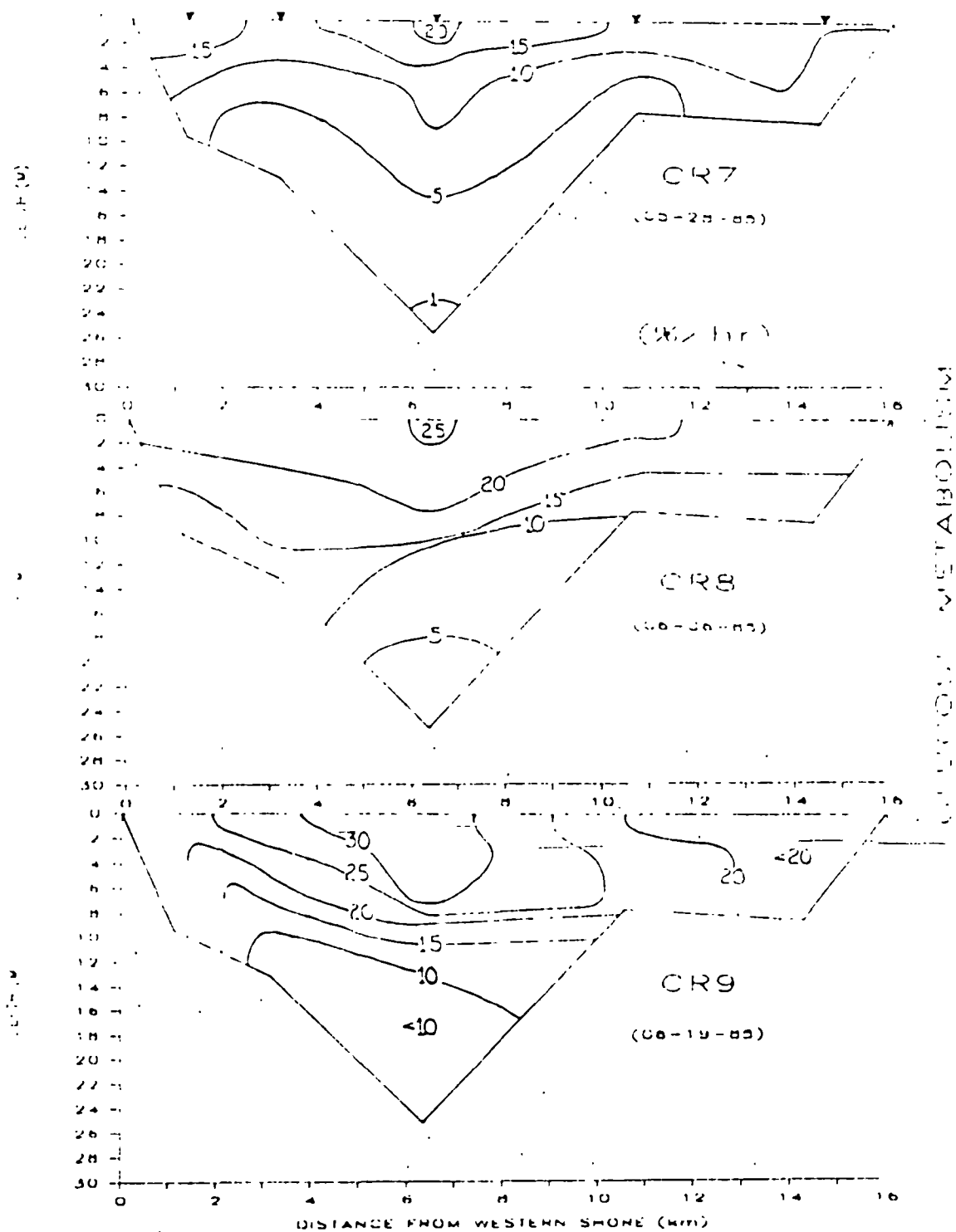


Figure 64. Lateral distribution of glucose metabolism, expressed as glucose turnover rates, along transect 2 for the period 28 May - 19 June 1985.

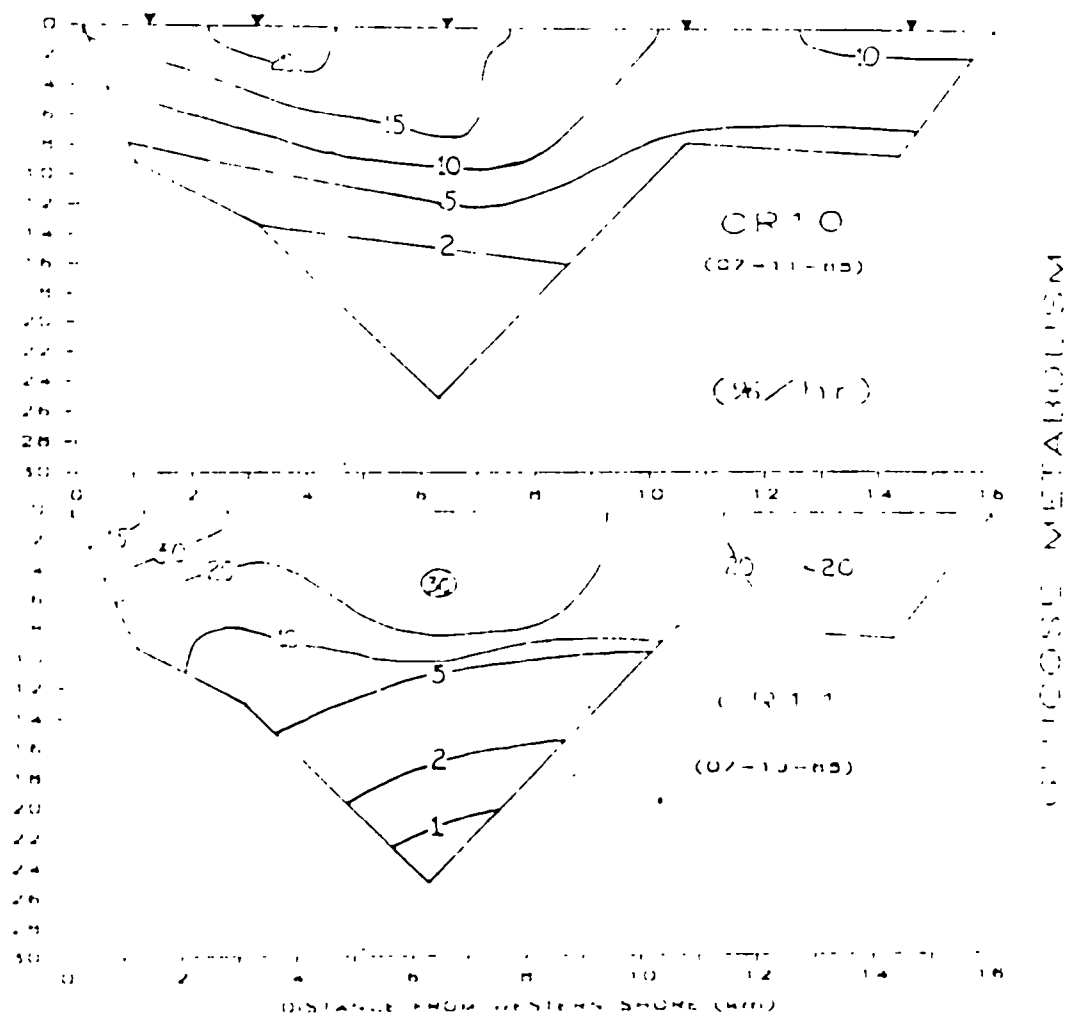


Figure 65. Lateral distribution of glucose metabolism, expressed as glucose turnover rates, along transect 2 for the period 11 Jul. - 19 Jul. 1986.

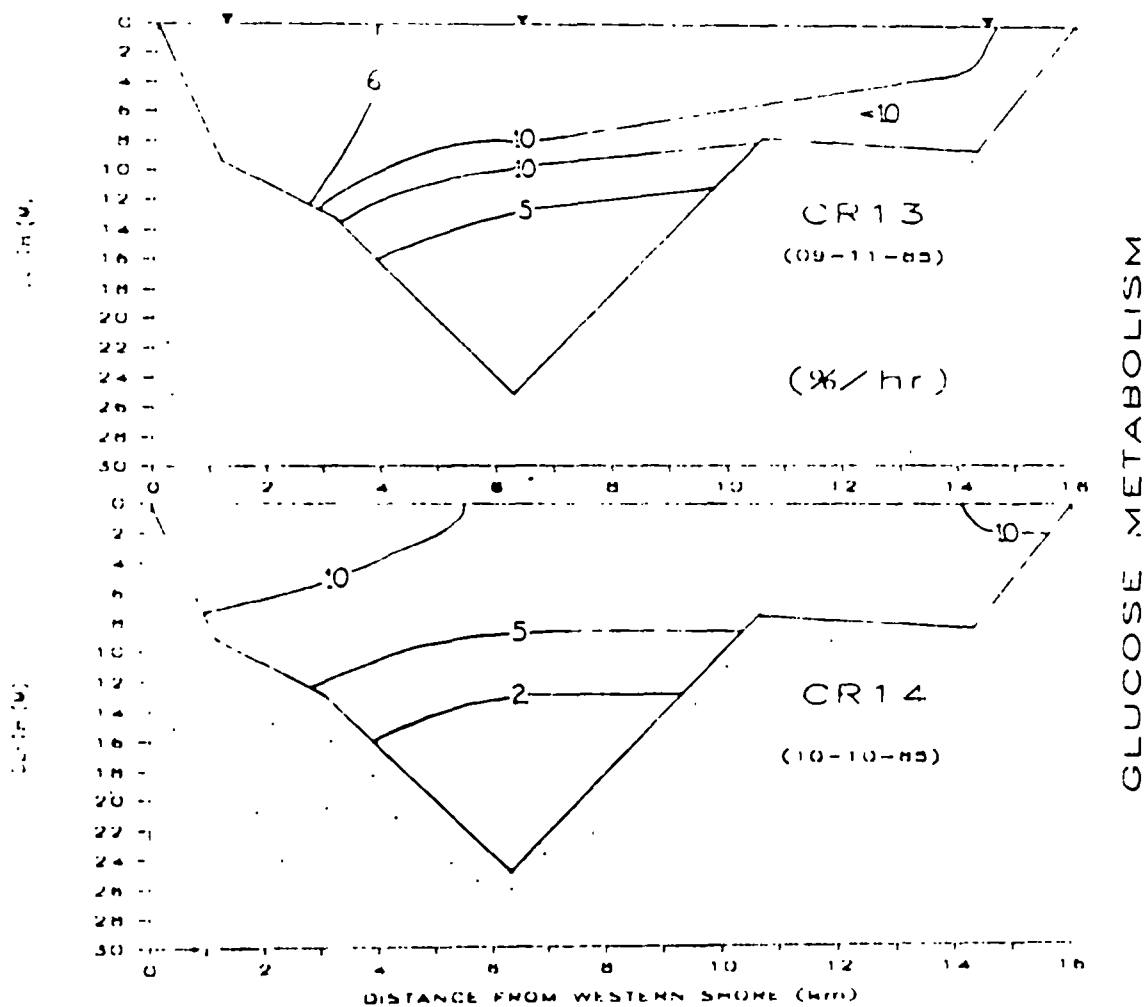


Figure 66. Lateral distribution of glucose metabolism, expressed as glucose turnover rates, along transect 2 for the period 11 Sep. - 10 Oct. 1985.

near the main channel of the Bay with maximum rates of 6-7%/h. Glucose turnover increased greatly by late April (Fig. 63), in concert with the spring phytoplankton maximum (Tables 2 and 3) and peaks of bacterial abundance (Fig. 24), production (Fig. 42), and amino acid metabolism (Fig. 53). Highest rates occurred in mid and deep water and along the eastern flank (Fig. 63). Glucose metabolism decreased dramatically (5 to 10-fold in mid and deep water) in mid-May (cruise 5, Fig. 63) with the bacterial decline, but nearly doubled one week later in the surface water as phytoplankton biomass and production decreased (Tables 2 and 3). Following a second decline at the end of May, glucose turnover increased again into mid-June. Bottom water glucose metabolism on 19 June (cruise 9, Fig. 64) was exceeded only by rates found during the spring phytoplankton bloom.

Summer conditions predominated in July throughout the remainder of the study, i.e. high rates of glucose metabolism were found in near surface waters and lower and decreasing rates occurred beneath the pycnocline (Fig. 65 and 66). Unlike all the other bacterial parameters measured, however, this "summer" pattern was observed as early as 23 May and persisted through May and June (Figs. 63 and 64). Glucose metabolism decreased in September and October as water temperatures began to decline (Fig. 66).

Except for cruise 3 (Fig. 62), cruise 7 (Fig. 64), and possibly cruise 5 (Fig. 63), glucose turnover isoclines were similar to salinity profiles across the transect (Figs. 29-32). In this respect, glucose metabolism tended to follow bacterial production (Figs. 42-45) more closely than did amino acid metabolism (Figs. 53-56).

Differences with Depth

Mean glucose turnover rates below the euphotic zone exceeded rates

within the euphotic zone until the mid-May bacterial decline (Fig. 67). The timing of this change was consistent with bacterial production (Fig. 46) and amino acid turnover (Fig. 57), but occurred two weeks earlier than the shift in bacterial abundance (Fig. 34). However, the mid-May change occurred only at transects 1 and 2 (Figs. 68 and 69). Across transect 3, mean glucose turnover within the euphotic zone was always greater than below it.

North to South Differences

From early June to late July when measurements at transects 1 and 3 had to be discontinued, mean glucose metabolism at the northern-most transects was usually higher than at transect 3 (Figs. 68 and 69). This was not true in late April when glucose metabolism at transect 3 within the euphotic zone, but not below it, exceeded glucose metabolism at the more northern transects. Glucose metabolism nearly always exceeded amino acid metabolism in both surface and bottom waters, often by a factor of 2 or more. Assuming that natural glucose and amino acid concentrations in Bay water were similar, we suggest that carbohydrates were preferred over amino acids as carbon and energy sources for microheterotrophic growth and metabolism. However, this cannot be proven in the absence of measurements of carbohydrate and amino acid concentrations.

Beginning with the bacterial decline in mid-May, mean glucose metabolism on the flanks exceeded glucose metabolism over the deep channel (Fig. 70). No discernible pattern was observed in east and west flank glucose turnover rates.

Oxygen Consumption

Mean oxygen consumption data for the mesohaline portion of the Bay are

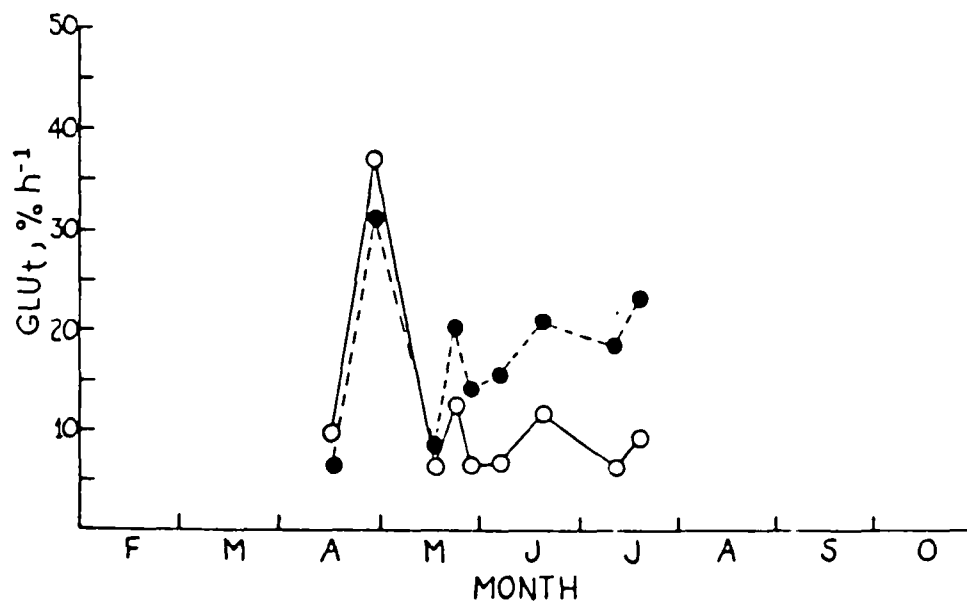


Figure 67. Mean glucose metabolism, expressed as glucose turnover rates, within (●) and below (○) the euphotic zone for transects 1-3 during 1985.

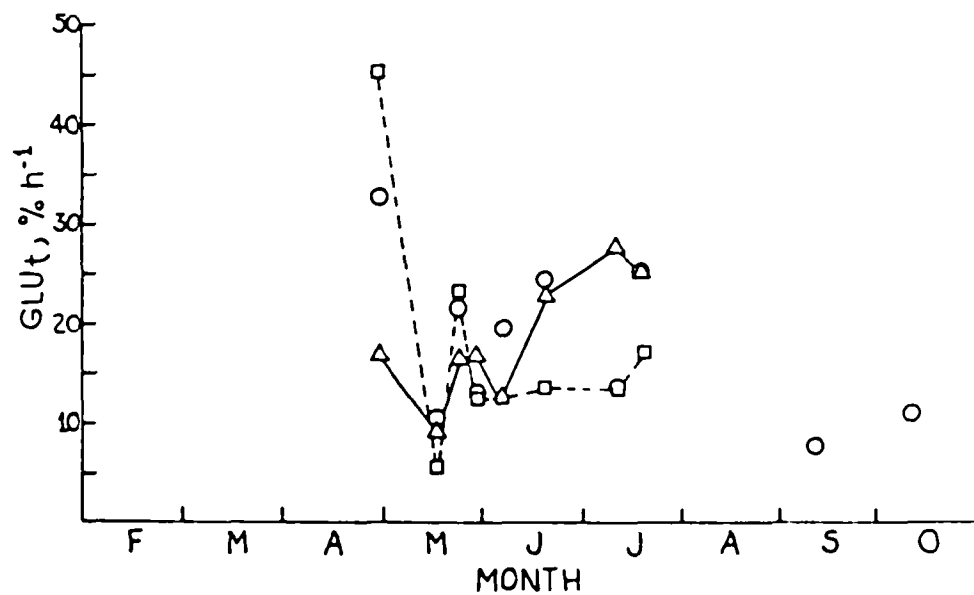


Figure 68. Mean glucose metabolism, expressed as glucose turnover rates, within the euphotic zone along transects 1 (△), 2 (○), and 3 (□) during 1985.

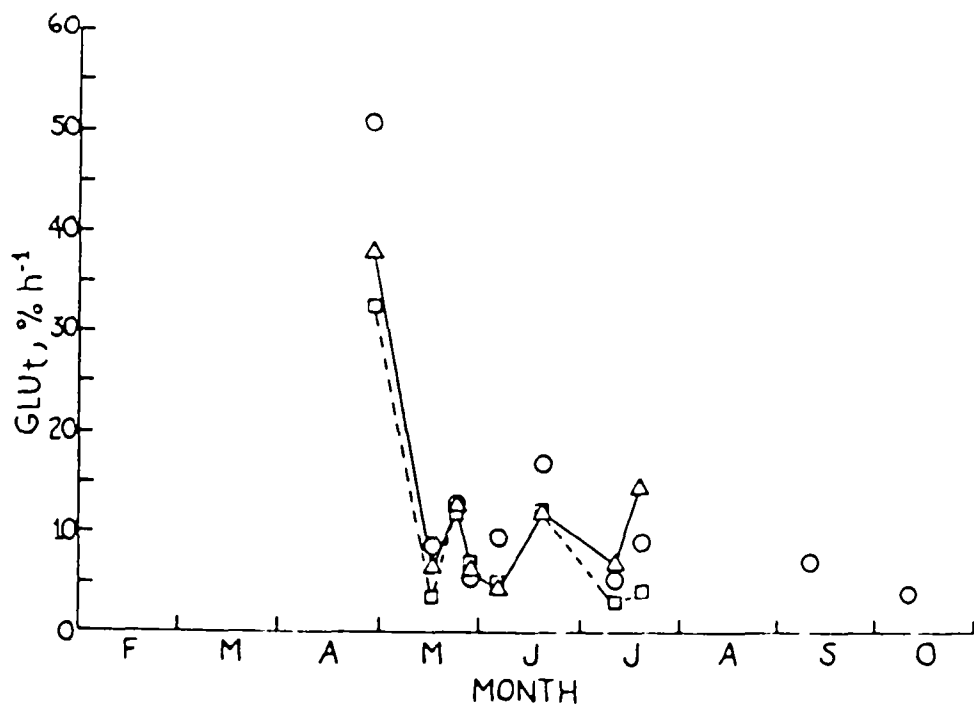


Figure 69. Mean glucose metabolism, expressed as glucose turnover rates, below the euphotic zone along transects 1 (Δ), 2 (\circ), and 3 (\square) during 1985.

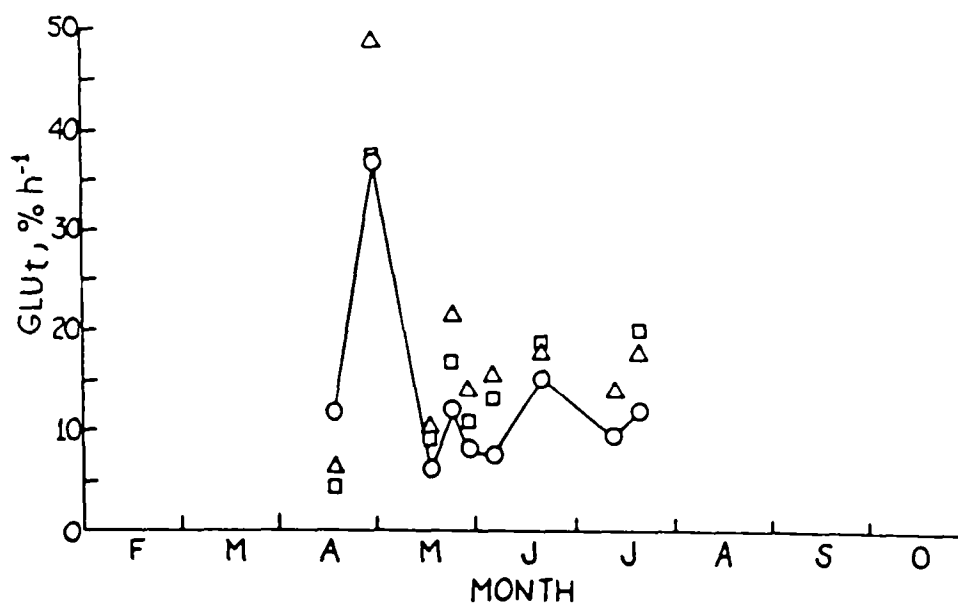


Figure 70. Mean glucose metabolism, expressed as glucose turnover rates, along the west flank (Δ), main channel (O), and east flank (\square) of Chesapeake Bay during 1985. Values are means of data from all three lateral transects.

plotted in Fig. 71. Apart from the decrease in oxygen consumption rates within the euphotic zone from mid-February to mid-April, the data indicate an increasing trend in oxygen consumption rates culminating in a late July to mid-August euphotic zone peak and peaks below the euphotic zone in early June and late July. Higher mean oxygen consumption rates below the euphotic zone, calculated by averaging to 15m depth compared to averaging to the bottom, reflect decreases in oxygen consumption rates with depth as well as elevated oxygen consumption rates near the pycnocline.

Elevated euphotic zone oxygen consumption rates from late April to late May coincide with the spring phytoplankton bloom (Table 3) while the summer euphotic zone oxygen consumption maximum corresponds with high primary production during the same time period (Table 4). Despite this, there are no clear-cut relationships among the deep water oxygen consumption maxima and bacterial or phytoplankton parameters on a cruise-by-cruise basis. However, bacterial abundance and activity tended to be uniformly high during the summer period. We cannot rule out the possibility that organisms other than bacteria might have been responsible for a portion of the observed oxygen consumption.

Oxygen consumption below the euphotic zone was usually greatest at the northern-most and least at the southern-most lateral transect (Fig. 72). Peak mean values along transect 1 in early June and transect 2 in early July do not correspond with peaks in bacterial or phytoplankton parameters. However, the generally high deep water oxygen consumption rates which occurred along transects 1 and 2 are consistent with high phytoplankton production and high bacterial abundances and activity characteristic of summer conditions. Higher oxygen consumption rates along the northern-most transects are also

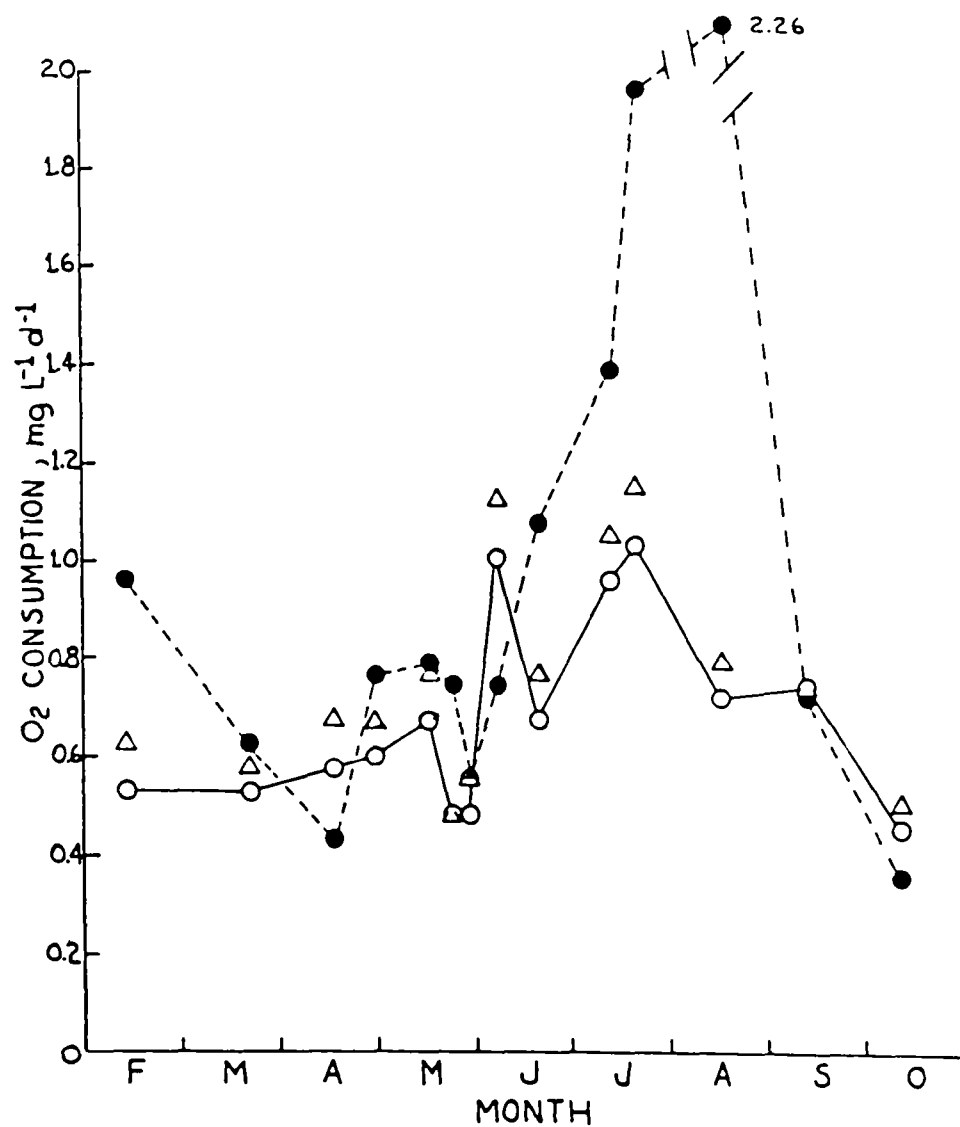


Figure 71. Mean oxygen consumption within the euphotic zone (●), beneath the euphotic zone to the benthos (○), and beneath the euphotic zone to 15m depth (△) during 1985. Values are means of data from all three lateral transects.

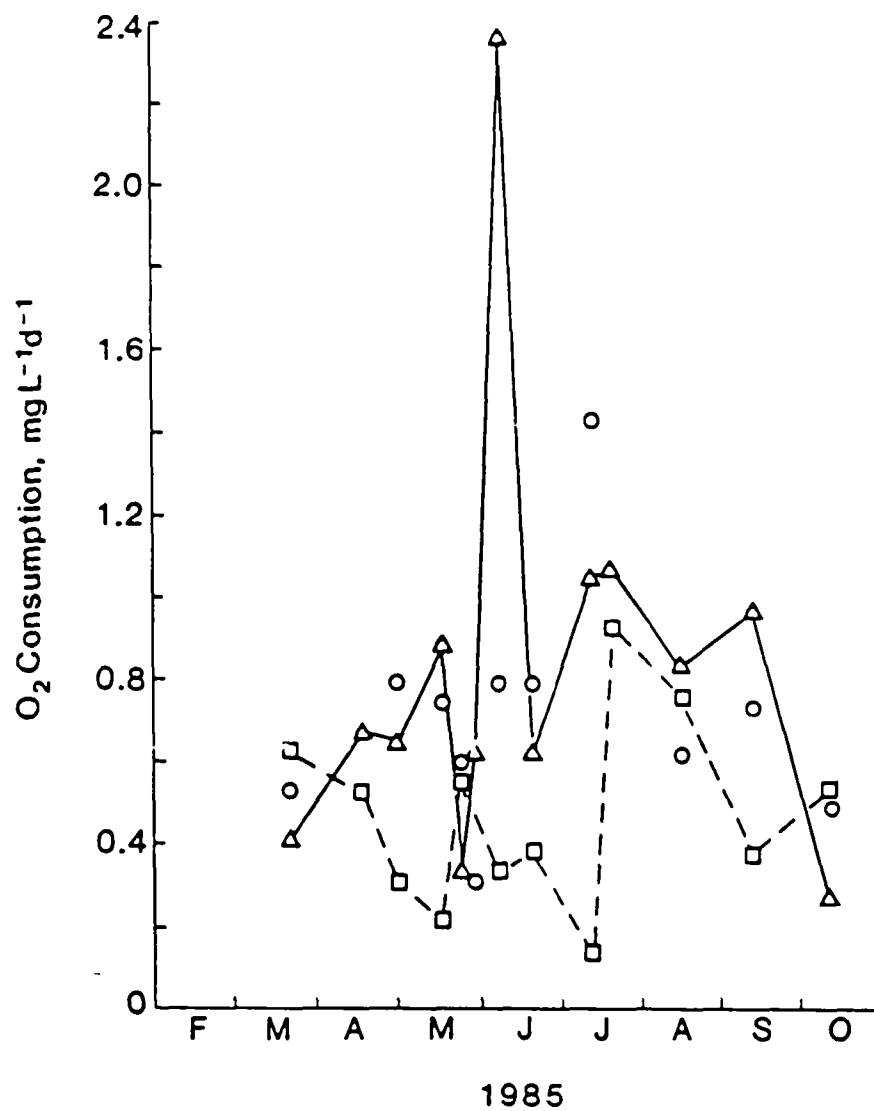


Figure 72. Mean oxygen consumption beneath the euphotic zone along transects 1 (Δ), 2 (\circ), and 3 (\square) during 1985.

consistent with oxygen depletion observed at the deep stations throughout the study period (Figs. 9 and 21).

Despite improvements in our experimental procedures for measuring oxygen consumption rates (see SECTION 4) we still observed, as in our 1984 data (Tuttle et al. 1985), considerable scatter in the oxygen consumption determinations. However, when we aggregated oxygen consumption data according to time periods based upon season and degree of stratification (1984 data, Tuttle et al. 1985) or by seasonal periods only (1985 data) and further separated the resulting aggregates into euphotic zone and below euphotic zone means, we found surprisingly good agreement between mean oxygen consumption rates and bacterial abundances (Fig. 73). Attempts to repeat this exercise with bacterial production estimates and bacterial metabolism measurements were unsuccessful. The apparent relationship between oxygen consumption rate and bacterial abundance required further statistical evaluation. Nevertheless, the ability to estimate oxygen consumption by measuring bacterial abundance, a much easier and more precise determination than directly measuring oxygen consumption, could prove to be a useful addition to Bay monitoring efforts.

Carbon Sources for Bacteria and Oxygen Consumption

We have previously discussed variations in phytoplankton biomass and productivity in terms of phytoplankton dynamics. In this section, we focus on phytoplankton as a source of carbon fueling bacterial metabolism and oxygen consumption.

Chlorophyll

Mean chlorophyll concentrations within and below the euphotic zone for

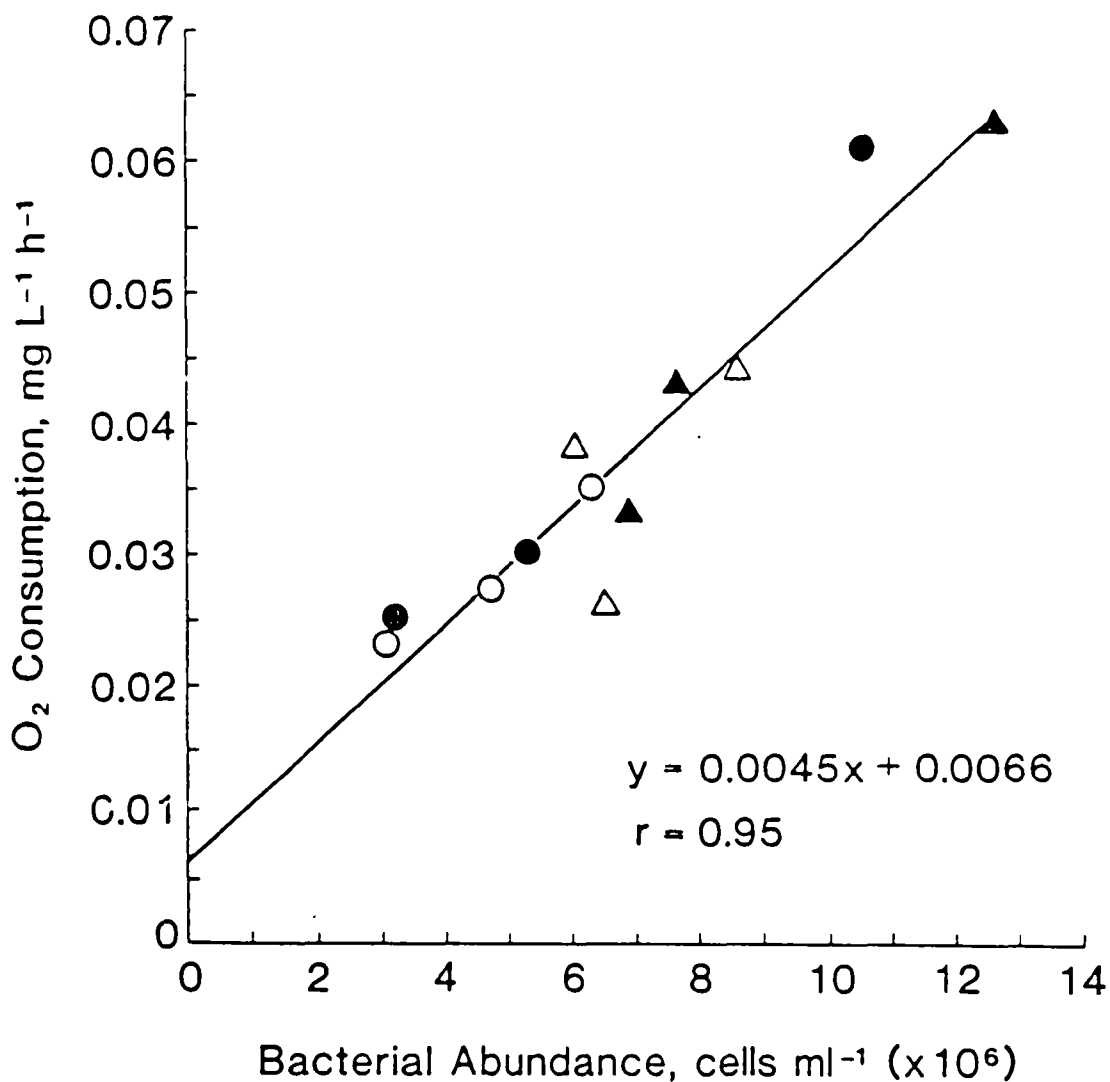


Figure 73. Linear regression of mean oxygen consumption on bacterial abundance. Symbols: (▲) euphotic zone means for the time periods 20 Aug. - 11 Sep., 14 Sep. - 3 Oct., and 5 Oct. - 2 Nov. 1984; (●) beneath euphotic zone means for 1984 data collected in the time periods given above; (△) euphotic zone means for the time periods 12 Feb. - 17 Apr., 29 Apr. - 7 June, and 19 June - 12 Sep. 1985; (○) beneath euphotic zone means for 1985 data collected in the time periods given above. Means were calculated using data from all transects.

each cruise are plotted in Figure 74. Early in the year, mean chlorophyll below the euphotic zone exceeded euphotic zone chlorophyll. This pattern reversed in late April and mean euphotic zone chlorophyll thereafter continued to exceed mean chlorophyll concentrations found below the euphotic zone.

Two distinct chlorophyll maxima were observed within the euphotic zone (Fig. 74). The first of these, extending from mid-April to mid-May, was indicative of the spring phytoplankton bloom (Tables 3 and 4) while the second, occurring in late July, represented a summer production maximum. Below the euphotic zone, however, chlorophyll a concentrations decreased consistently from mid-April to late May and then remained relatively low through mid-October. This pattern suggests that removal of intact phytoplankton below the euphotic zone by zooplankton grazing and/or by bacterial degradation increased after mid-April.

The variations of mean chlorophyll content of the euphotic zone were qualitatively similar to each of the east-west transects (Fig. 75A). Below the euphotic zone, however, significant inputs of chlorophyll occurred during the summer at transect 1 (Fig. 75B). During both the spring and summer maxima of phytoplankton biomass, higher concentrations of chlorophyll were found at transect 1 than at transect 3 (Figs. 74A and 74B). This relationship was true both within and below the euphotic zone.

From late April to mid-August, mean chlorophyll concentrations over the Bay flanks were greater than over the main channel (Fig. 76). This pattern is consistent with measurements of bacterial abundance (Fig. 36), bacterial production (Fig. 50), and bacterial metabolism (Figs. 60 and 70). However, the same was not necessarily true of primary productivity (Table 4) or of

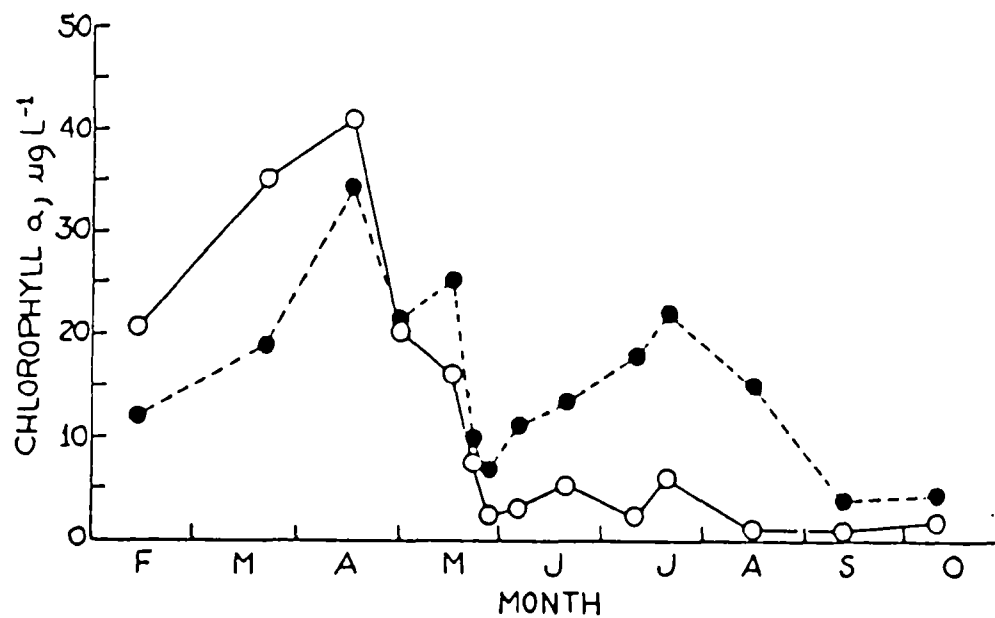


Figure 74. Mean chlorophyll *a* concentrations within (●) and below (○) the euphotic zone during 1985. Values are means of data from all three lateral transects.

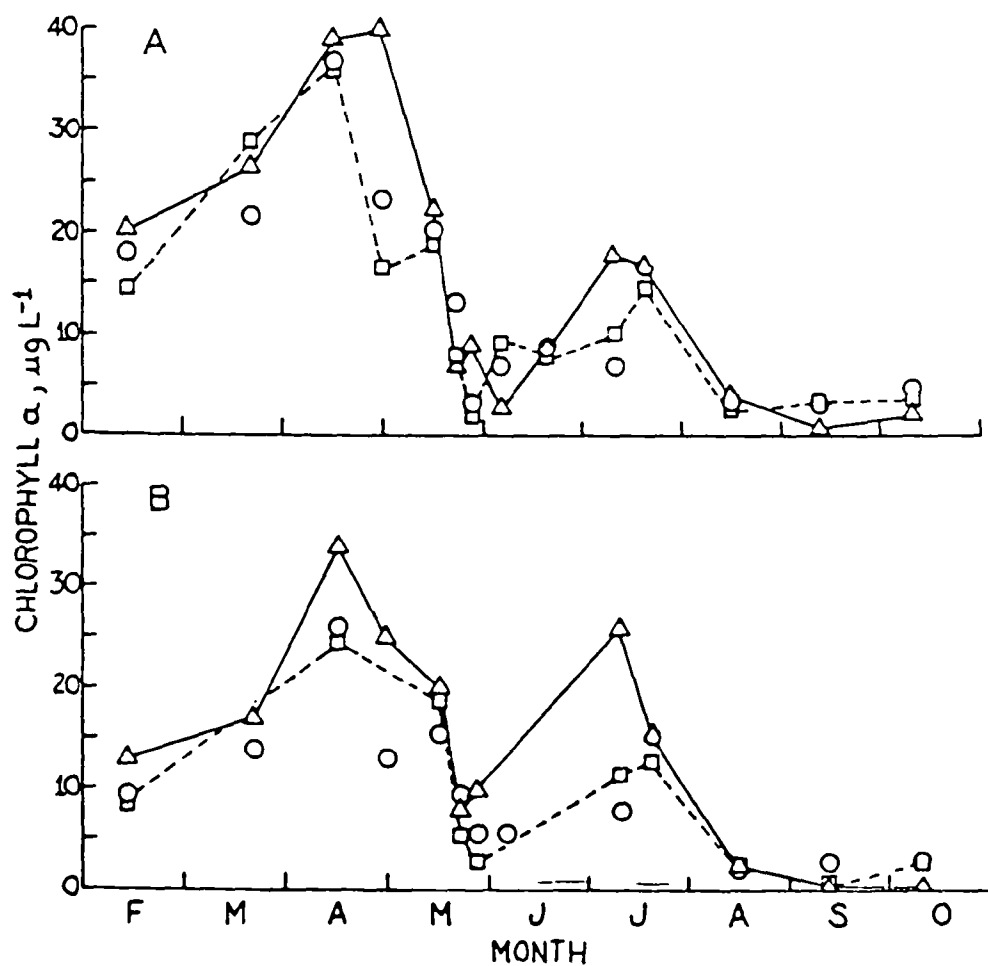


Figure 75. Mean chlorophyll *a* concentrations within (A) and below (B) the euphotic zone across transects 1 (Δ), 2 (○), and 3 (□) during 1985.

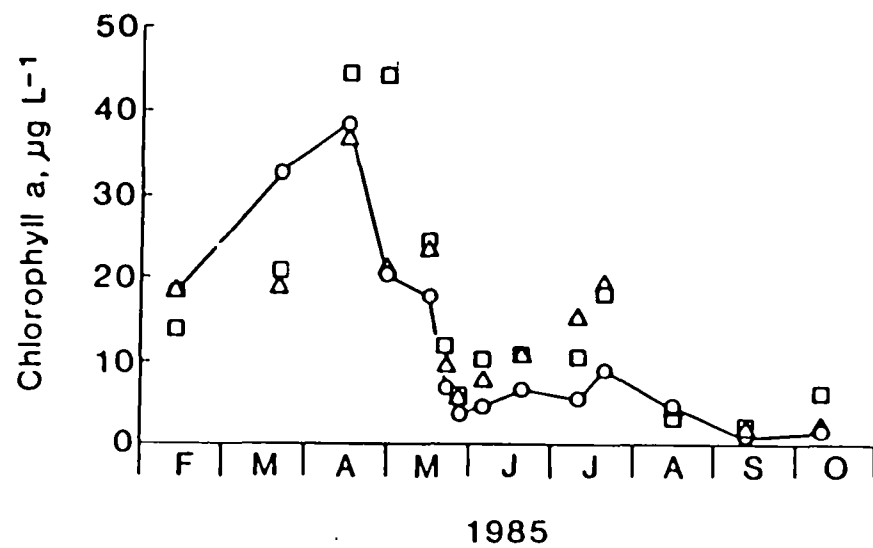


Figure 76. Mean chlorophyll *a* concentrations along the west flank (Δ), main channel (O), and east flank (□) of Chesapeake Bay during 1985. Values are means of data from all three lateral transects.

euphotic zone chlorophyll (Table 7) measured across transect 2. The apparent discrepancy is likely due to the fact that the means plotted in Figure 76 included measurements, made within and below the euphotic zone and at all three transects, whereas the data compiled in Tables 4a and 7 represent transect 2 measurements made only within the euphotic zone.

Phaeopigments

Mean phaeopigment concentrations (Fig. 77) tended to follow mean chlorophyll concentrations through time (Fig. 74). Both spring and summer peaks were observed within the euphotic zone, but the magnitude of the mid-July phaeopigment peak relative to the spring phaeopigment maximum was greater than expected from the ratio of mean summer maximum to mean spring maximum chlorophyll (Fig. 74). We attribute this difference to increased metabolism of phytoplankton biomass within the euphotic zone during the summer on the basis that high phaeopigment to chlorophyll ratios were indicative of phytoplankton decay. Our interpretation is consistent with the notion that the system shifted from phytoplankton to detrital dominance following the phytoplankton decline in mid-May (Fig. 12).

Particulate Organic Nitrogen

Mean particulate organic nitrogen (PON) concentrations (Fig. 78) within the euphotic zone exhibited a pattern consistent with phaeopigments (Fig. 77), i.e. the summer maximum exceeded the spring maximum. Below the euphotic zone, PON peaks in late June, late July, and mid-September coincided with peaks of bacterial production (Fig. 46) and amino acid metabolism (Fig. 57), but the trend over the summer indicated relatively low PON in deeper waters during the summer compared with the spring. Given that

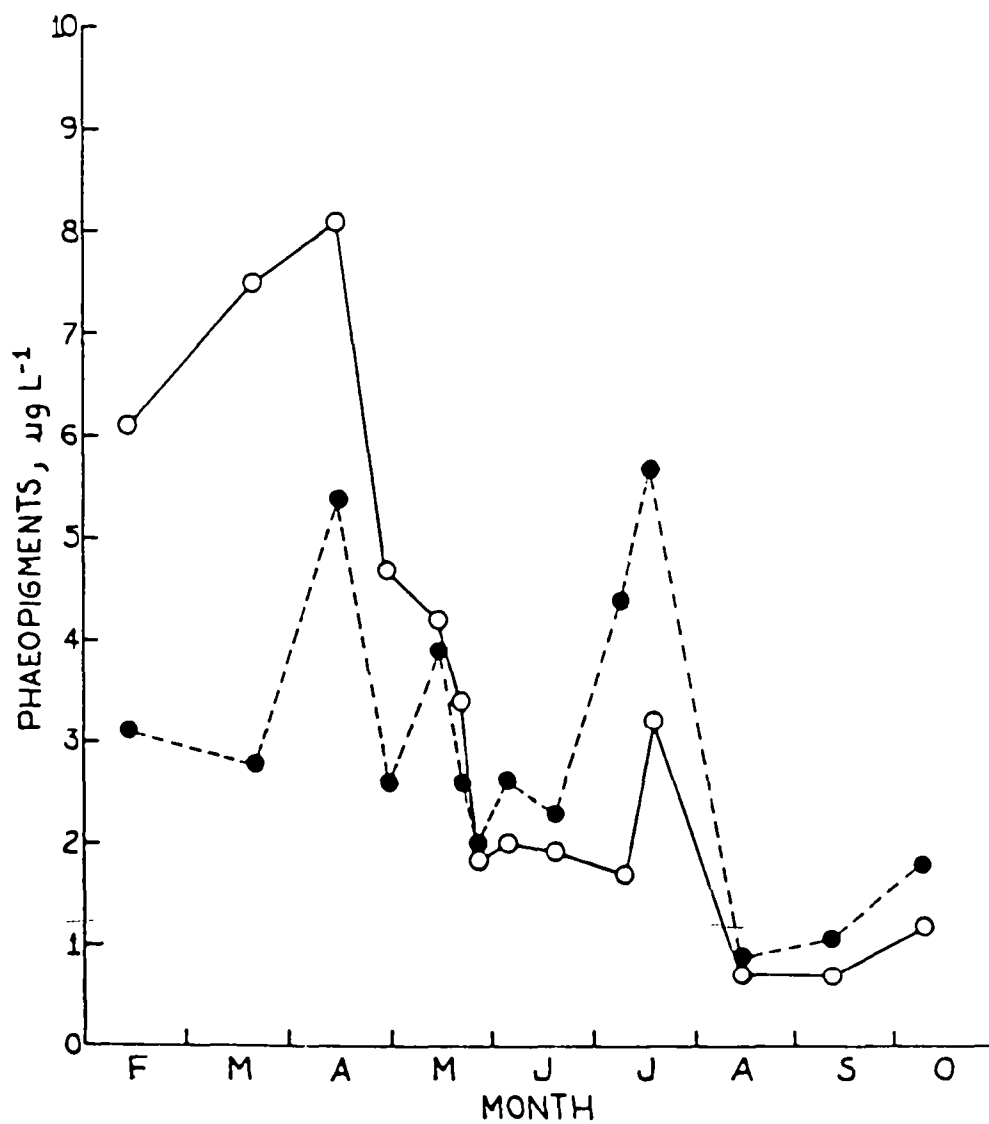


Figure 77. Mean phaeopigment concentrations within (●) and below (○) the euphotic zone during 1985. Values are means of data from all three lateral transects.

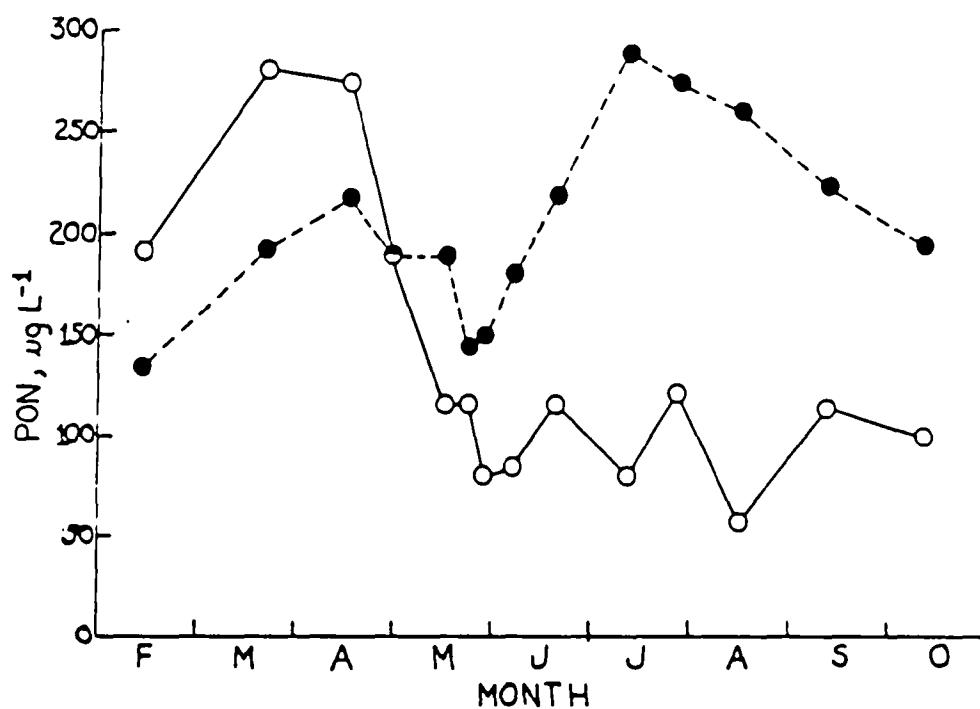


Figure 78. Mean PON concentrations within (●) and below (○) the euphotic zone during 1985. Values are means of data from all three lateral transects.

bacterial biomass and production remained at high levels during summer conditions, the PON data suggest a decreased bacterial dependence upon particulate organic matter below the euphotic zone during the summer compared to other seasons.

Mean PON concentrations for each of the three lateral transects are shown in Figure 79. Except for the tendency of PON concentrations to be highest at transect 1 during the period mid-June to mid-August, there was no clear-cut trend among the transects. In contrast, mean PON concentrations were consistently greater over the Bay flanks than over the main channel from late April to mid-August (Fig. 80).

Particulate Organic Carbon

Variations in mean particulate organic carbon (POC) concentrations (Fig. 81) were similar to changes in PON (Fig. 78) except that euphotic zone POC began to exceed POC below the euphotic zone two weeks earlier than this shift was observed in PON and the summer euphotic zone POC maximum occurred in mid-August rather than in late July. POC peaks coincident with bacterial production (Fig. 46) and amino acid metabolism (Fig. 57) occurred during the summer below the euphotic zone, but the trend of below euphotic zone POC indicated increasing accumulation of POC in deep water following the phytoplankton decline in late May which continued until the end of the study. This trend suggests that from late spring through the summer, POC may have been less susceptible to bacterial attack below the euphotic zone than it had been earlier in the year.

Where POC data are available for each of the three lateral transects (Fig. 82), we found no evidence for consistently higher POC at one transect compared to the others. However, in agreement with PON (Fig. 79), POC at

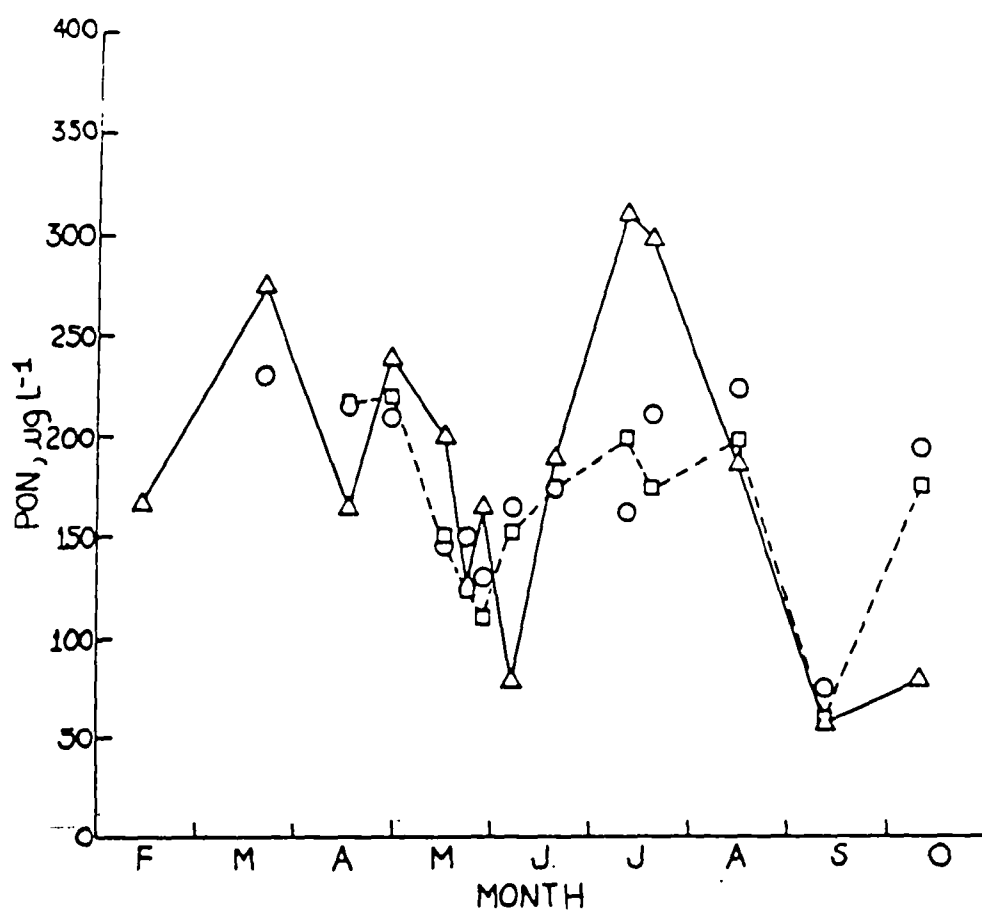


Figure 79. Mean PON concentrations along transects 1 (△), 2 (○), and 3 (□) during 1985. Means include data from within and below the euphotic zone.

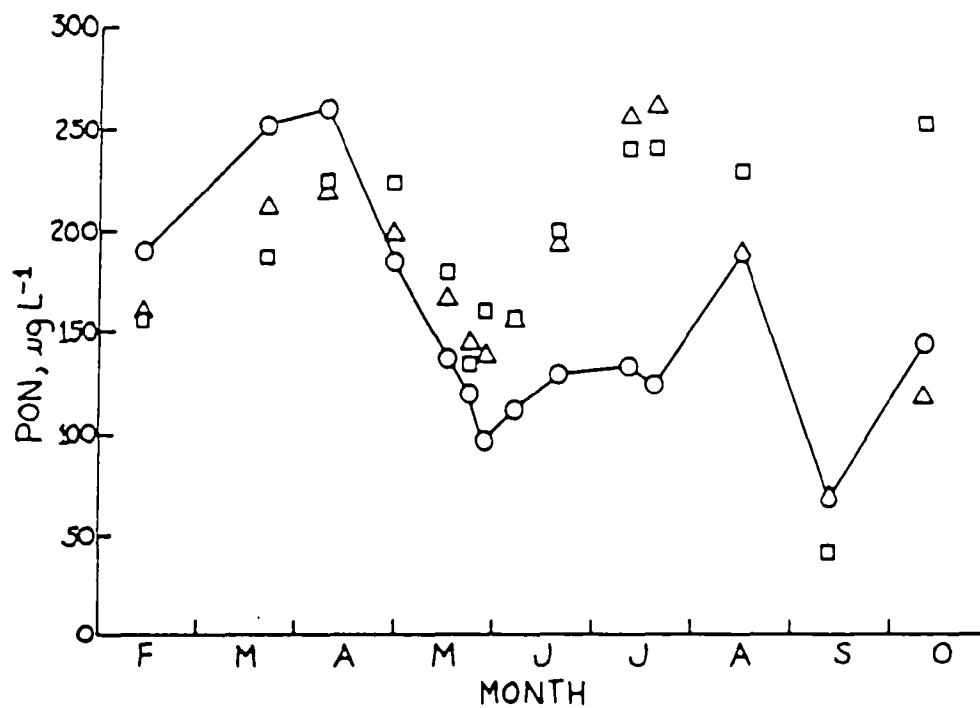


Figure 80. Mean PON concentrations along the west flank (Δ), main channel (\circ), and east flank (\square) of Chesapeake Bay during 1985. Values are means of data from all three lateral transects.

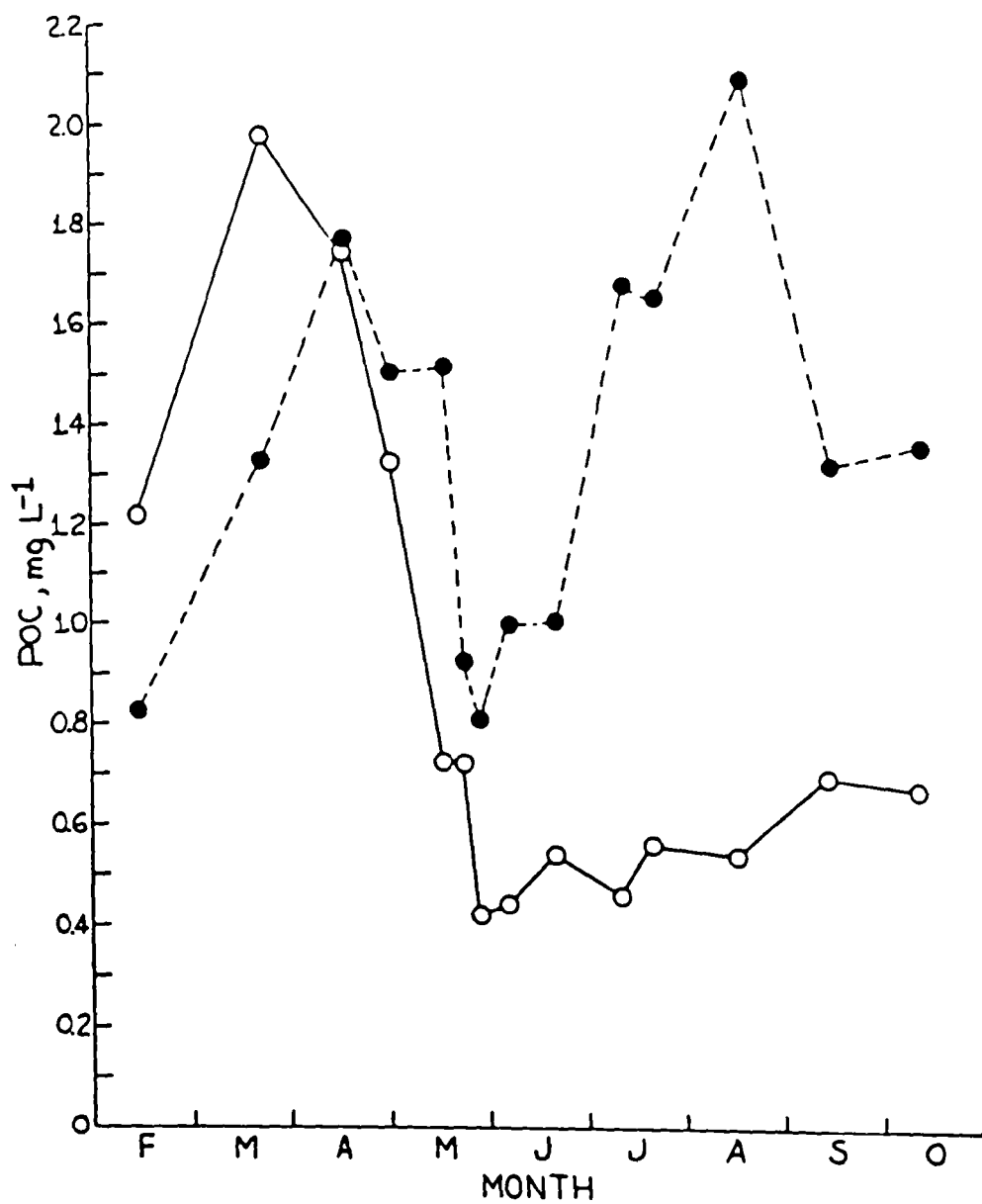


Figure 81. Mean POC concentrations within (●) and below (○) the euphotic zone during 1985. Values are means of data from all three lateral transects.

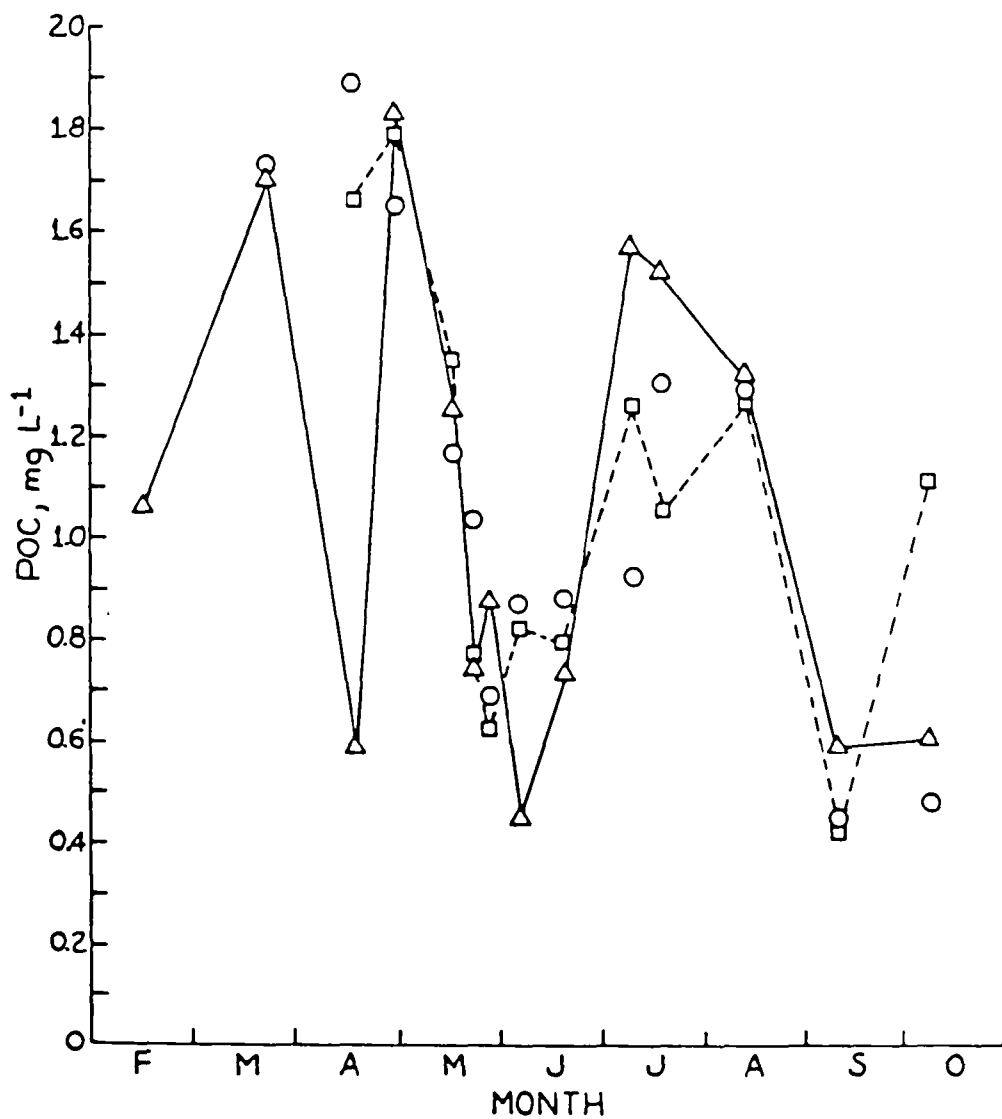
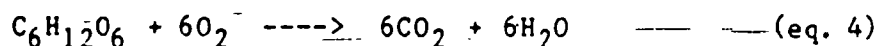


Figure 82. Mean POC concentrations along transects 1 (Δ), 2 (O), and 3 (\square) during 1985. Means include data from within and below the euphotic zone.

transect 1 exceeded POC at transects 2 and 3 during mid-summer. Insufficient data are available to calculate within and below euphotic zone means for each of the transects. Mean POC concentrations were greater over the flanks than over the main channel from late spring to at least mid-August (Fig. 83). This difference is consistent with chlorophyll (Fig. 76) and PON (Fig. 80).

Biochemical Oxygen Demand

We emphasize that only degradable organic carbon (defined here as that organic matter subject to bacterial metabolism) can fuel oxygen consumption. While amino acid and carbohydrate analyses would have been useful for comparison with amino acid and glucose metabolism measurements, budgetary restraints necessitated our use of biochemical oxygen demand (BOD) determinations to estimate labile carbon. Experimentally determined oxygen consumption was converted to carbon equivalence according to equation 4.



The use of carbohydrates to calculate carbon equivalence is supported by our finding that glucose turnover exceeded amino acid turnover.

Mean total BOD throughout the water column was variable during the spring when no single transect exhibited consistently high or low BOD in relation to the other two (Fig. 84). During the summer, however, mean total BOD remained significantly higher to the north at transect 1 than to the south at transect 3. This difference was due mainly to BOD within the euphotic zone (Fig. 85) rather than below it (Fig. 86), even though BOD below the euphotic zone also tended to be greater to the north than to the south (Fig. 86). During rapid oxygen depletion of bottom waters in the spring (Fig. 21), total BOD beneath the euphotic zone was greater to the north than

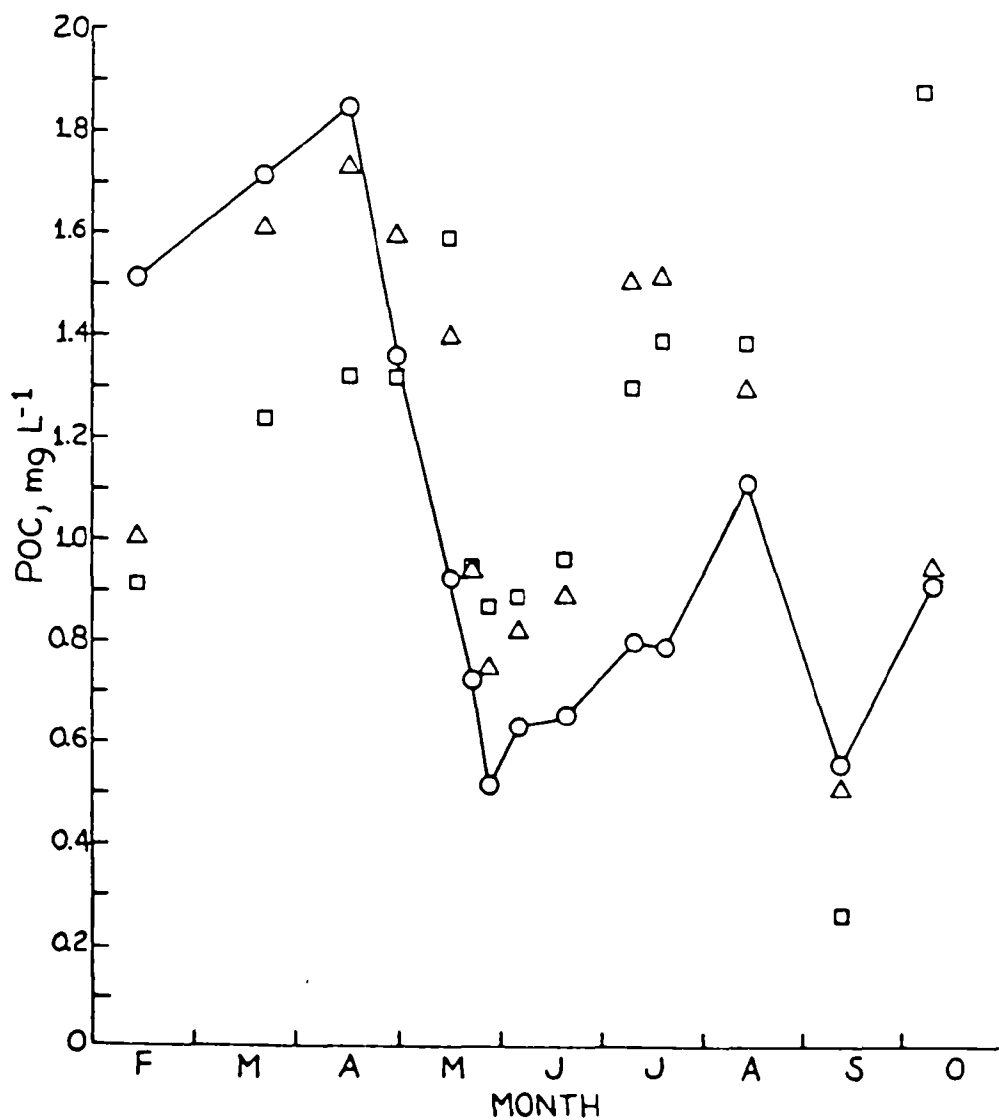


Figure 83. Mean POC concentrations along the west flank (Δ), main channel (\circ), and east flank (\square) of Chesapeake Bay during 1985. Values are means of data from all three lateral transects.

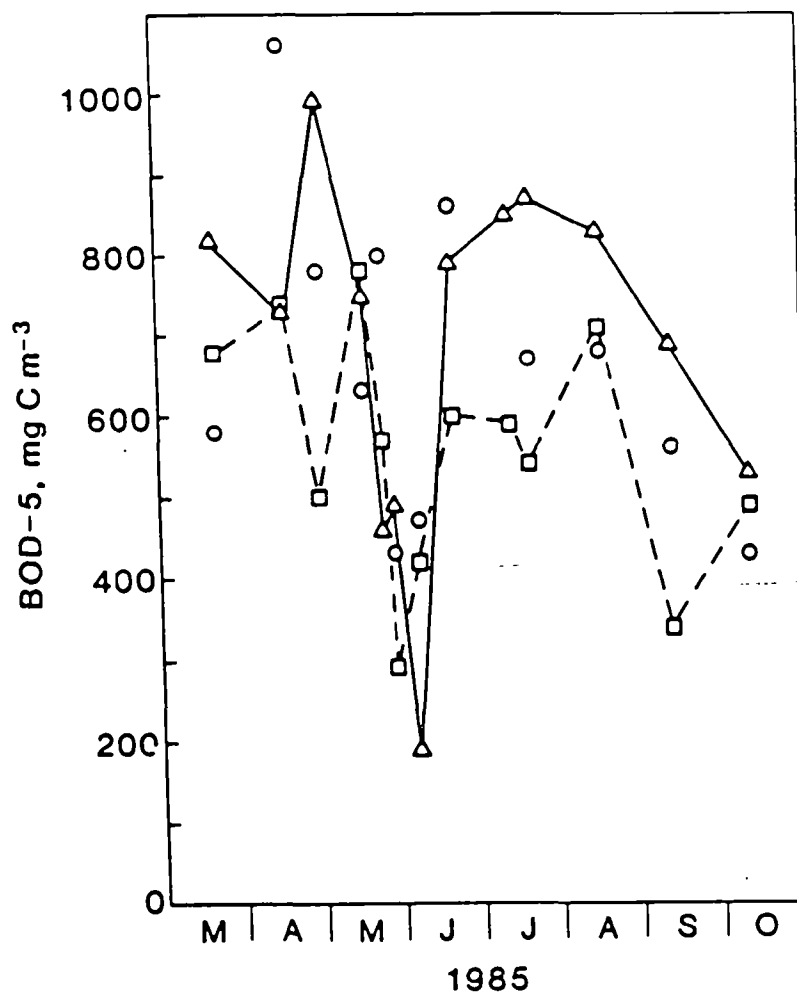


Figure 84. Mean total BOD-5 along transects 1 (△), 2 (○), and 3 (□) during 1985. Means include data from within and below the euphotic zone.

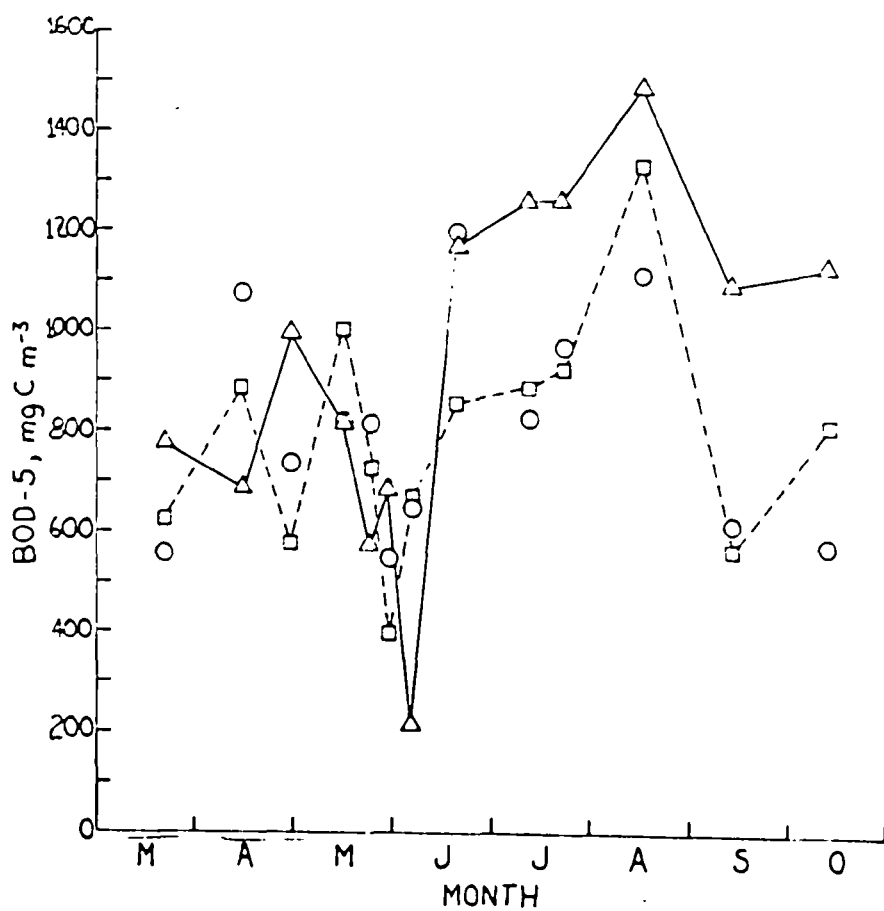


Figure 85. Mean total BOD-5 within the euphotic zone along transects 1 (Δ), 2 (\circ), and 3 (\square) during 1985.

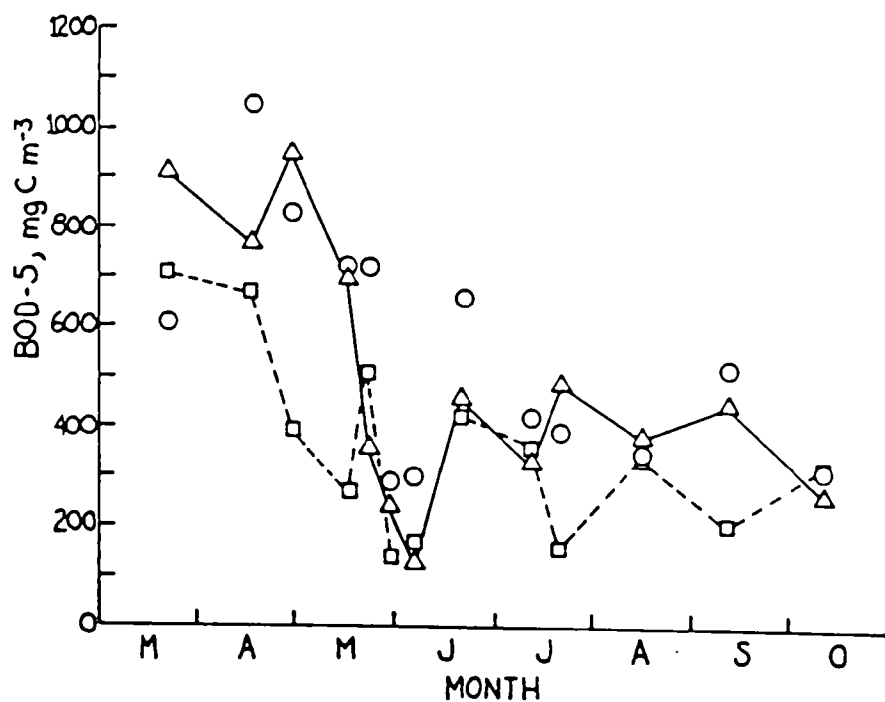


Figure 86. Mean total BOD-5 below the euphotic zone along transects 1 (Δ), 2 (○), and 3 (□) during 1985.

to the south (Fig. 86) whereas euphotic zone BOD showed no coherent pattern among the three transects (Fig. 85). The May declines of bacteria and phytoplankton coincided with BOD decreases at all three transects. These decreases were more severe and times slightly later at transect 1 than farther south (Figs. 84-86).

Within the euphotic zone, summer BOD concentrations equaled or exceeded spring levels (Fig. 85) whereas below the euphotic zone, summer concentrations tended to average about half the spring means (Fig. 86). These differences are consistent with mean PON (Fig. 78) and POC (Fig. 81) concentrations and suggest that increased bacterial production and metabolism below the euphotic zone during the summer tends to maintain BOD at relatively low levels and/or the flux of particulate BOD to deep water decreases during summer conditions.

Total mean BOD concentrations over the flanks exceeded those over the main channel from late April through mid-October (Fig. 87). Apart from the period of mid-May to early June when east flank BOD concentrations were higher than to the west, there were no consistent differences in east and west flank BOD means.

Mean total BOD within the euphotic zone reflected the spring phytoplankton biomass maximum and high summer phytoplankton production (Fig. 88). Following the May phytoplankton decline, euphotic zone BOD increased into the summer, reaching concentrations higher than during the spring peaks. Particulate BOD within the euphotic zone changed in concert with total BOD, but it usually comprised a smaller portion of total BOD in the summer than it did in the spring (Figs. 88 and 89) comprising as little as 30 to 40% of total euphotic zone BOD in July and September (Fig. 89B).

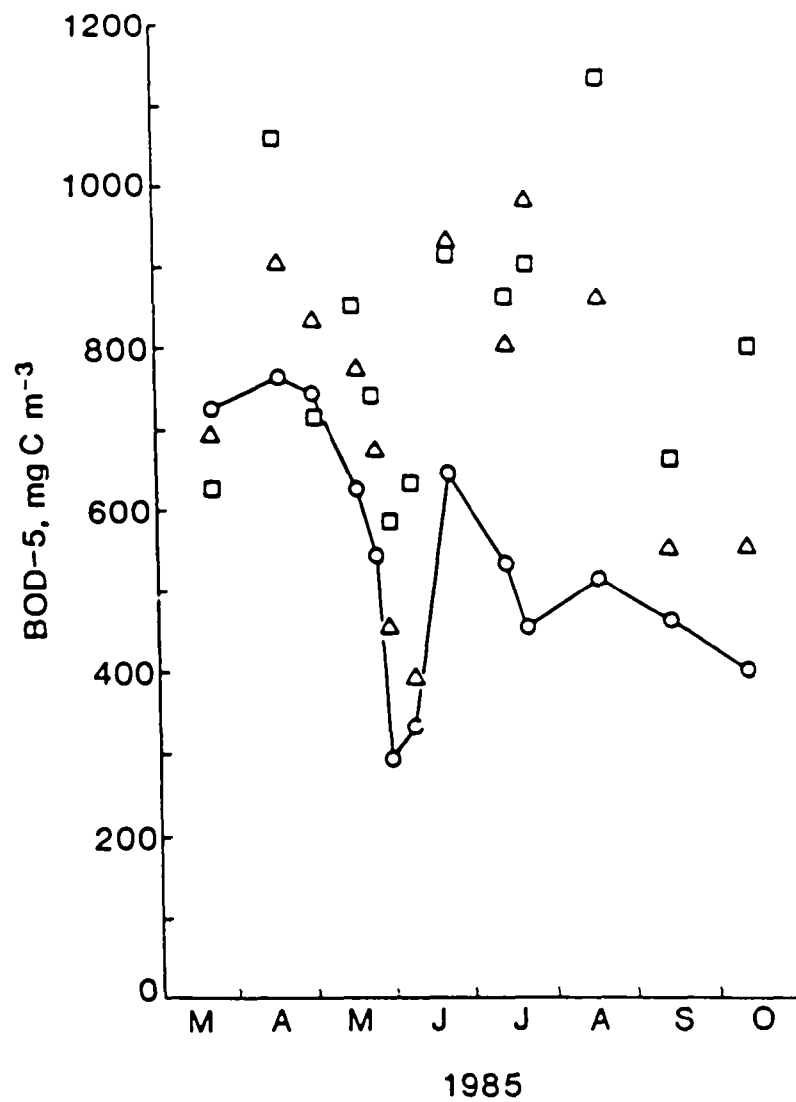


Figure 87. Mean total BOD-5 along the west flank (Δ), main channel (O), and east flank (\square) of Chesapeake Bay during 1985. Means include data from within and below the euphotic zone.

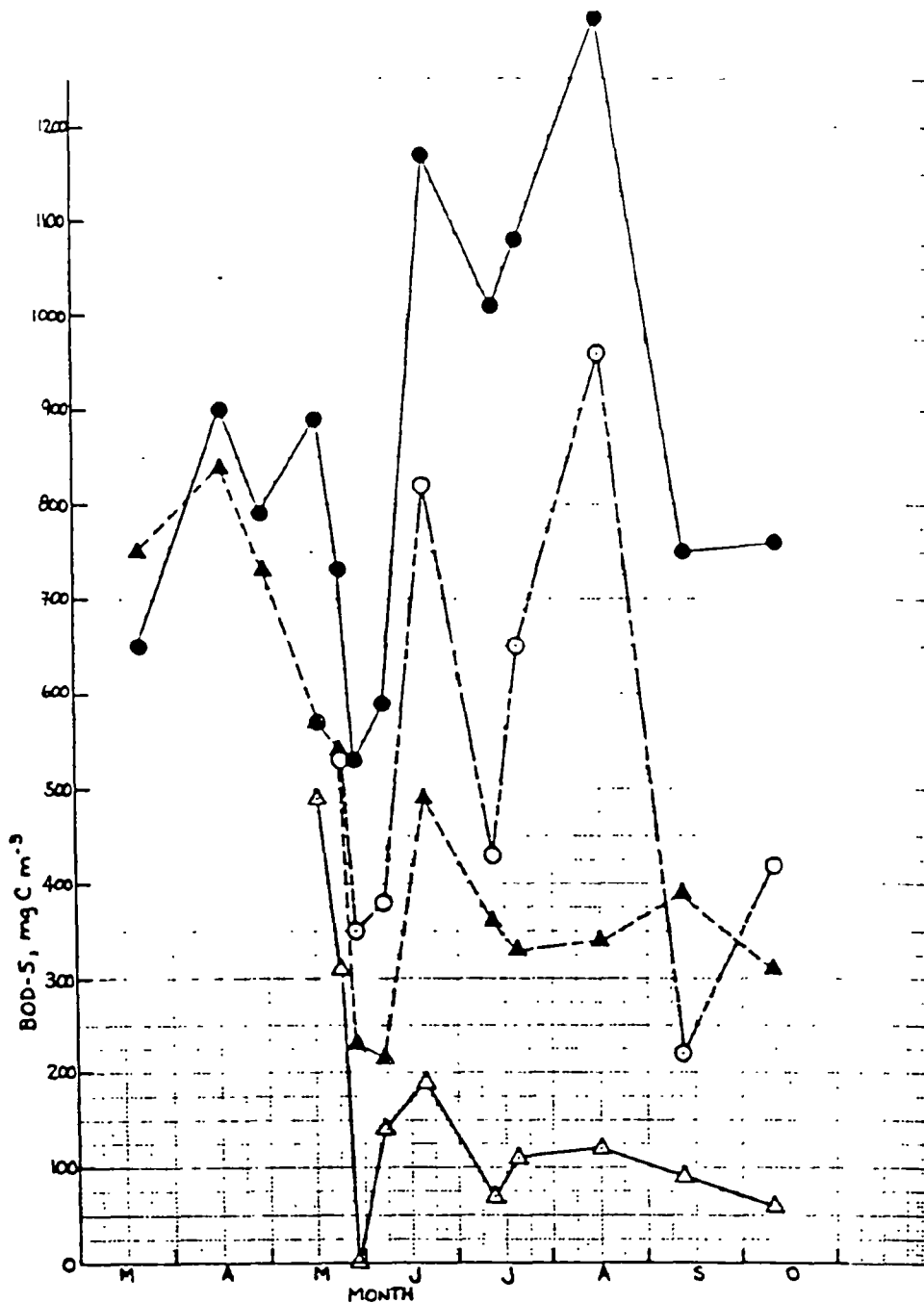


Figure 88. Mean total BOD-5 (closed symbols) and particulate BOD-5 (open symbols) in the mesohaline portion of Chesapeake Bay during 1985. Circles represent values within the euphotic zone and triangles represent values beneath the euphotic zone. Means include data from all three lateral transects.

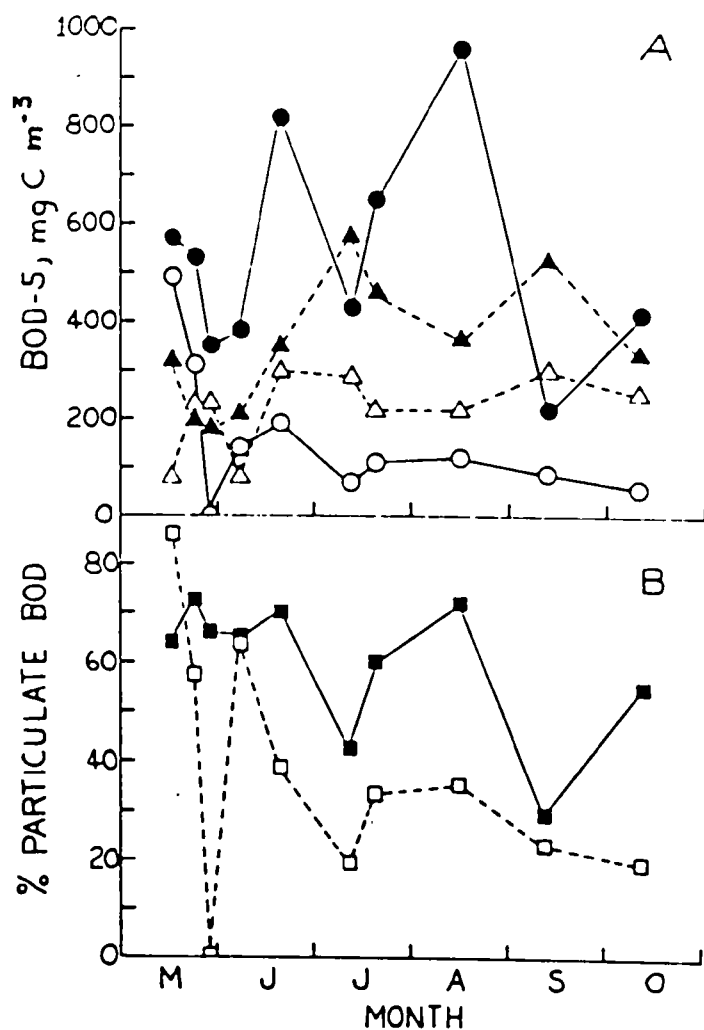


Figure 89. Comparisons of mean particulate BOD-5 with mean filterable BOD-5 (A) and % of total BOD-5 comprised of particulate BOD-5 (B) in the mesohaline portion of Chesapeake Bay during 1985. Values are means of data from all three lateral transects. Symbols: (●) particulate BOD-5 within the euphotic zone; (▲) filterable BOD within the euphotic zone; (○) particulate BOD-5 beneath the euphotic zone; (△) filterable BOD-5 beneath the euphotic zone; (■) % particulate BOD-5 within the euphotic zone; (□) % particulate BOD-5 beneath the euphotic zone.

Below the euphotic zone, the shift in the proportion of particulate BOD to total BOD was even more striking (Figs. 89A and 89B). From mid-June into October, dissolved BOD was about double the particulate BOD (Fig. 89A). Particulate BOD below the euphotic zone during this time period accounted for no more than 20 to 40% of the total BOD (Fig. 89B).

Mean particulate BOD (Fig. 89A) below the euphotic zone remained reasonably constant through the summer while POC exhibited an increasing trend (Fig. 81). For example, particulate BOD accounted for about 35% of POC in late June but only about 15% of POC in mid-September.

During the summer, mean % PBOD/POC averaged 51% within the euphotic zone (n=34), 26% within the region of the pycnocline (n=23), and 18% beneath the pycnocline (n=18). We suspect that most of the particulate organic material which reached the deep water below the pycnocline during the summer is either reasonably refractory or is composed of relatively large material which rapidly sinks to the bottom and is metabolized in the sediments. Therefore, bacteria in the deep water are likely supported chiefly by dissolved organic matter. This contention is supported by the fact that FBOD below the euphotic zone comprises about 2/3 or more of total BOD there and that the mean ratios of euphotic zone FBOD : below euphotic zone FBOD does not differ by more than 10% from the ratios of euphotic zone bacterial abundance : below euphotic zone bacterial abundance over the summer. Thus, the summer pattern of bacterial abundance (see e.g. Figs. 26, 27, and 33) can be explained to a first approximation in terms of FBOD.

1984 AND 1985 INTERANNUAL CONTRASTS - MICROBIOLOGY

As we have discussed earlier in this report, 1984 and 1985 were sharply

contrasting years in terms of rainfall, water column stability (Figs. 16 and 21), surface salinity (Fig. 16), and oxygen regime (Fig. 9). We have also documented differences in phytoplankton biomass during the summer seasons of the two years (Fig. 19), marked by substantially higher standing stocks in 1984 than in 1985. However, average summer phytoplankton production was comparable in both years. In this section, we compare bacterial parameters.

Microheterotrophs

Comparisons of bacterial parameters between the summers of 1984 and 1985 are difficult to make due to the differing boundaries of the study areas investigated, frequency of cruises, and time spans covered. For example, we have found and reported herein differences in a north to south direction in 1985 while no apparent differences existed over the more limited north to south range of the 1984 study. Furthermore, bacterial parameters were measured beginning only in late summer (20 August) of 1984. Were we able to match time periods for the two years, we would have at best 1985 data from only the September cruise. Fortunately, we observed similar patterns in the bacterial parameters during summer conditions in both years, namely high values near the surface and decreasing with depth (e.g. Figs. 26, 27, 44, 55, and 56). Therefore, we compare here data for transect 2 (Choptank transect) for the period 8 August to 11 September 1984 and 11 July to 12 September 1985 when the "typical" summer patterns were observed.

Bacterial abundances were remarkably similar in both years, particularly below the euphotic zone (Table 8). Therefore, despite higher phytoplankton biomass in 1984 than in 1985, there appeared to be sufficient organic carbon input below the euphotic zone in 1985 to support a high bacterial biomass

Table 8. Comparison of the means of key bacterial parameters measured during summer conditions in 1984 (cruises 11-18, 8/20/84 to 9/11/84) and in 1985 (cruises 10-13, 7/11/85 to 9/12/85).

	<u>EUPHOTIC ZONE</u>	<u>BELOW EUPHOTIC ZONE</u>
BACTERIAL PRODUCTION*	2.92×10^8 ('84)	1.92×10^8 ('84)
(cells L ⁻¹ h ⁻¹)	5.32×10^8 ('85)	3.08×10^8 ('85)
BACTERIAL ABUNDANCE	1.37×10^{10} ('84)	8.44×10^9 ('84)
(cells L ⁻¹)	1.09×10^{10} ('85)	7.02×10^9 ('85)
BACTERIAL TURNOVER	0.52 ('84)	0.55 ('84)
(d ⁻¹)	1.17 ('85)	1.05 ('85)
O _W CONSUMPTION	1.48 ('84)	1.04 ('84)
(mg L ⁻¹ d ⁻¹)	1.31 ('85)	1.02 ('85)
O ₂ CONSUMPTION**	1.64 ('84)	1.07 ('84)
(mg L ⁻¹ d ⁻¹)	1.34 ('85)	0.92 ('85)

*Based upon 2×10^{18} cells produced mol⁻¹ ³H thymidine incorporated.

**Based upon bacterial abundance according to the relationship given in Figure 72.

nearly equal to that found in 1984.

Bacterial production increased in summer 1985 compared to 1984 (Table 8). The magnitude of this increase was 82% within the euphotic zone and 60% beneath it, resulting in doublings of summer bacterial turnover rates (biomass specific growth rates) in 1985 compared to 1984. We suggest that this increase in bacterial production and turnover may have been caused by increased predation pressure on the bacterial community in 1985 as appears to have occurred with phytoplankton. Thus, widespread anoxia, such as in 1984, may exert a major influence on predation of both phytoplankton and bacterial communities.

Directly measured oxygen consumption rates were also similar in 1984 and 1985, particularly below the euphotic zone (Table 8). Within the euphotic zone where oxygen consumption is unimportant to deep water oxygen depletion since oxygen is replenished by phytoplankton, directly measured oxygen consumption averaged only 11% lower in 1985 than in 1984. Comparable oxygen consumption values were found by calculating oxygen consumption from average bacterial abundances (Table 10, Fig. 73). In this case, oxygen consumption rates decreased 19% within the euphotic zone and 14% below it.

We conclude that despite major differences in climatic conditions and in the oxygen regime between 1984 and 1985, the bacterial parameters, including oxygen consumption rates, were remarkably similar under summer conditions in both years. These similarities, in concert with nearly identical phytoplankton production in both years, suggest that a major ecological shift has occurred in the mesohaline portion of Chesapeake Bay during the summer (and perhaps the spring as well) such that a large portion of phytoplankton production is processed directly by pelagic microheterotrophs rather than by

higher organisms. This implies that the extent and duration of anoxia in the Bay is determined not by major differences in biological parameters but rather by oxygen replenishment into deep waters which in turn is a function of physical factors such as water column stability, freshwater flow, pycnocline tilting, and wind mixing. The existing biological conditions are such that we expect widespread anoxia to occur whenever the appropriate physical conditions obtain.

The Role of Sulfur Cycling

As we have recounted earlier in this report, sulfur cycling can also be a major mechanism for oxygen depletion in the mesohaline reaches of Chesapeake Bay. Although not a part of the Sea Grant/EPA study, we feel it appropriate to discuss briefly the results of ongoing sulfur cycling studies which have been conducted during 1984-1986 (Tuttle, unpublished) within the study area of the 1985 Sea Grant/EPA investigation.

Hydrogen sulfide is produced during the metabolism of organic matter by obligately anaerobic sulfate-reducing bacteria. In the mid-Bay, this process appears to be most intense in deep channel anoxia sediments. Rates of sediment sulfate reduction measured during 1984 and 1985 indicate that sulfide production in the channel sediments increased throughout the late spring and summer, reaching a peak in mid-September in both years. This implies not only that sulfate reduction is highly temperature-dependent (maximum bottom water temperatures peaked during the August-September period of both years), but that it may be strongly influenced by the accumulation of organic matter from the annual summer phytoplankton maximum in the sediments. During April to November 1984, sulfide production in deep Bay sediments averaged 75 mmol

$\text{m}^{-2} \text{d}^{-1}$ and in 1985, the average rate ($68 \text{ mmol m}^{-2} \text{d}^{-1}$) was comparable.

Therefore, we conclude that despite the decreased phytoplankton biomass during summer 1985, sufficient organic matter reached the sediments to support a rate of sulfate reduction similar to that found the previous year.

Oxygen consumption results when sulfide is oxidized (see eq. 2). If the water column is not anoxic, as was the case during much of 1985 (Fig. 9), then sulfide oxidation in surficial sediments contributes to sediment oxygen demand. When the water column becomes anoxic, sulfide rises to the pycnocline where it is oxidized within as narrow depth band (ca. 1m) in which oxygen and sulfide coexist. Rates of water column sulfide oxidation measured in 1984 and in 1985 near the pycnocline during anoxic events gave average oxygen consumption rates of $9 \text{ mg O}_2 \text{ l}^{-1} \text{ h}^{-1}$. When the water column is not anoxic, mean microheterotroph oxygen consumption below the euphotic zone is about $1 \text{ mg O}_2 \text{ l}^{-1} \text{ h}^{-1}$ (Table 8). However, microheterotrophic oxygen consumption is not limited to a narrow band, but occurs throughout the deep water. If we integrate over an average hypoxia thickness layer of 10 m (Fig. 15), then water column oxygen consumption by microheterotrophs is comparable to that due to sulfide oxidation.

REFERENCES

1. Azam, F. and Fenchel, T. The ecological role of water-column microbes in the sea. *Mar. Ecol. Prog. Ser.* 10:257-263, 1983.
2. Biggs, R.B. and Flemer, D.A. The flux of particulate carbon in an estuary. *Mar. Biol.* 12:11-17, 1972.
3. Boynton, W.R., Kemp, W.M. and Keefe, C.W. A comparative analysis of nutrients and other factors influencing estuarine phytoplankton production. In: *Estuarine Comparisons*, V.S. Kennedy, ed. Academic Press, New York, 1982, pp. 69-90.
4. Carpenter, J.H. The Chesapeake Bay Institute technique for the Winkler dissolved oxygen method. *Limnol. Oceanogr.* 10:141-143, 1965.
5. Chervin, M.B., Malone, T.C. and Neal, P.J. Interactions between suspended organic matter and copepod grazing in the plume of the Hudson River. *Estuar. Coast. Mar. Sci.* 13:169-184, 1981.
6. D'Elia, C.F. Nutrient enrichment of Chesapeake Bay: an historical perspective. In: *Chesapeake Bay Program Technical Studies: A Synthesis*. U.S. Environmental Protection Agency, 1982, pp. 45-102.
7. Ducklow, H.W. Chesapeake Bay nutrient and plankton dynamics. I. Bacterial biomass and production during spring tidal destratification in the York River, Virginia, estuary. *Limnol. Oceanogr.* 27:651-659, 1982.
8. Ducklow, H.W. The production and fate of bacteria in the oceans. *BioScience*. 33:494-501, 1983.
9. Flemer, D.A. and Biggs, R.B. Particulate carbon:nitrogen relations in northern Chesapeake Bay. *J. Fish. Res. Bd. Canada* 28:911-918, 1971.
10. Fuhrman, J.A. and Azam, F. Bacterioplankton secondary production estimated for coastal waters of British Columbia, Antarctica, and California. *Appl. Environ. Microbiol.* 39:1085-1095, 1980.
11. Fuhrman, J.A. and Azam, F. Thymidine incorporation as a measure of heterotrophic bacterioplankton production in marine surface waters: evaluation and field studies. *Mar. Biol.* 66:109-120, 1982.
12. Heinle, D.R., D'Elia, C.F., Taft, J.L., Wilson, J.S., Cole-Jones, M., Caplins, A.B. and Cronin, L.E. Historical review of water quality and climatic data from Chesapeake Bay with emphasis on effects of

enrichment. Final Report, UMCEES Ref. No. 80-15CBL. Univ. of Md. Center for Environmental and Estuarine Studies, Chesapeake Biological Laboratory, Solomons, Maryland, 1980.

13. Hobbie, J.E., Daley, R.J. and Jasper, S. Use of Nuclepore filters for counting bacteria by fluorescence microscopy. *Appl. Environ. Microbiol.* 34:1225-1228, 1977.
14. Malone, T.C., Kemp, W.M., Ducklow, H.W., Boynton, W.R., Tuttle, J.H. and Jonas, R.B. Lateral variation in the production and fate of phytoplankton in a partially stratified estuary. *Mar. Ecol. Prog. Ser.* 32:149-160, 1986.
15. Muller, P.J. C/N ratios in Pacific deep-sea sediments: effect of inorganic ammonium and organic nitrogen compounds sorbed by clays. *Geochim. Cosmochim. Acta* 41:765-776, 1977.
16. Officer, C.B., Biggs, R.B., Taft, J.L., Cronin, I.E., Tyler, M.A. and Boynton, W.R. Chesapeake Bay anoxia: origin, development, and significance. *Science* 223:22-27, 1984.
17. Schneider, E. 1987. The Maryland aquaculture project: project summary (Draft)
18. Seliger, H.H., Boggs, J.A. and Biggley, W.H. Catastrophic anoxia in Chesapeake Bay in 1984. *Science* 228:70-73, 1985.
19. Steele, J.H. The Structure of Marine Ecosystems. Harvard University Press, Cambridge, Massachusetts, 1974.
20. Strickland, J.D.H. Production of organic matter in the primary stages of the marine food chain. In: *Chemical Oceanography*, J.P. Riley and G. Skirnow, eds. Academic Press, New York, 1965, pp. 478-610.
21. Taft, J.L. Nutrient processes in Chesapeake Bay. In: *Chesapeake Bay Program Technical Studies: A Synthesis*. U.S. Environmental Protection Agency, Annapolis, Maryland, 1982, pp. 103-149.
22. Taft, J.L., Taylor, W.R., Hartwig, E.D. and Loftus, R. Seasonal oxygen depletion in Chesapeake Bay. *Estuaries* 3:242-247, 1980.
23. Tuttle, J., Malone, T., Jonas, R., Ducklow, H. and Cargo, D. Nutrient-dissolved oxygen dynamics: roles of phytoplankton and microheterotrophs under summer conditions. Final Report to U.S. Environmental Protection Agency, Chesapeake Bay Program, Annapolis, Maryland, 1985, 121 pp.
24. Williams, P.J. LeB. Incorporation of microheterotrophic processes into the classical paradigm of the planktonic food web. *Kieler Meeresforsch.* 5:1-28, 1981.

25. Williams, P.J. LeB. and Askew, C. A method of measuring the mineralization of micro-organisms of organic compounds in seawater. *Deep-Sea Res.* 15:365-375, 1968.
26. Williams, P.J. LeB., Berman, T., and Holm-Hansen, O. Amino acid uptake and respiration by marine heterotrophs. *Mar. Biol.* 35:41-47, 1976.
27. Wright, R.T., and Coffin, R.B. Factors affecting bacterioplankton density and productivity in salt marsh estuaries. In: *Current Perspectives in Microbial Ecology*. C.A. Reddy and M.J. Klug, eds. Am. Soc. Microbiol., Washington, D.C., 1984, pp. 485-494.